

Relevance of cross sections for indirect dark matter detection

Mattia Di Mauro



Cross sections for Cosmic Rays @
CERN, October 16-19 2024

Outline of the talk

- Introduction about dark matter (DM) evidences and searches
- Indirect search of DM
 - Gamma rays and Neutrinos
 - Positrons
 - Antiprotons
 - Anti-D (anti-He3)

<https://github.com/dimauromattia/CRXS> AstroP XS

<https://github.com/ajueid/CosmiXs> DM spectra

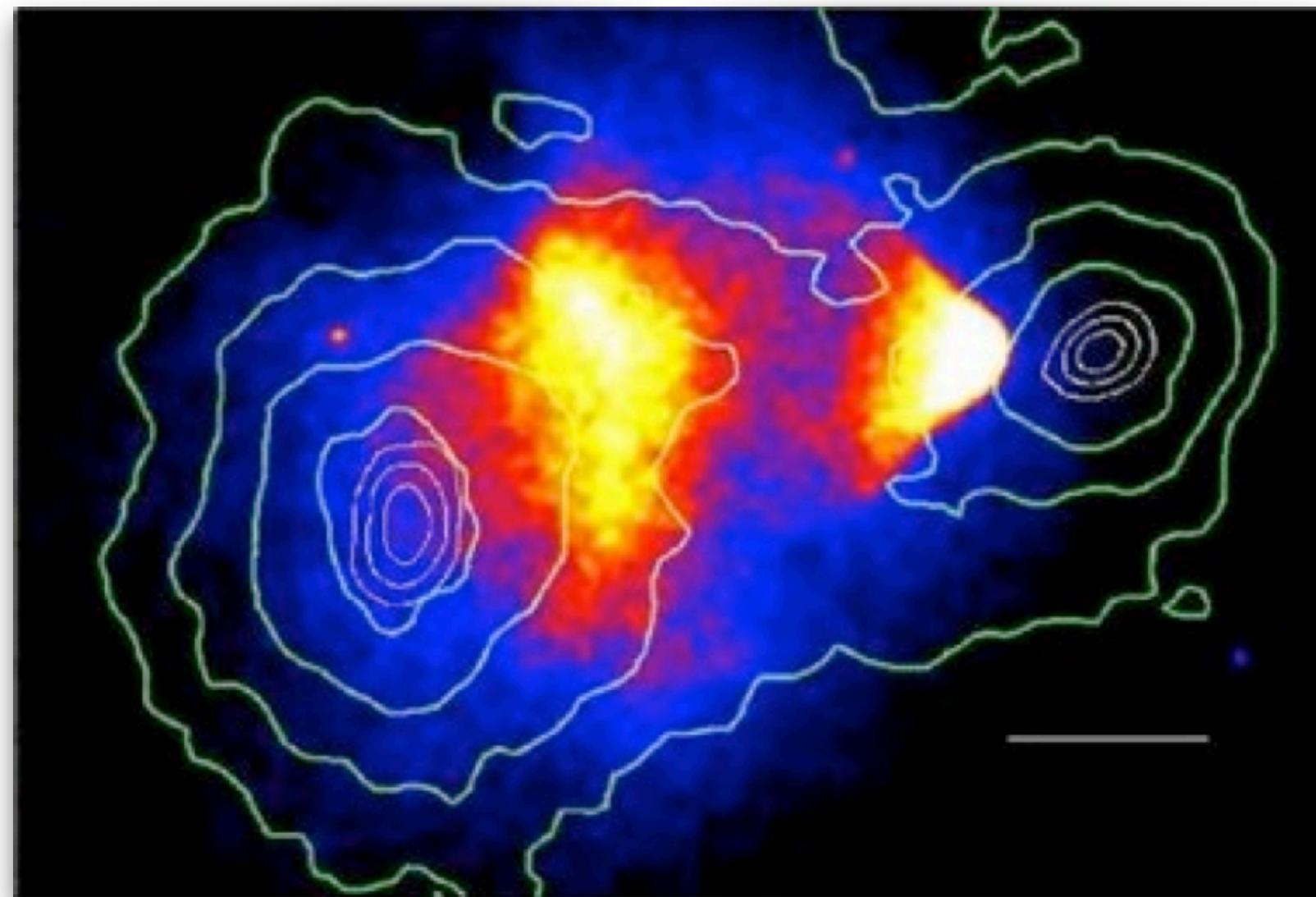
- **XS e+e-:** *Phys.Rev.D* 105 (2022) 12, 123021 Orusa, DM, Korsmeier, Donato
- **XS gamma:** *Phys.Rev.D* 107 (2023) 8, 083031 Orusa, DM, Korsmeier, Donato
- **XS pbar:** *Phys.Rev.D* 97 (2018) 10, 103019 Korsmeier, Donato, DM
- **Dbar:** Di Mauro, Ruiz, Jueid, Fornengo, Bellini - in preparation -

Dark matter: gravitational evidences

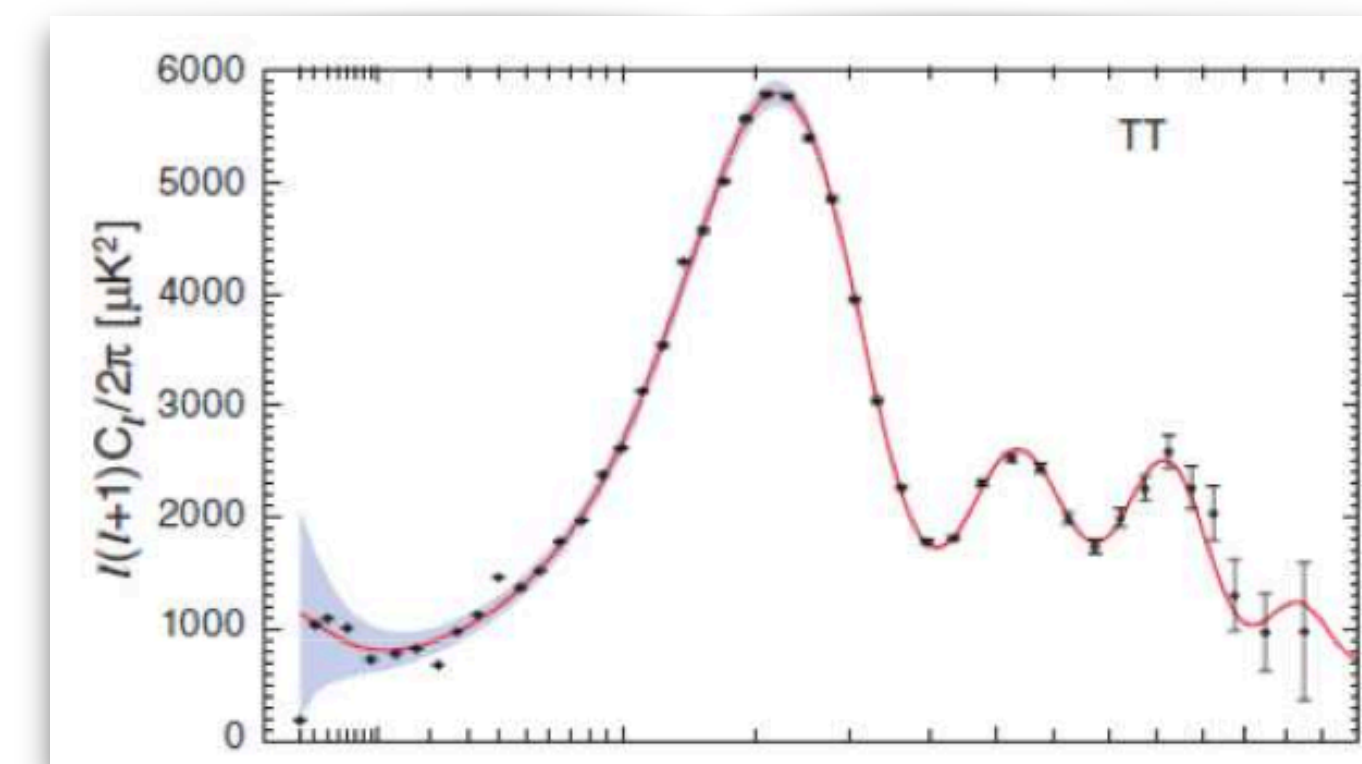
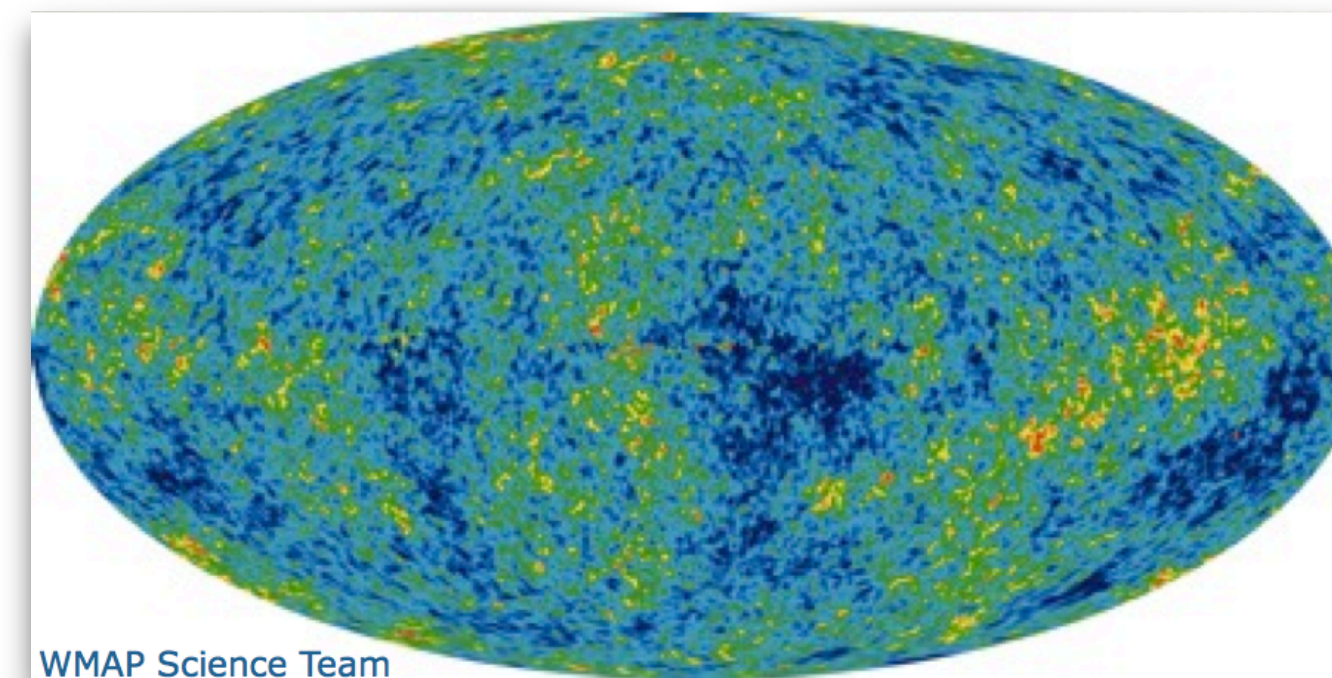
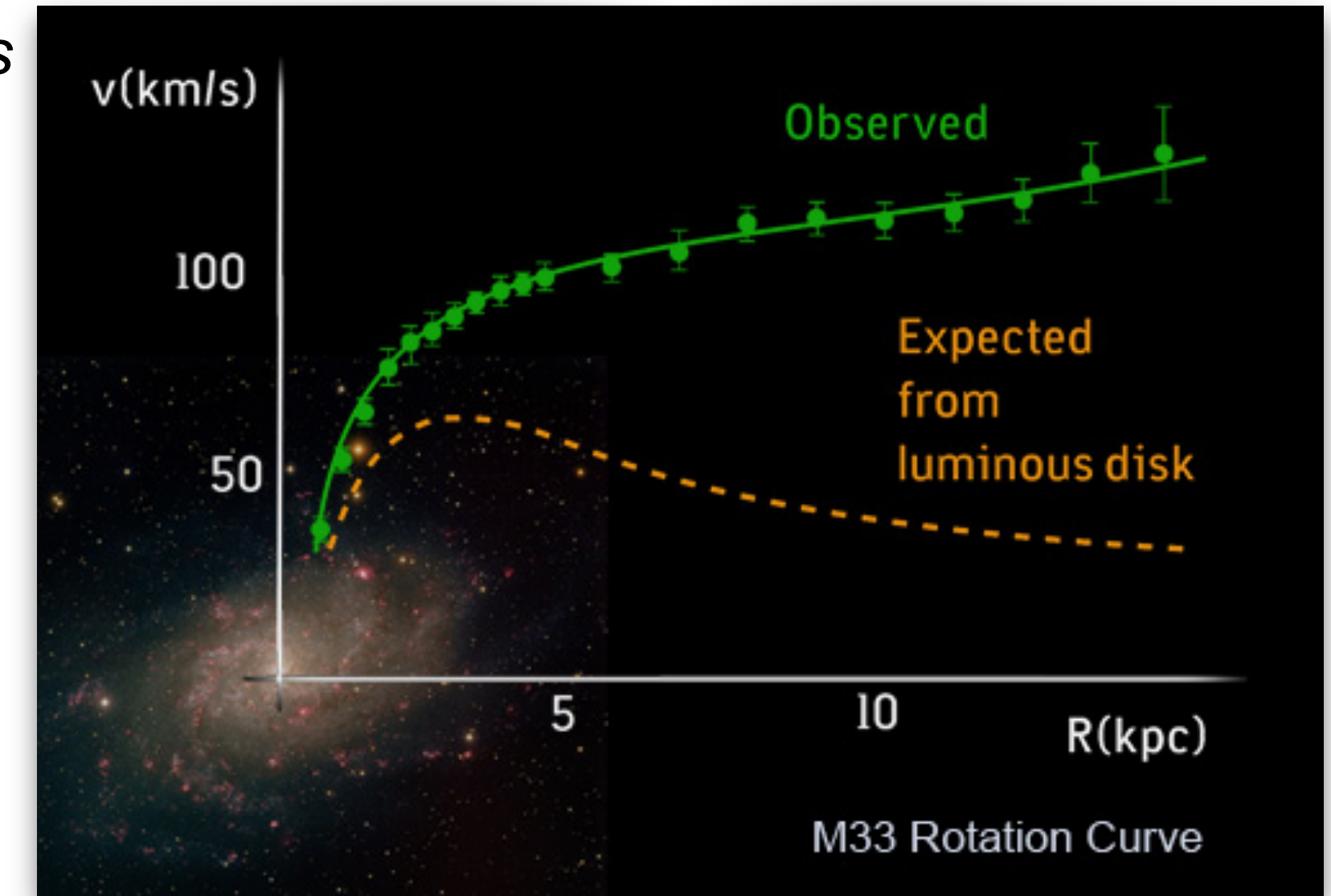


Comprises **majority of mass** in Galaxies
Missing mass on Galaxy Cluster scale
(Zwicky (1937))

Almost **collisionless**
Bullet Cluster



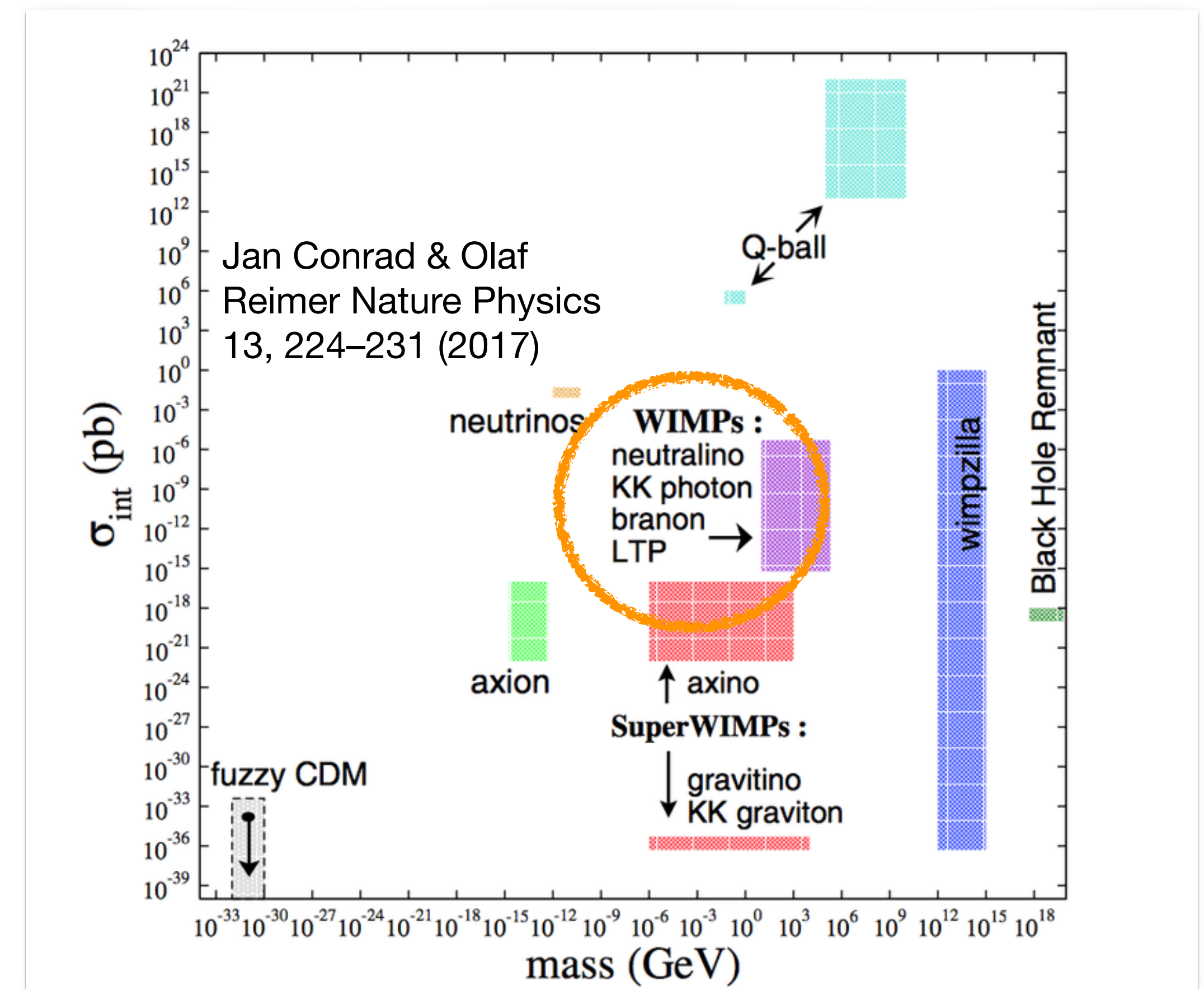
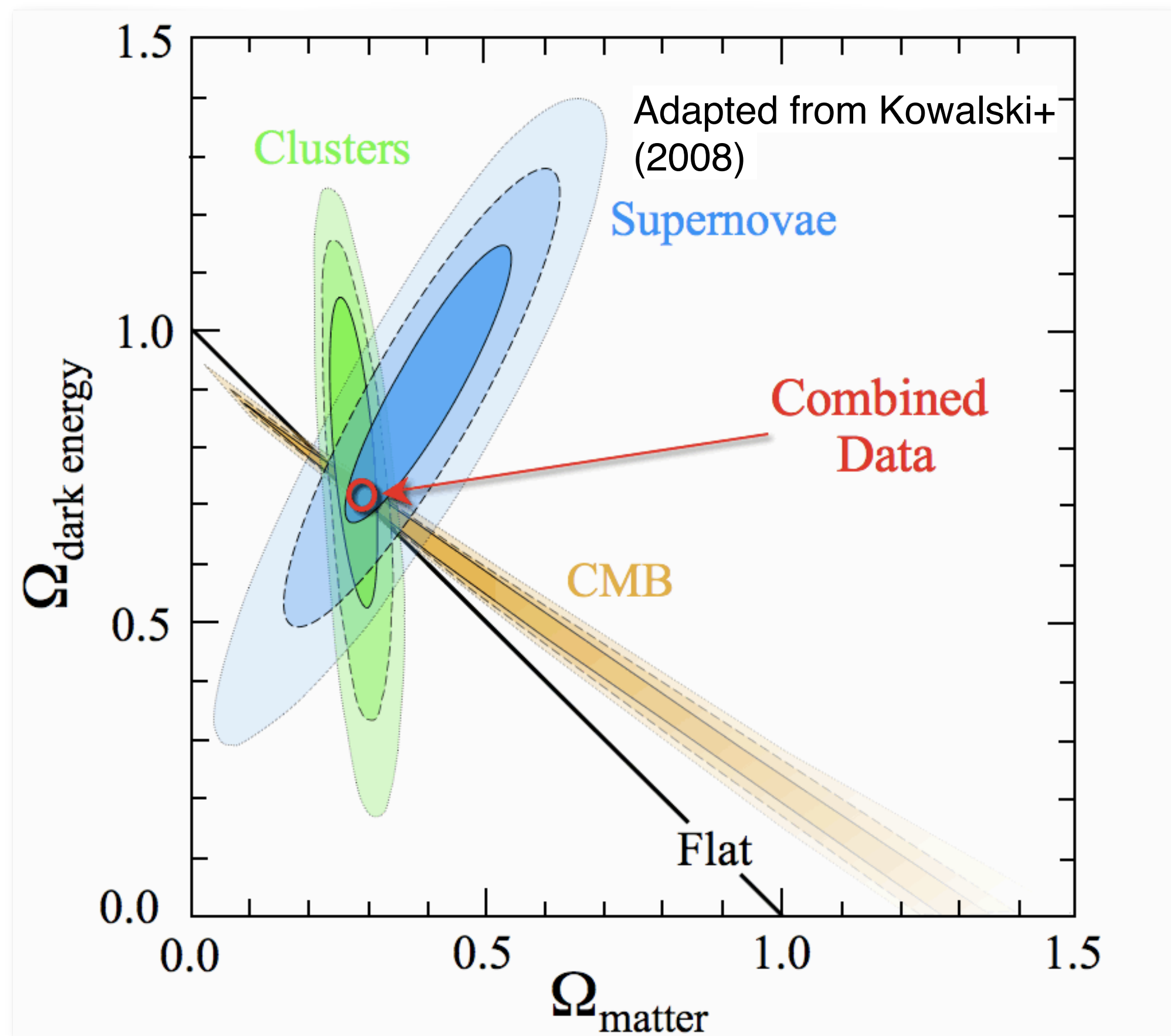
Large **halos** around Galaxies
Rotation Curves
Rubin+(1980)



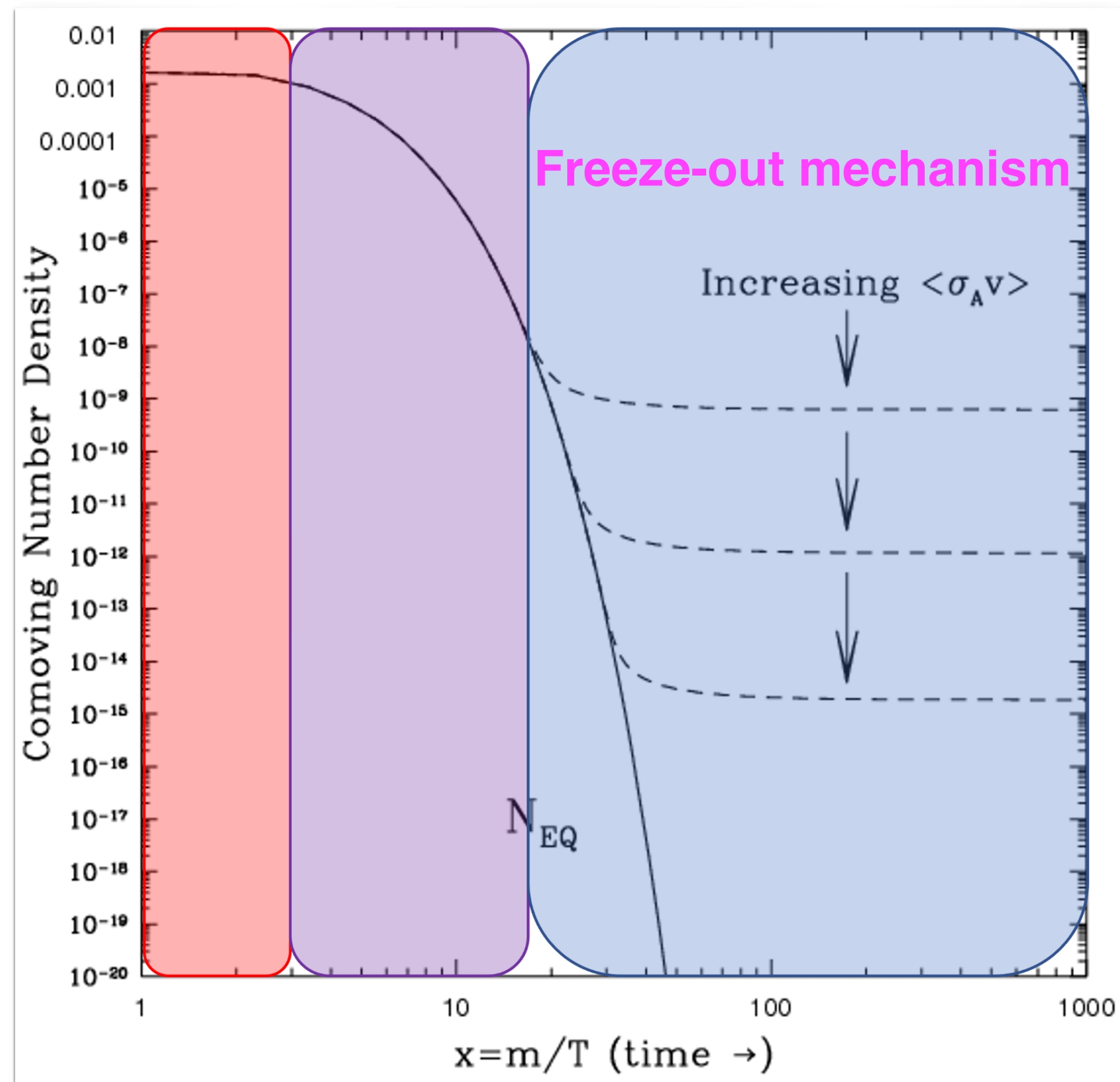
Non-Baryonic
Big-Bang Nucleosynthesis,
CMB Acoustic Oscillations
WMAP(2010), Planck(2015)

A plethora of dark matter candidates

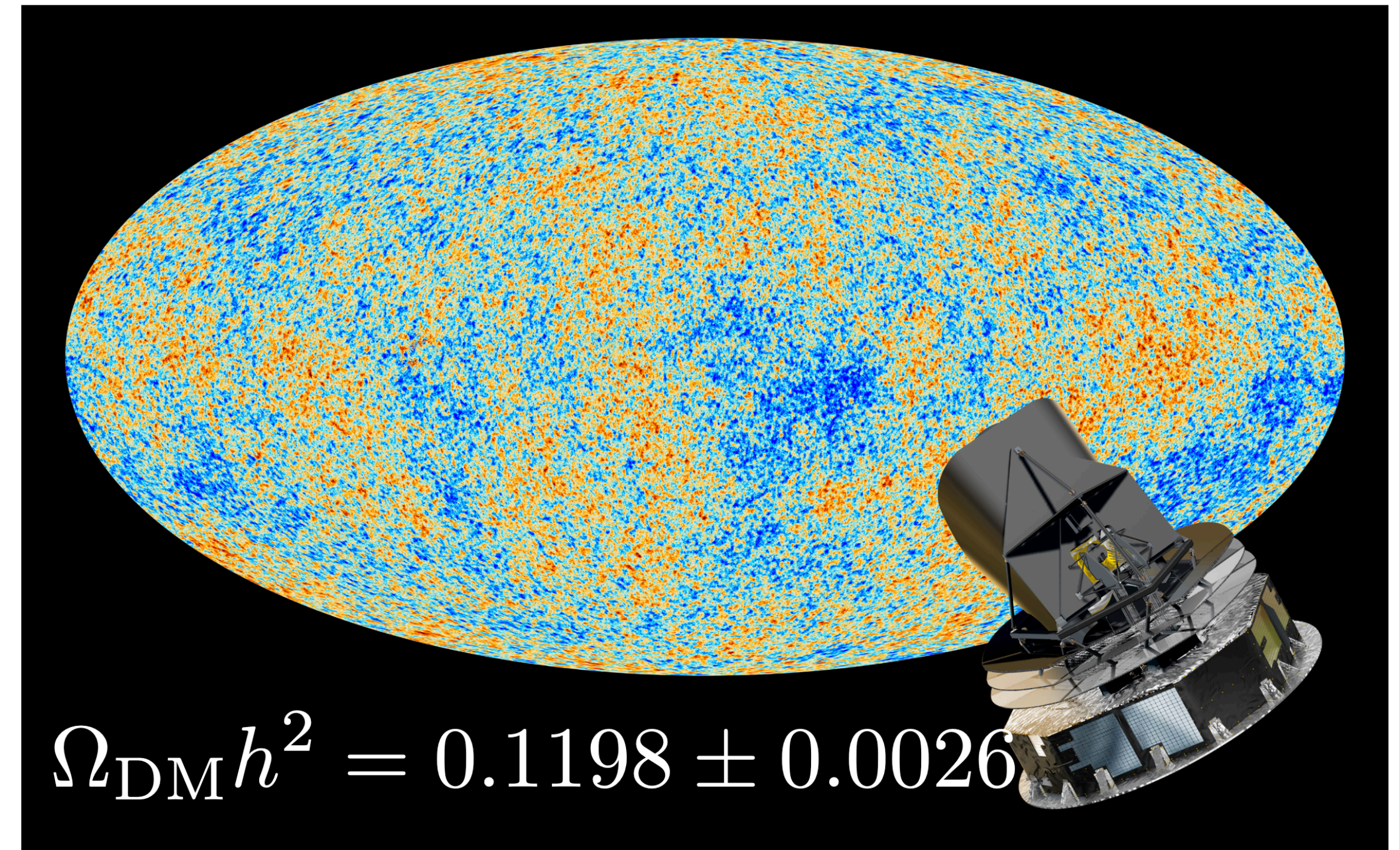
- No Standard Model particle matches the known properties of dark matter
- Weakly interacting massive particle, or WIMP, among the most popular candidate



The WIMP 'miracle'



CMB temperature anisotropy

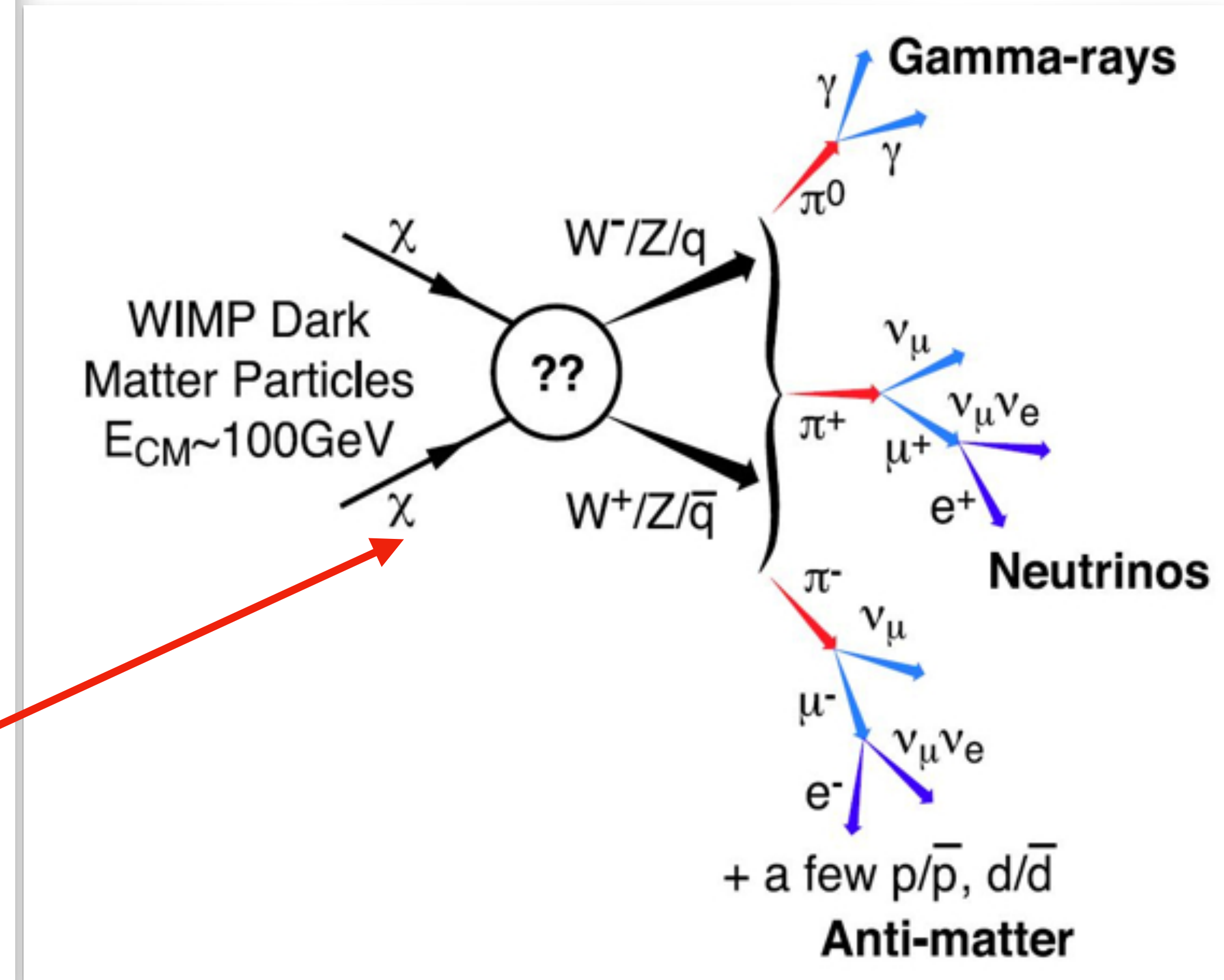
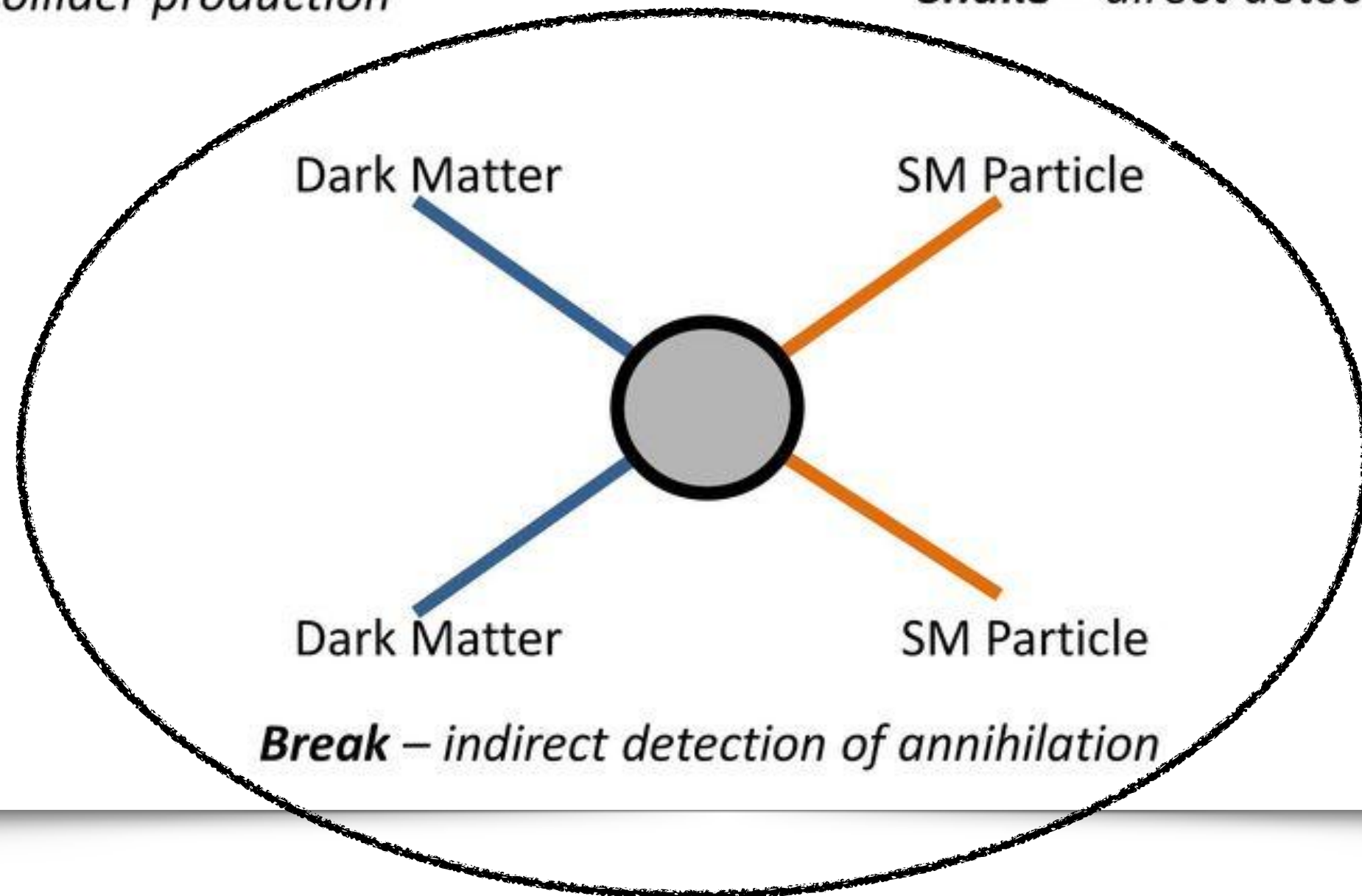
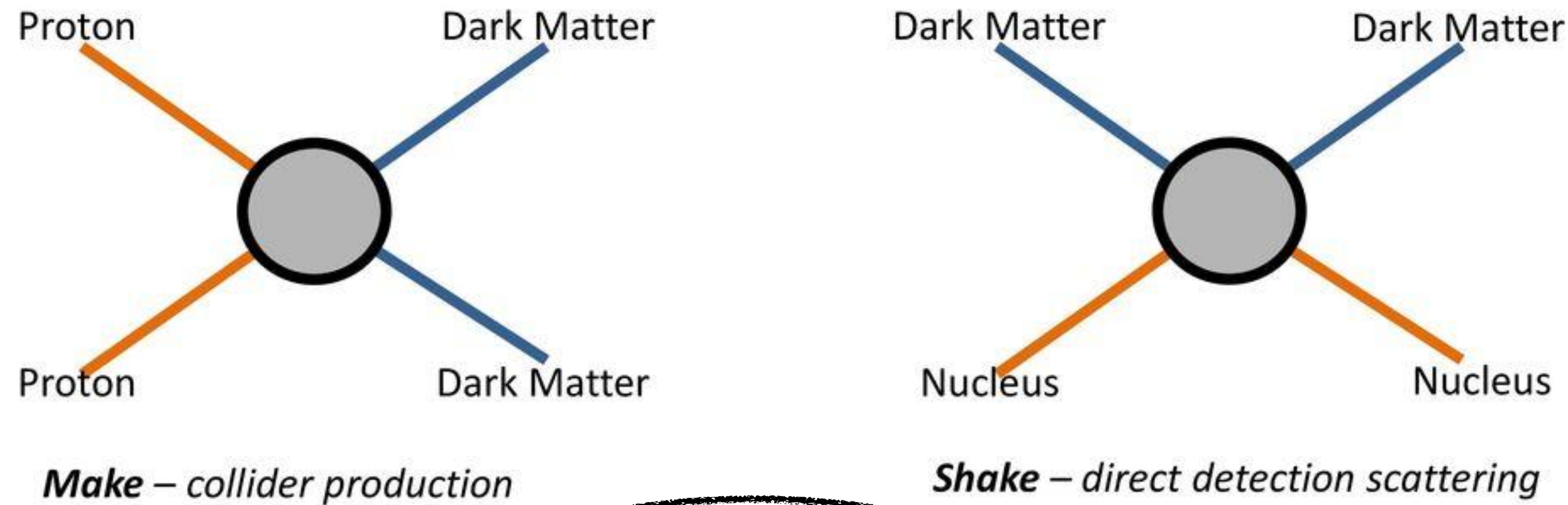


$$\Omega_{\text{DM}} h^2 \sim \frac{10^{-27} \text{ cm}^3 / \text{s}}{\langle \sigma(\text{DM DM} \rightarrow \text{SM SM})_v \rangle}$$

$$\langle \sigma(\text{DM DM} \rightarrow \text{SM SM})_v \rangle \sim 3 \times 10^{-26} \text{ cm}^3 / \text{s}$$

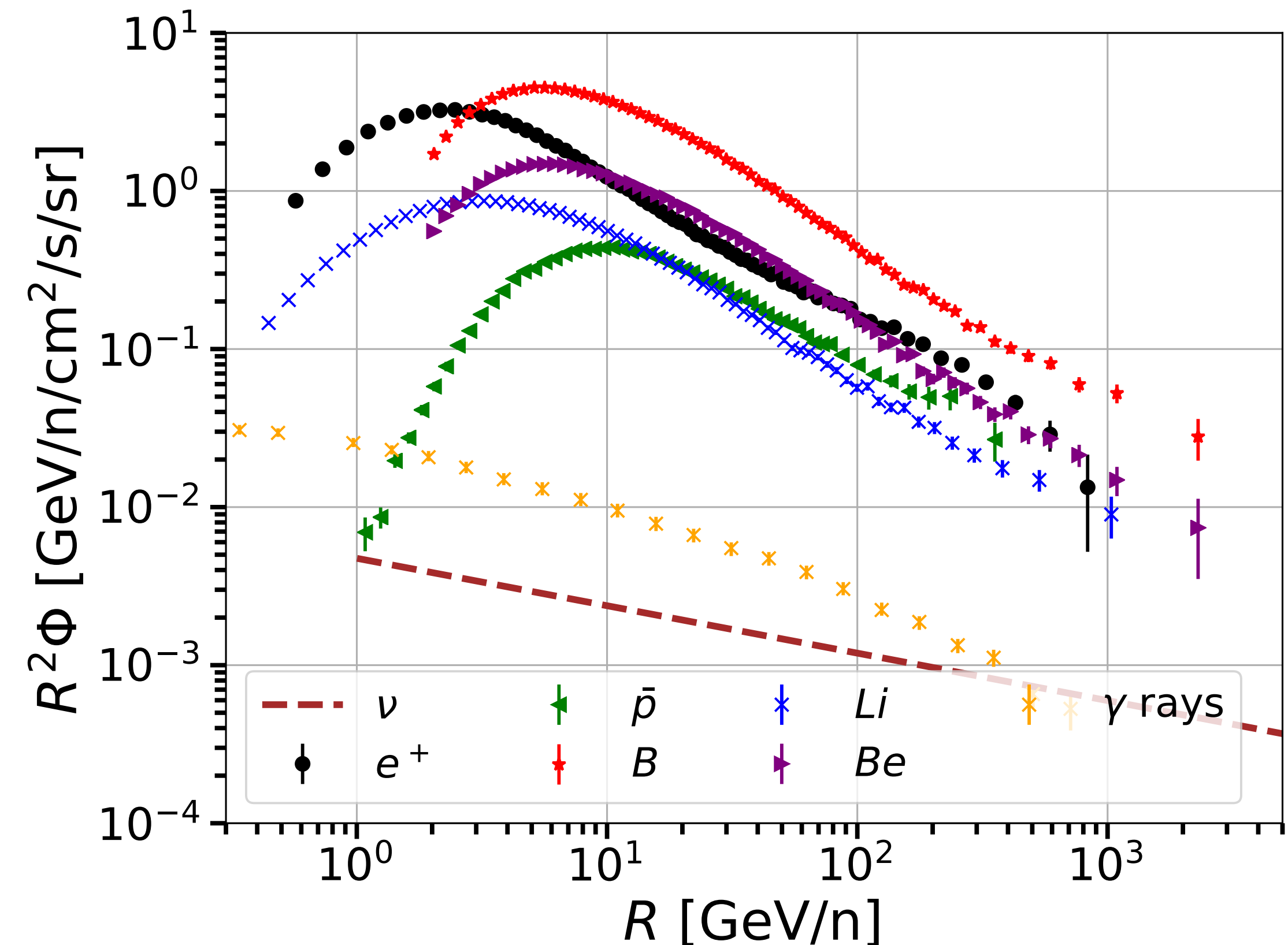
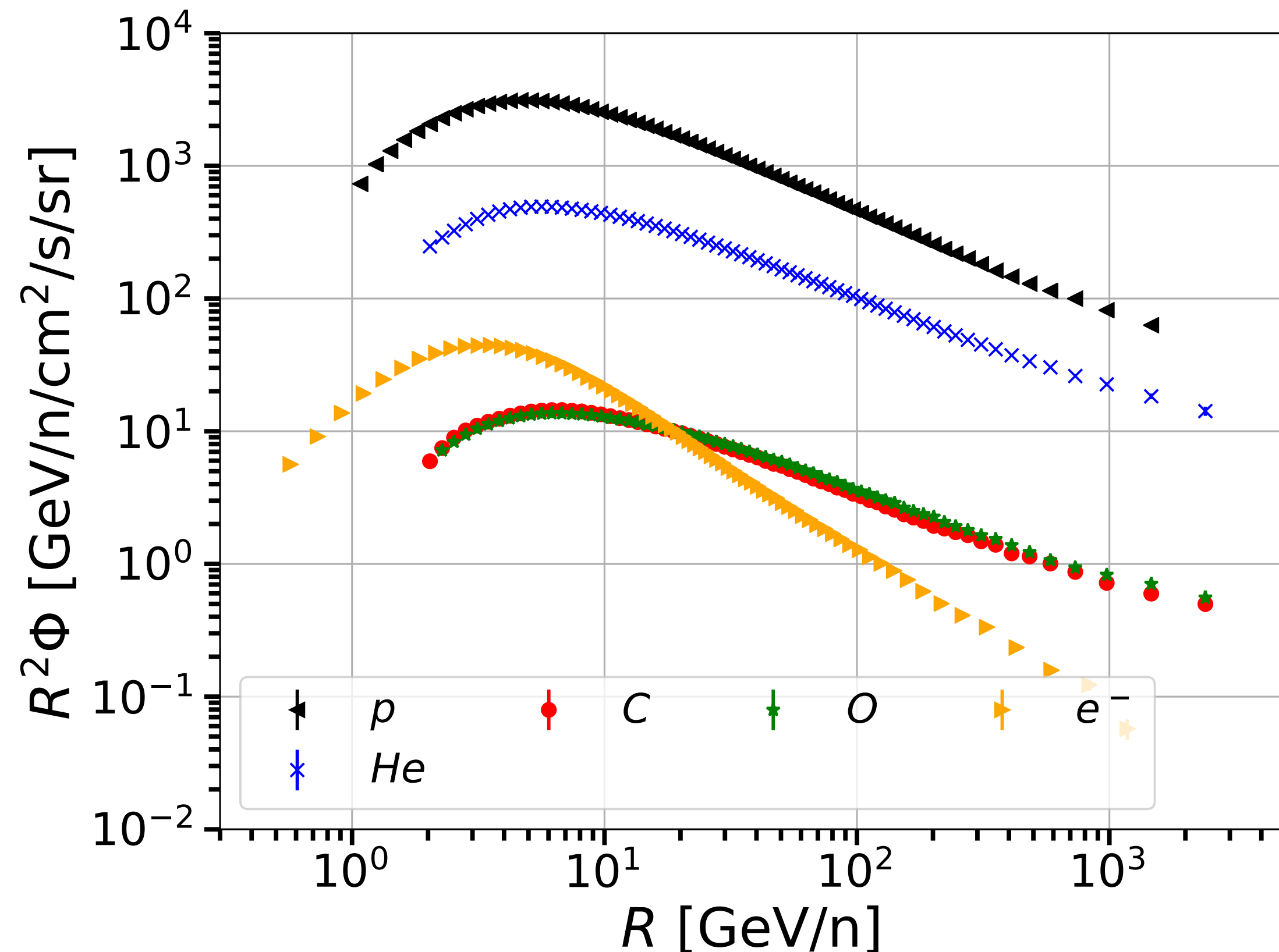
Dark matter searches

Ways to Detect Dark Matter – *Make, Shake and Break*



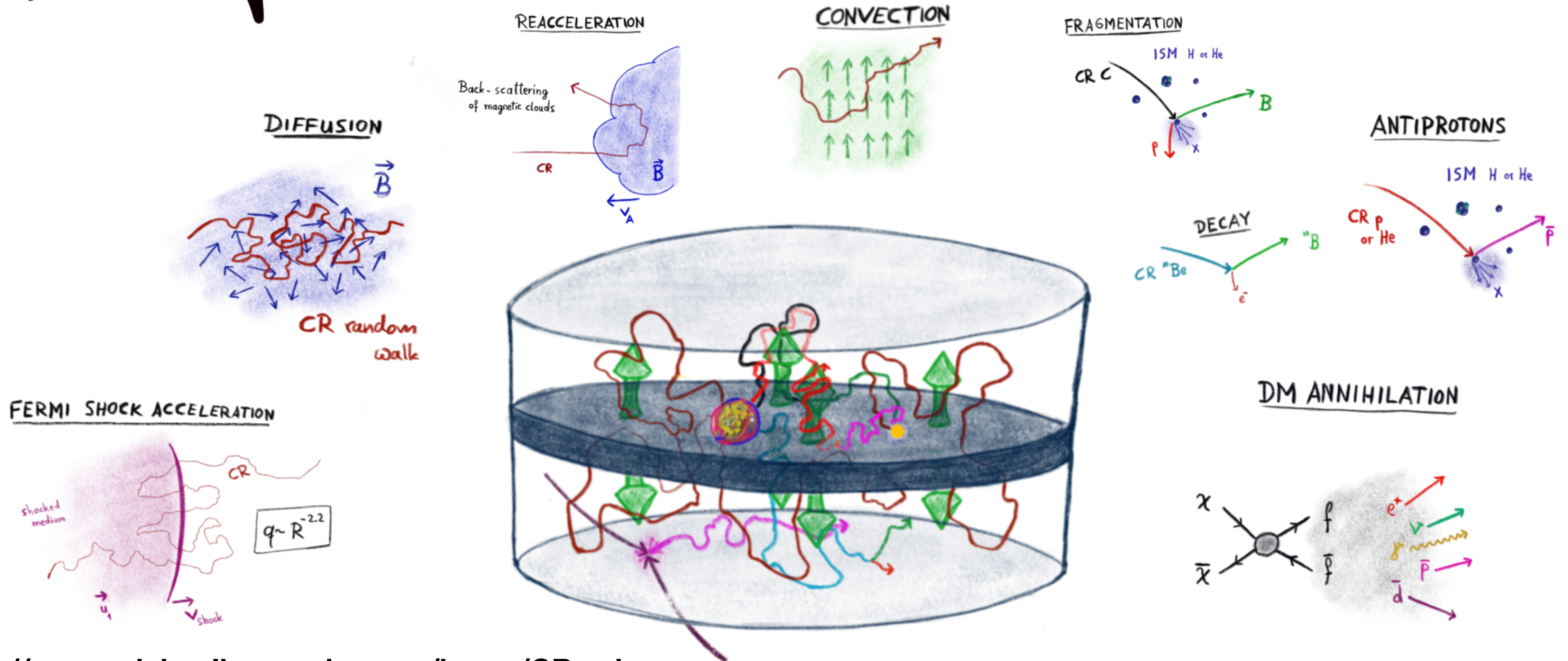
Cosmic particles

- Antiprotons, antinuclei, positrons, gamma rays and neutrinos are the rarest CRs and the most studied for DM indirect detection.
- Antinuclei are particularly promising because the DM production could exceed by at least 1 odg the secondary one for $K < 1 \text{ GeV/n}$.



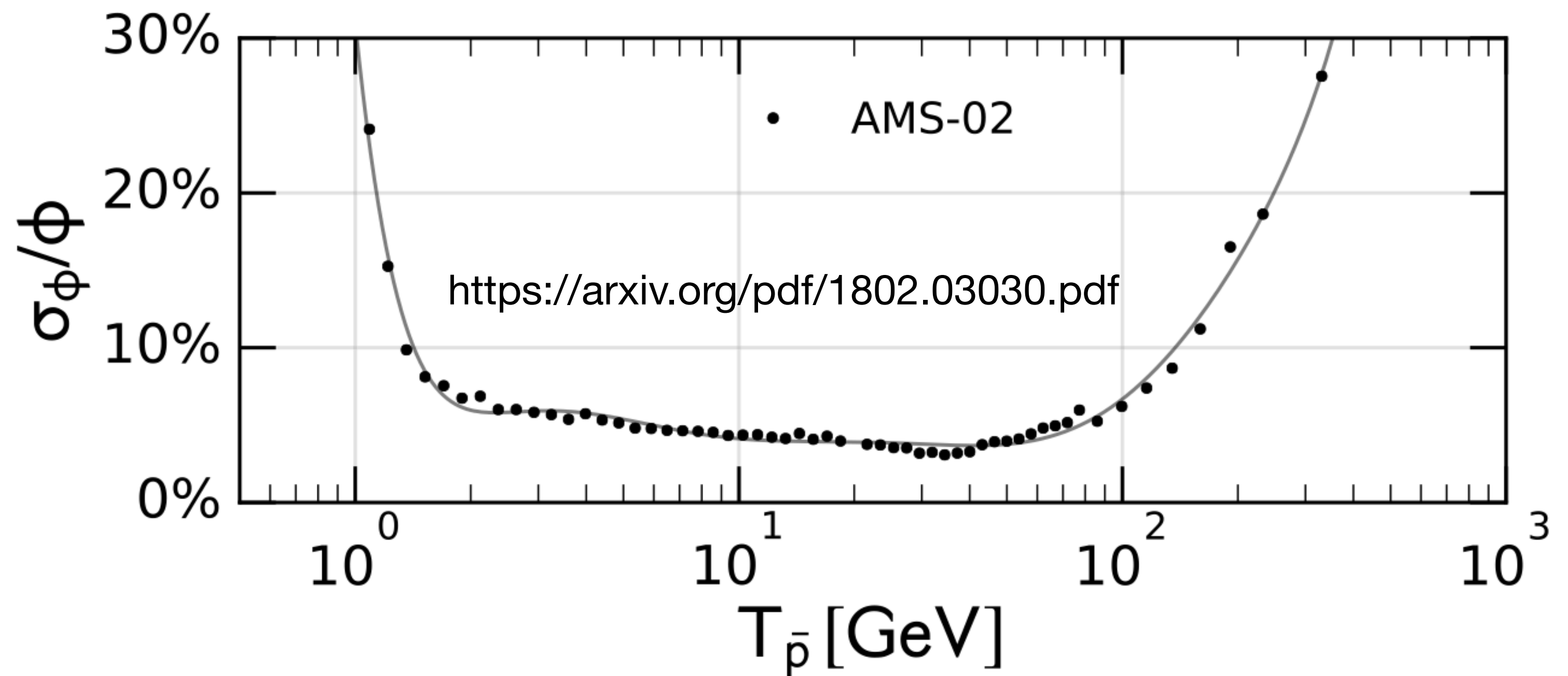
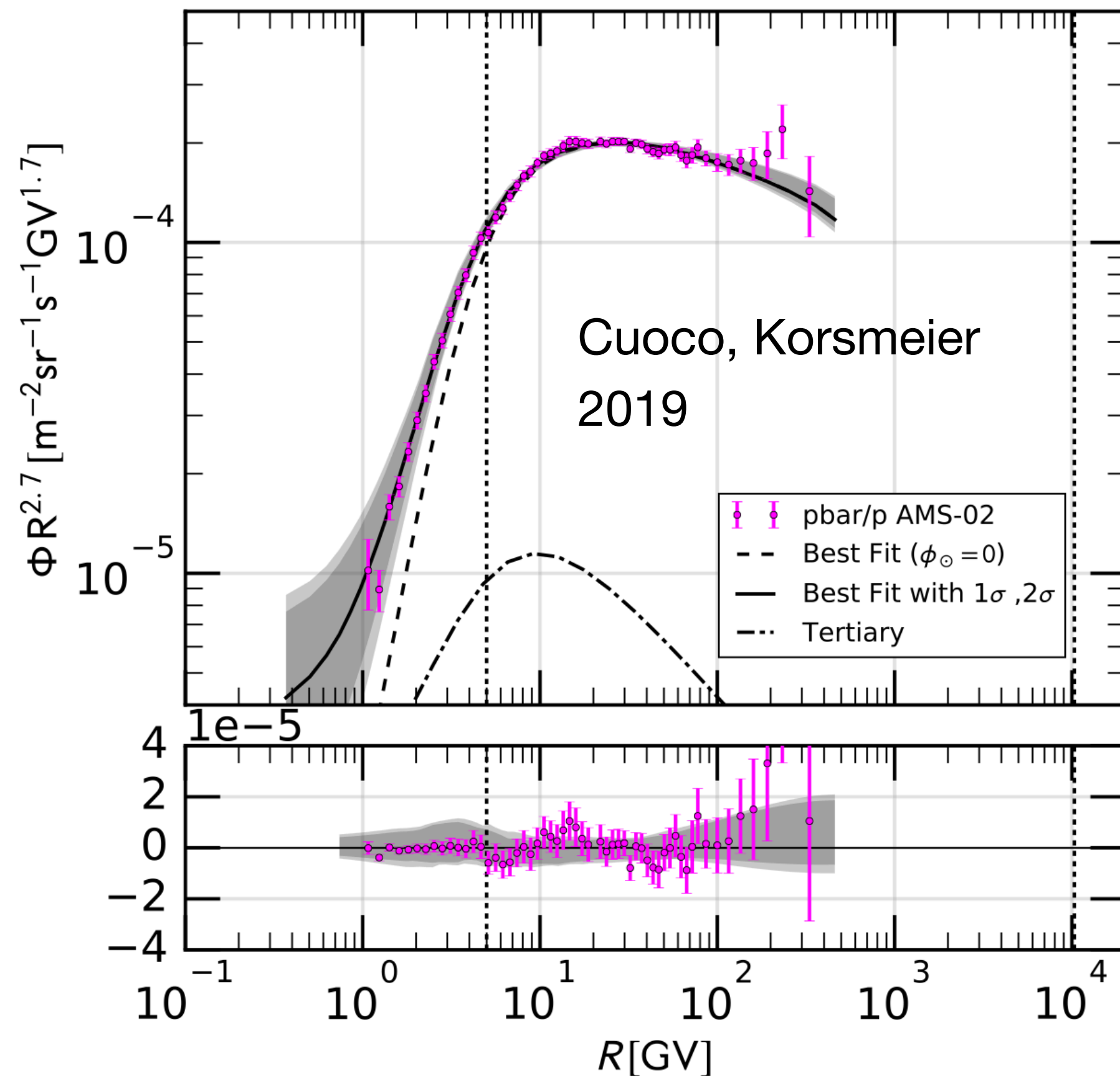
Cosmic-ray propagation

CR propagation



Antiprotons AMS-02 data and DM

- The AMS-02 data reach a precision of about 3-6%.
- Errors of cross section data and theoretical models should reach about this precision.
- This is particularly relevant for CR physics and searches for DM signals.



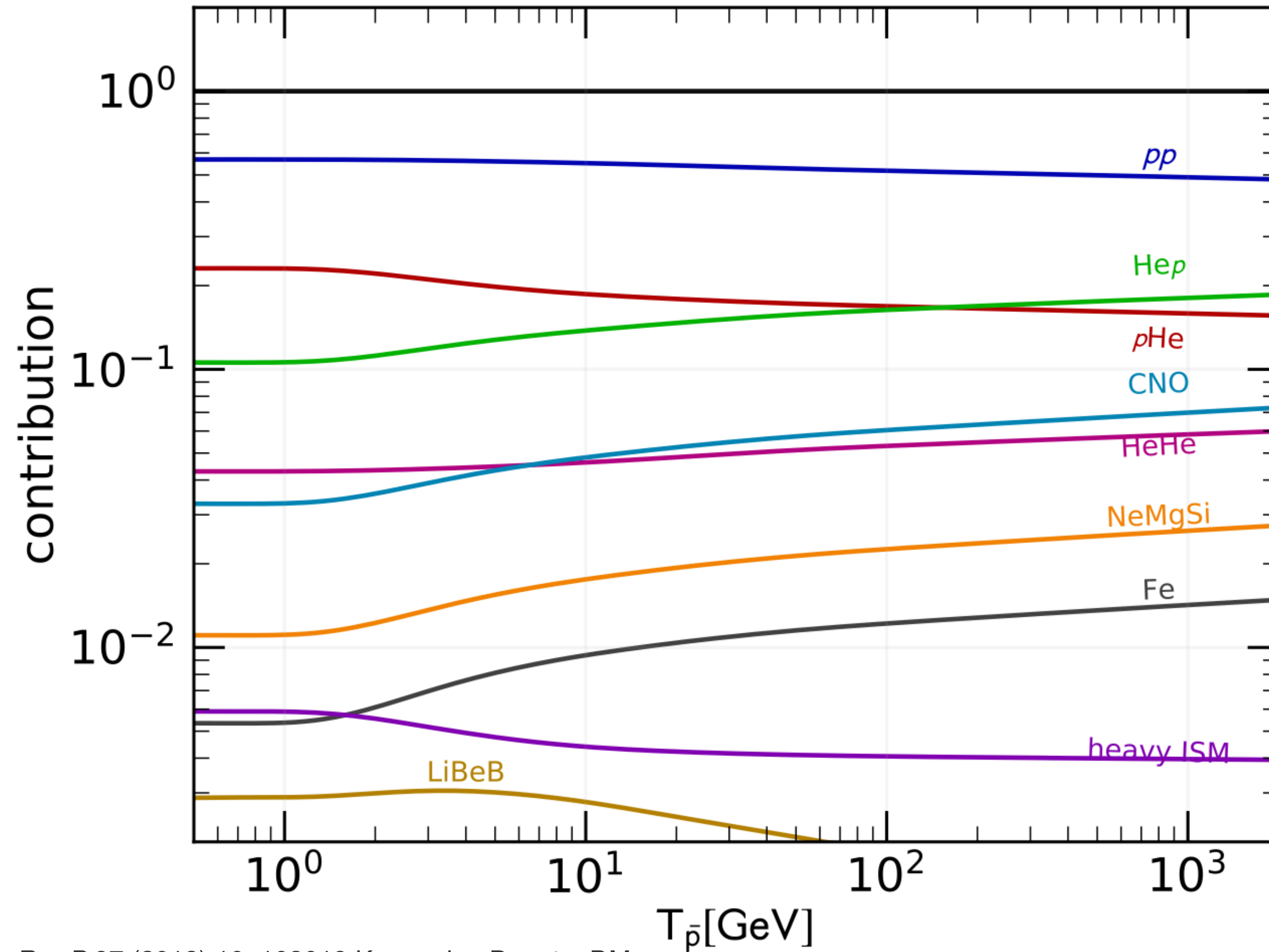
Secondary antiproton source term

$$q_{ij}(T_{\bar{p}}) = \int_{T_{\text{th}}}^{\infty} dT_i 4\pi n_{\text{ISM},j} \phi_i(T_i) \frac{d\sigma_{ij}}{dT_{\bar{p}}}(T_i, T_{\bar{p}})$$

$$\sigma_{\text{inv}} = E \frac{d^3\sigma}{dp^3}(\sqrt{s}, x_{\text{R}}, p_{\text{T}}) \quad \frac{d\sigma_{ij}}{dT_{\bar{p}}}(T, T_{\bar{p}}) = p_{\bar{p}} \int d\Omega \sigma_{\text{inv}}^{(ij)}(T_i, T_{\bar{p}}, \theta)$$

| | Analytic Parametrization | Monte Carlo Event Generator |
|------------------|--|---|
| Procedure | <ul style="list-style-type: none"> • Parametrization of the (Lorentz invariant) cross section • Fit to experimental data • Integration over production angle | <ul style="list-style-type: none"> • Tuning of the MC event generator to the relevant experimental data • Generation of data • Extraction of the final cross section |
| Examples | <ul style="list-style-type: none"> • Antiprotons: [Tan&Ng '83; Winkler '17; Korsmeier '18] • Positrons: [Dermer '86, Orusa '22] • Nuclei: [GALPROP; DRAGON] | <ul style="list-style-type: none"> • Antiprotons: [AAfrag/QGS-Jet (Kachelriss '17)] • Positrons: [Kamae '05] • Nuclei: [FLUKA (della Torre Luque '22)] |

Antiproton production channels



- About 50% from pp and 50% from pHe, Hep, HeHe

$$\sigma_{\text{inv}}^{\text{Galaxy}} = \sigma_{\text{inv}} (2 + \Delta_{\text{IS}} + 2\Delta_{\Lambda})$$

Antiproton production cross sections: data

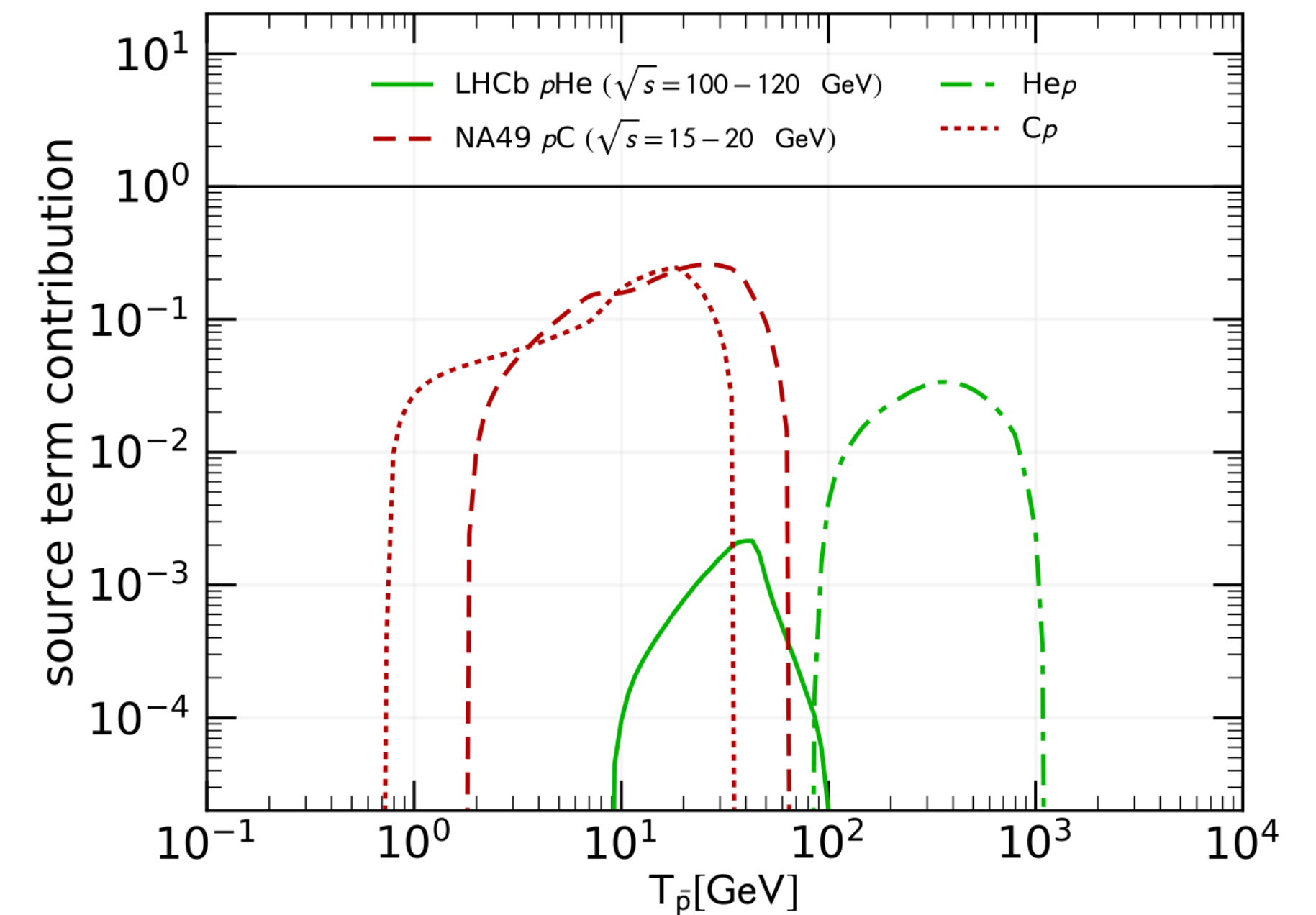
pp → anti-p X

| Experiment | \sqrt{s} [GeV] | σ_{scale} | I | II | Ref. |
|-----------------------|----------------------|-------------------------|---|----|------|
| NA49 | 17.3 | 6.5% | × | × | [26] |
| NA61 | 7.7, 8.8, 12.3, 17.3 | 5% | × | × | [24] |
| Dekkers <i>et al.</i> | 6.1, 6.7 | 10% | × | × | [36] |
| BRAHMS | 200 | 10% | × | | [38] |

pA → anti-p X

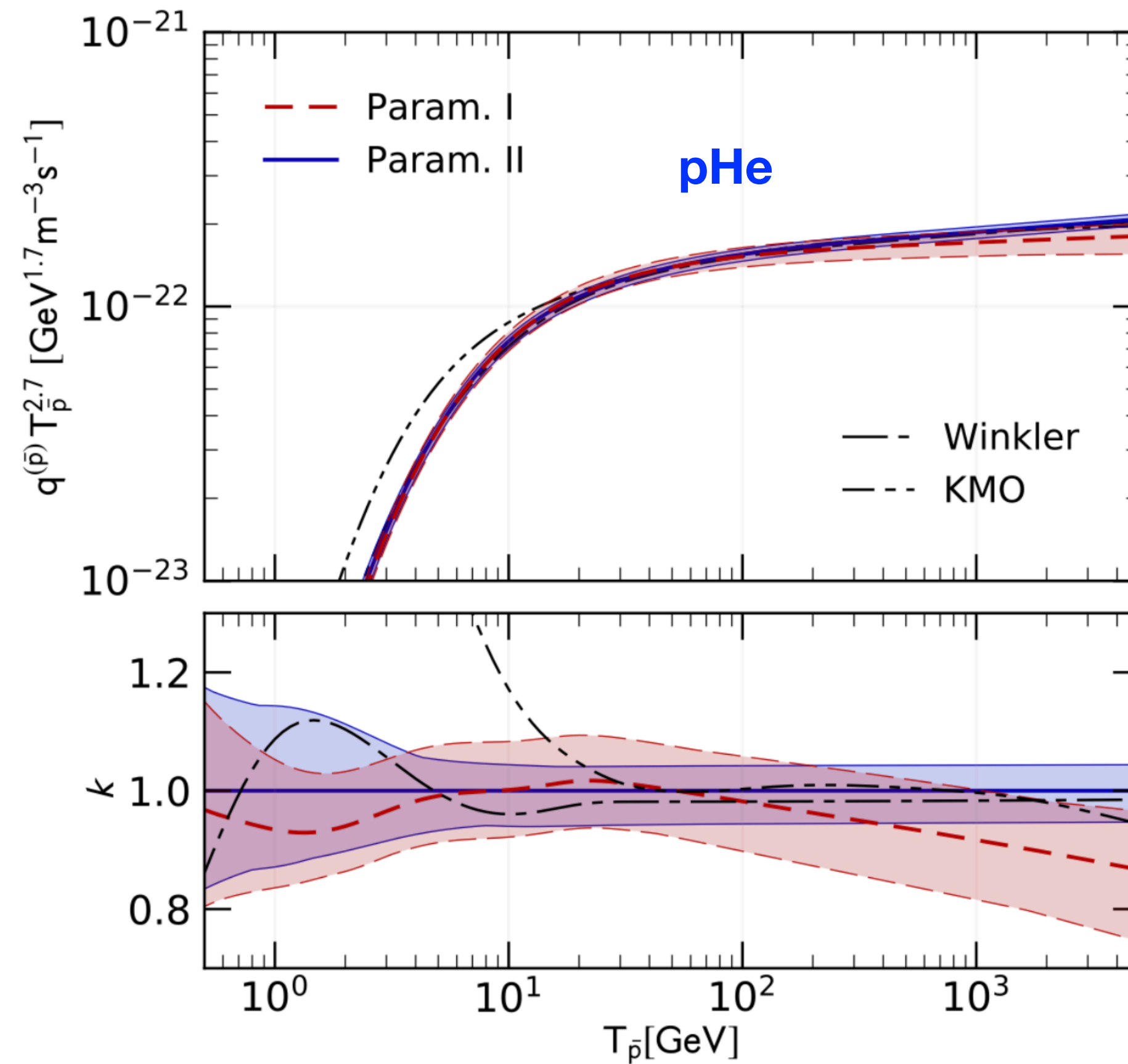
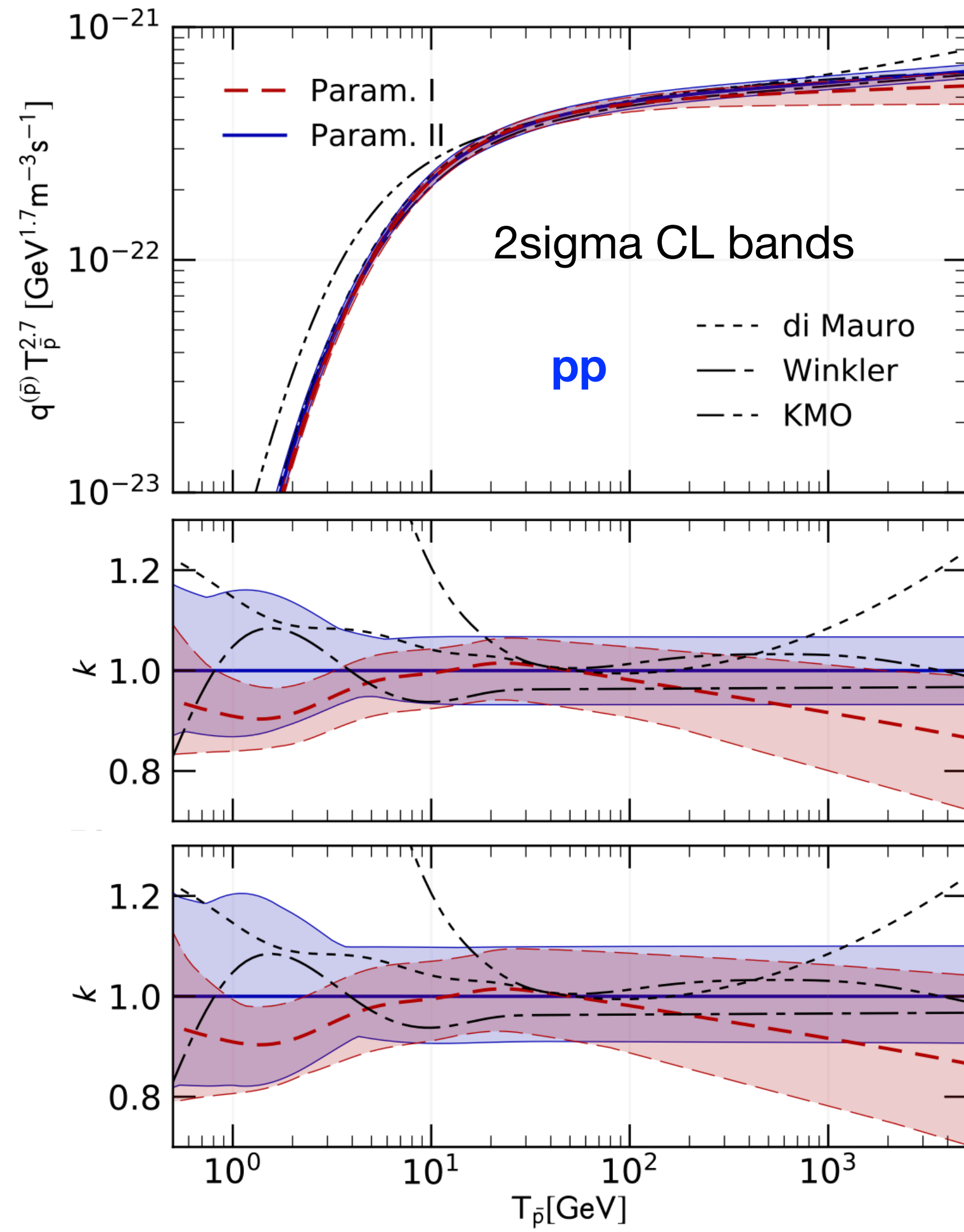
| | \sqrt{s} [GeV] | σ_{scale} | I-A | I-B | II-A | II-B | Ref. |
|------|------------------|-------------------------|-----|-----|------|------|------|
| NA49 | 17.3 | 6.5% | × | × | × | × | [35] |
| LHCb | 110 | 6.0% | | × | | × | [25] |

Ep=6.5 TeV



Antiproton data from AMS-02 are between 10-1000 GeV → sqrt(s) = 5-50 GeV (NA61, AMBER,...)

Antiproton production cross sections: results



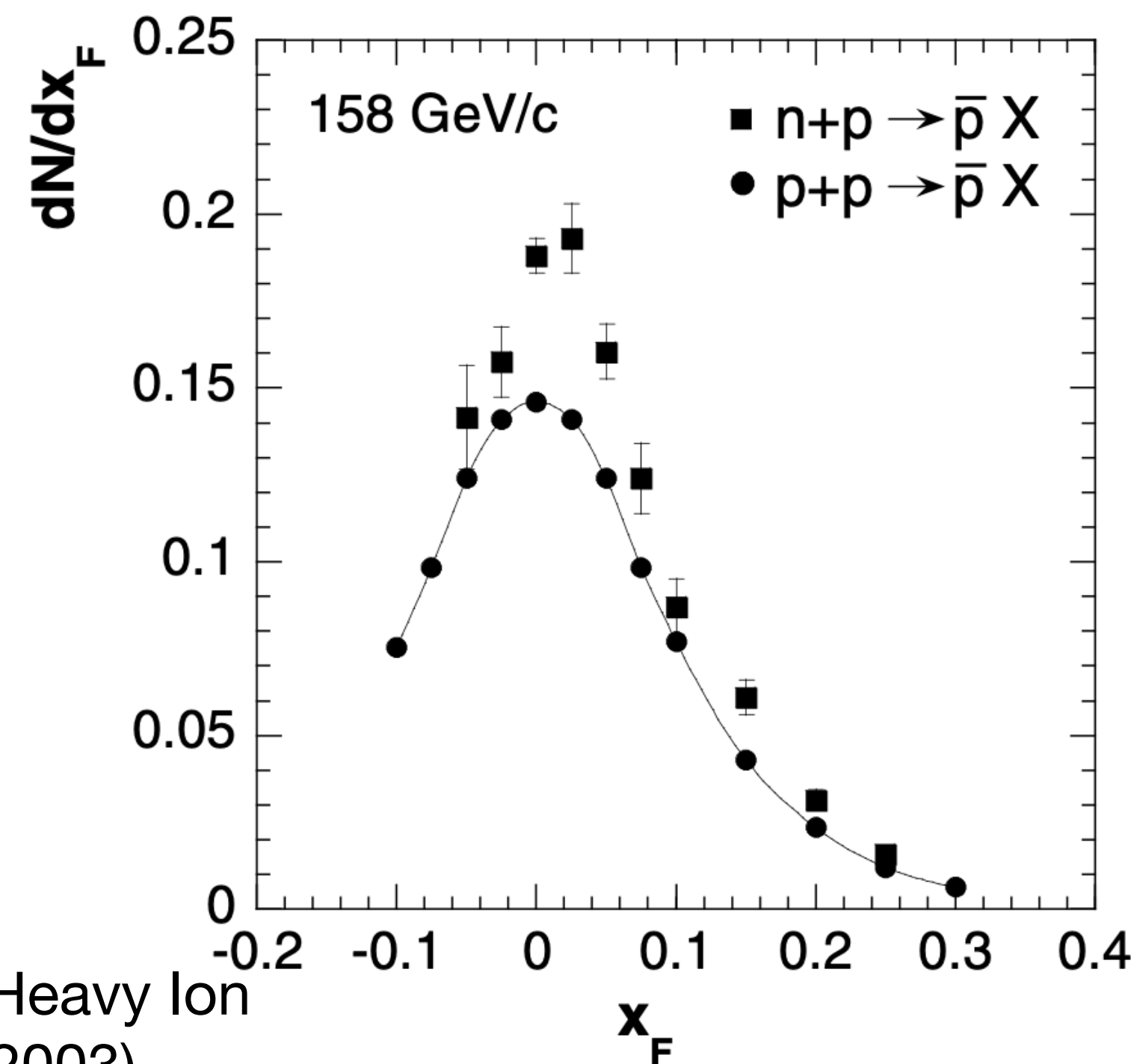
$$f^{pA} = A^{D_1} \left[A^{D_2} \left(1 + \frac{N}{A} \Delta_{\text{IS}} \right) F_{\text{pro}}(x_f) + F_{\text{tar}}(x_f) \right]$$

- The prompt pp channel has an uncertainty between 10-15%
- The uncertainty for the He part is about 15-20%

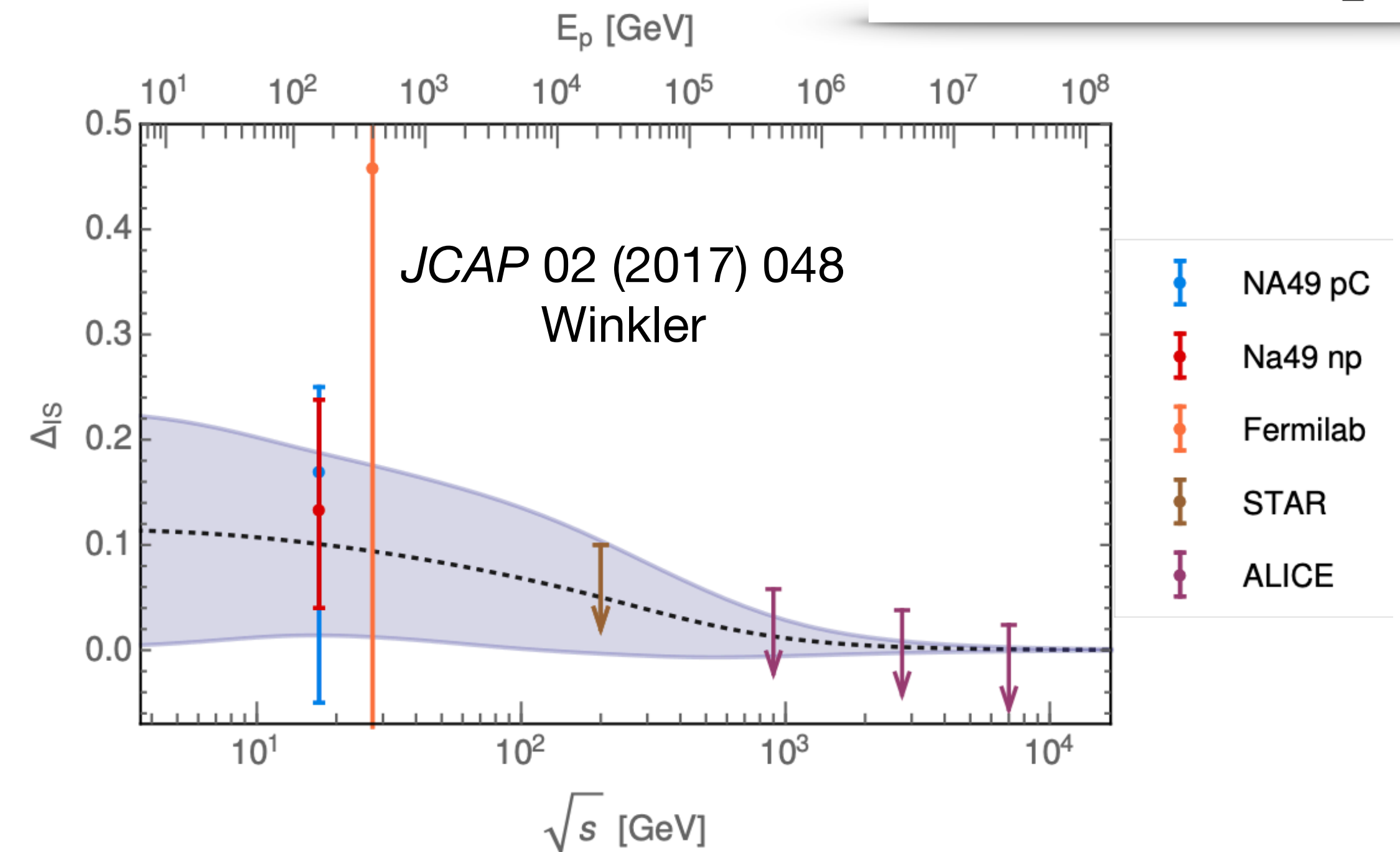
Antineutron production channel

- $pp \rightarrow \text{anti-n } X \rightarrow \text{anti-p } Y$ usually taken to be the same of $pp \rightarrow \text{anti-p } X$.
- NA49 proceeding found an isospin asymmetry at the level of 20-30% at $x_F=0$.
- **This is the main source of uncertainty in antiproton production cross sections.**

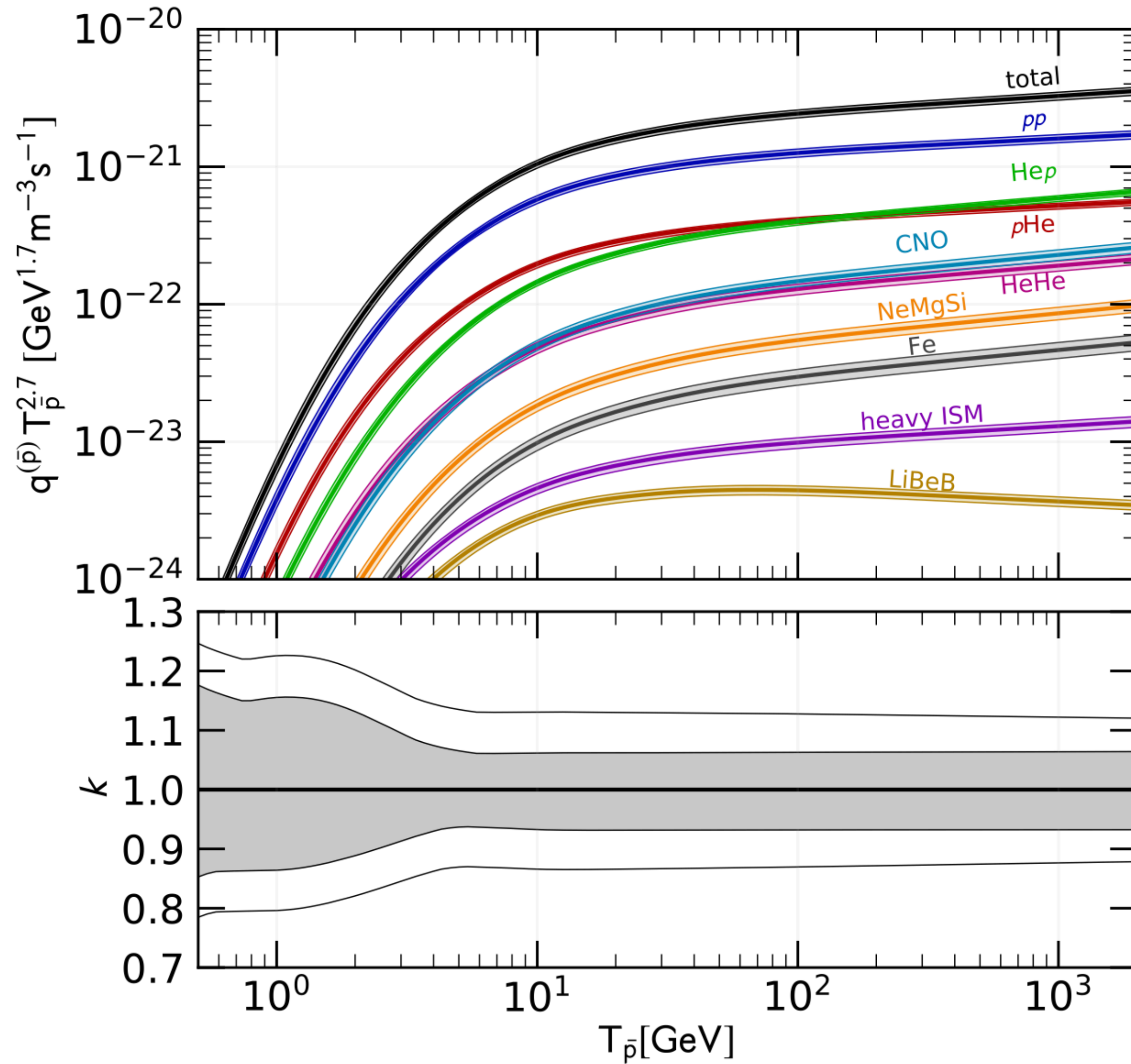
$$\Delta_{\text{IS}} = \frac{c_1^{\text{IS}}}{1 + (s/c_2^{\text{IS}})^{c_3^{\text{IS}}}}$$



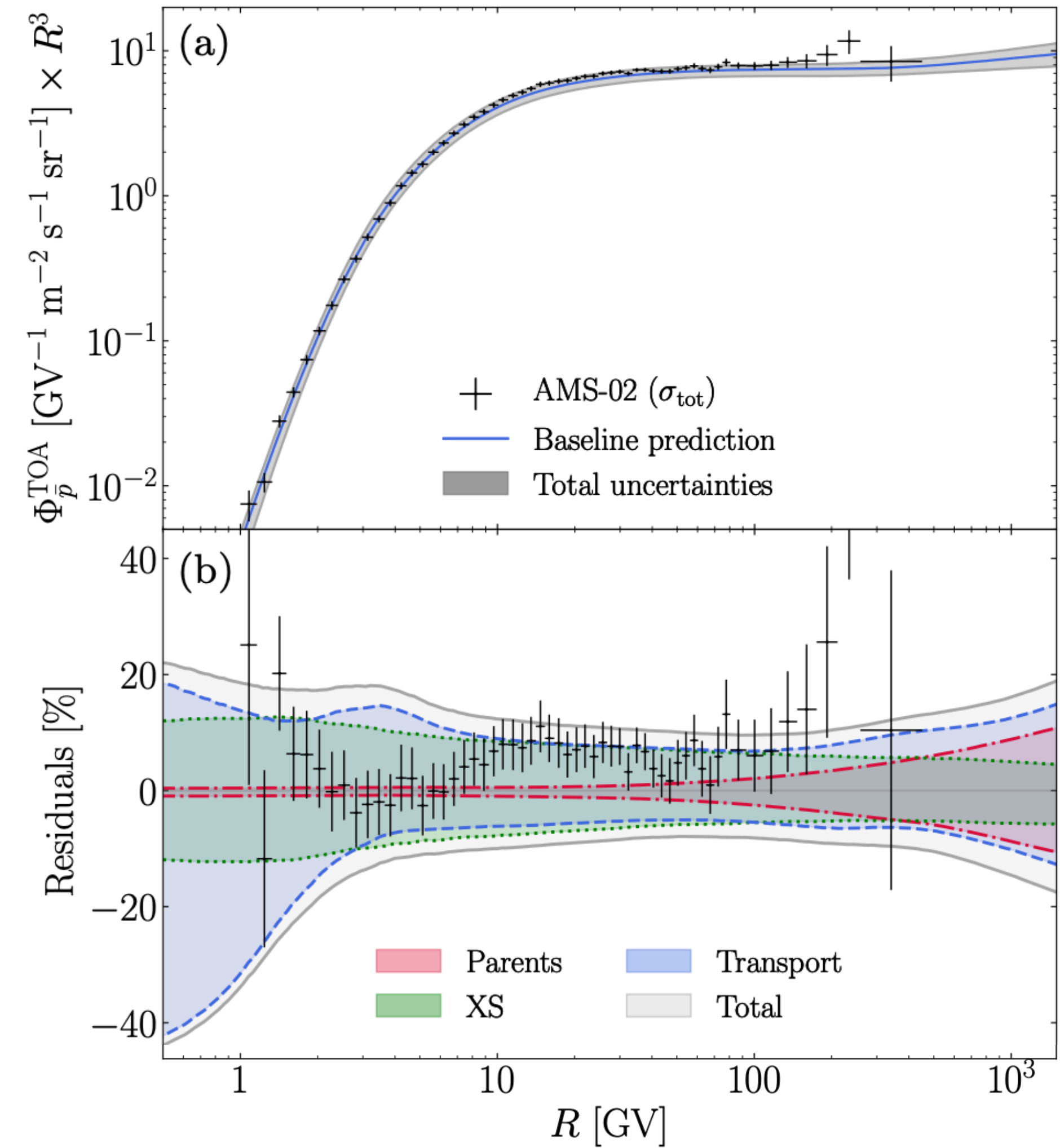
Fischer et al., Heavy Ion
Phys. 17 (2003)



Final uncertainty

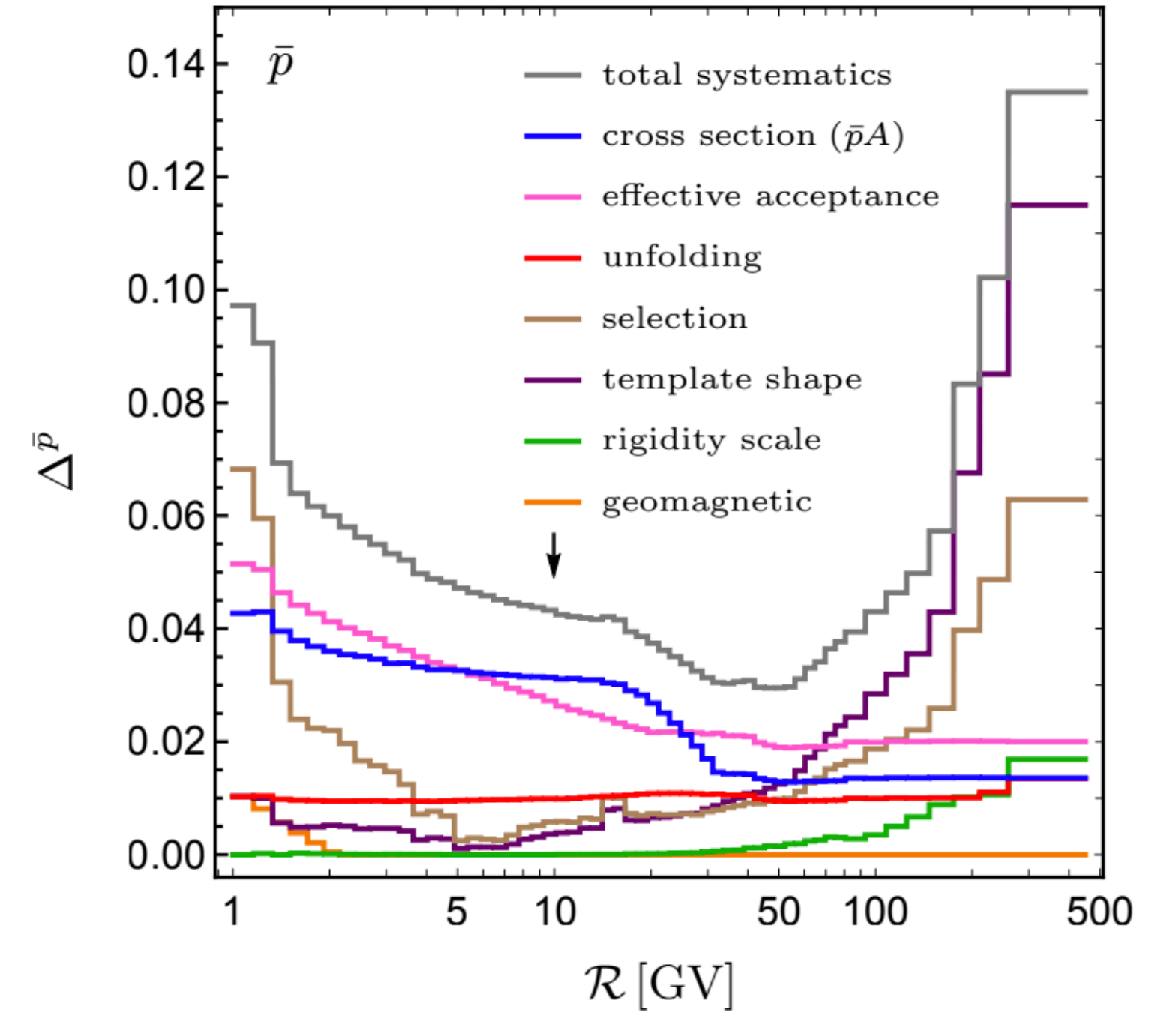
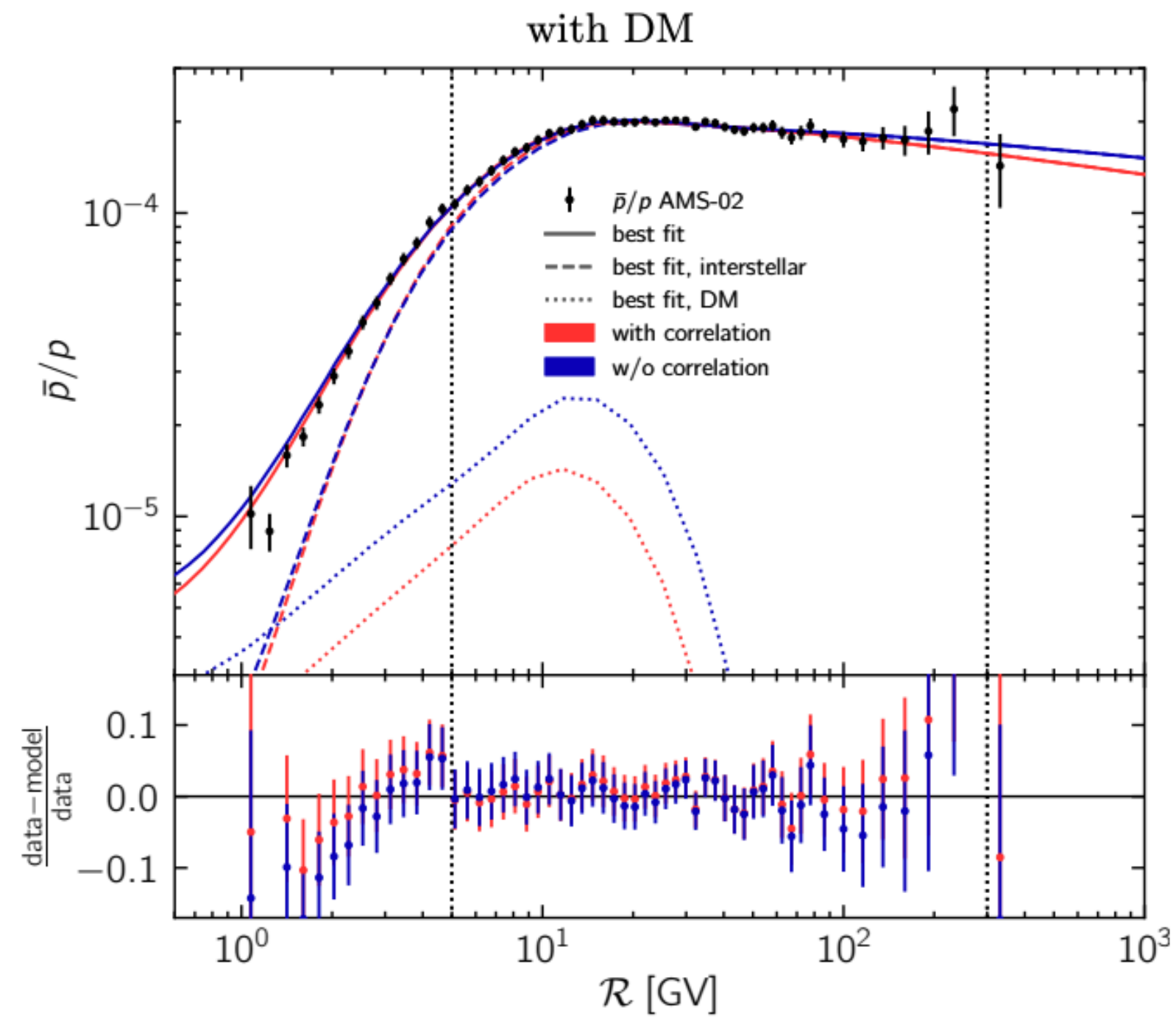
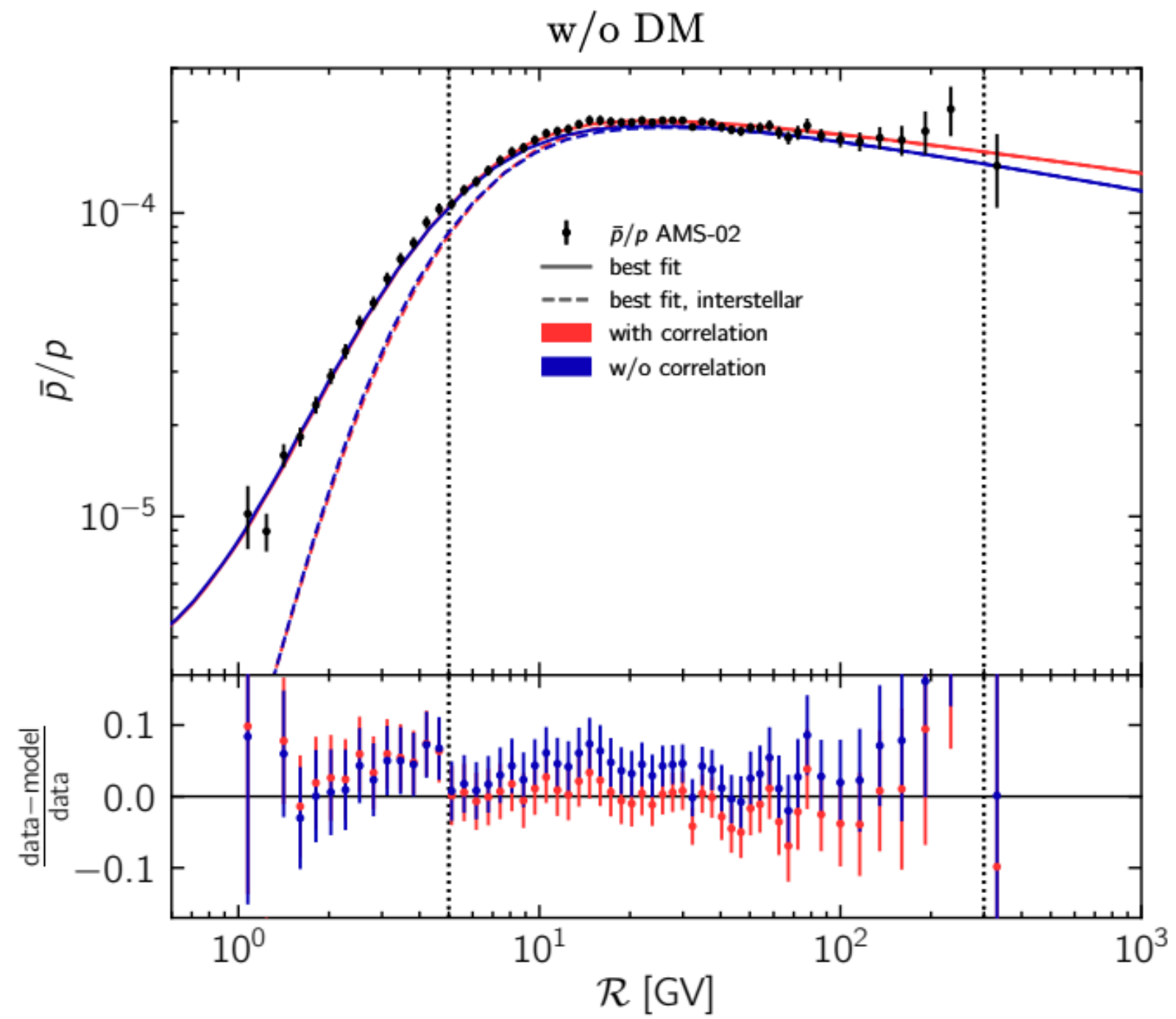


Phys.Rev.D 97 (2018) 10, 103019 Korsmeier, Donato, DM



Phys.Rev.Res. 2 (2020) 2, 023022, 163 Boudaud et al.

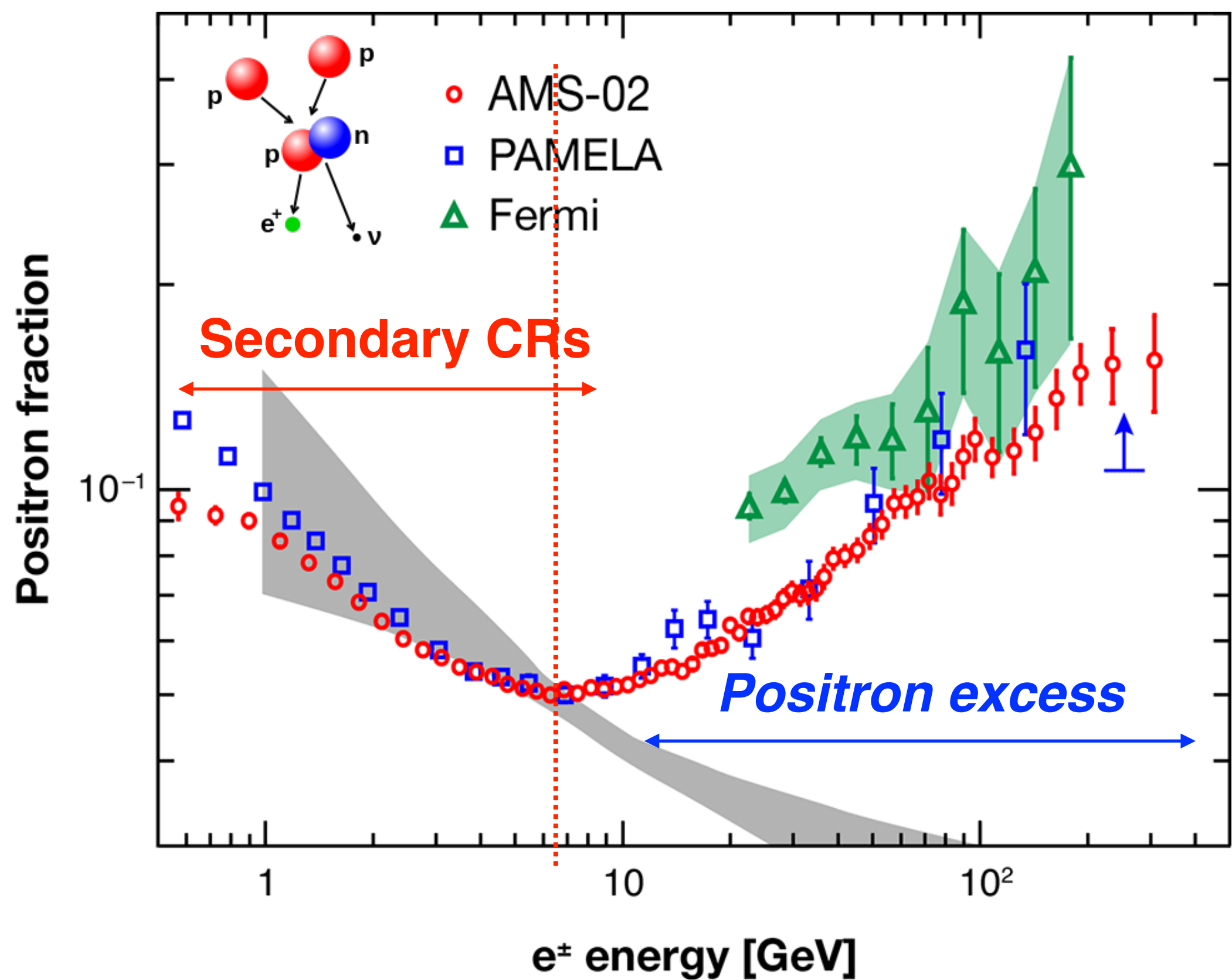
P-bar excess in AMS-02 data



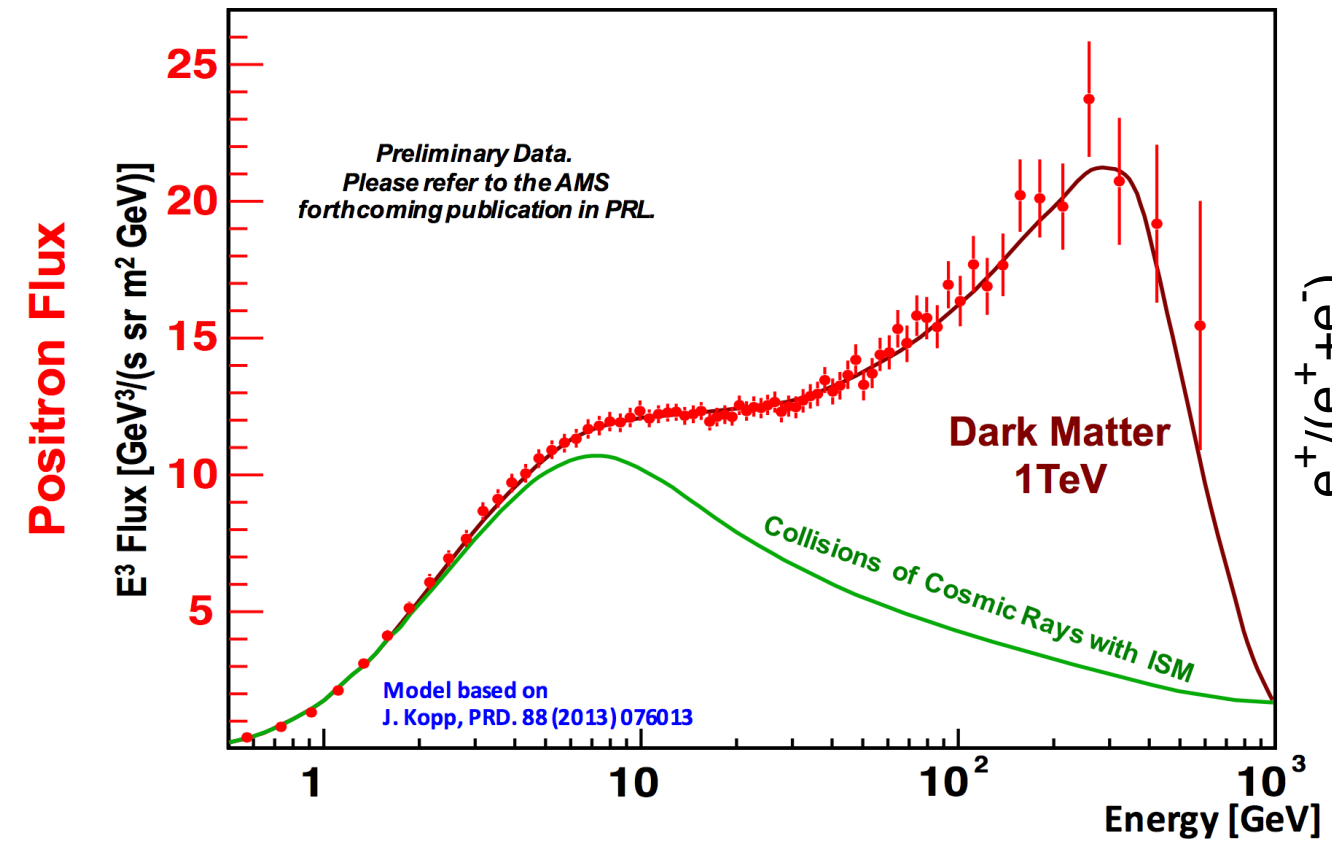
Phys.Rev.Res. 2 (2020) 4, 043017 Heisig et al.

| | | |
|---|--------------|---------------|
| χ_{tot}^2 | 20.3 (27.2) | 233.1 (236.3) |
| No. of fit param. | 16(18) | 16(18) |
| m_{DM} [GeV] | 76 | 66 |
| $\langle \sigma v \rangle$ [10^{-26} cm ³ /s] | 0.91 | 0.74 |
| $\Delta \chi_{\text{tot}}^2$ | 6.9 | 3.2 |
| local sig. | 2.6 σ | 1.8 σ |
| global sig. | 1.8 σ | 0.5 σ |

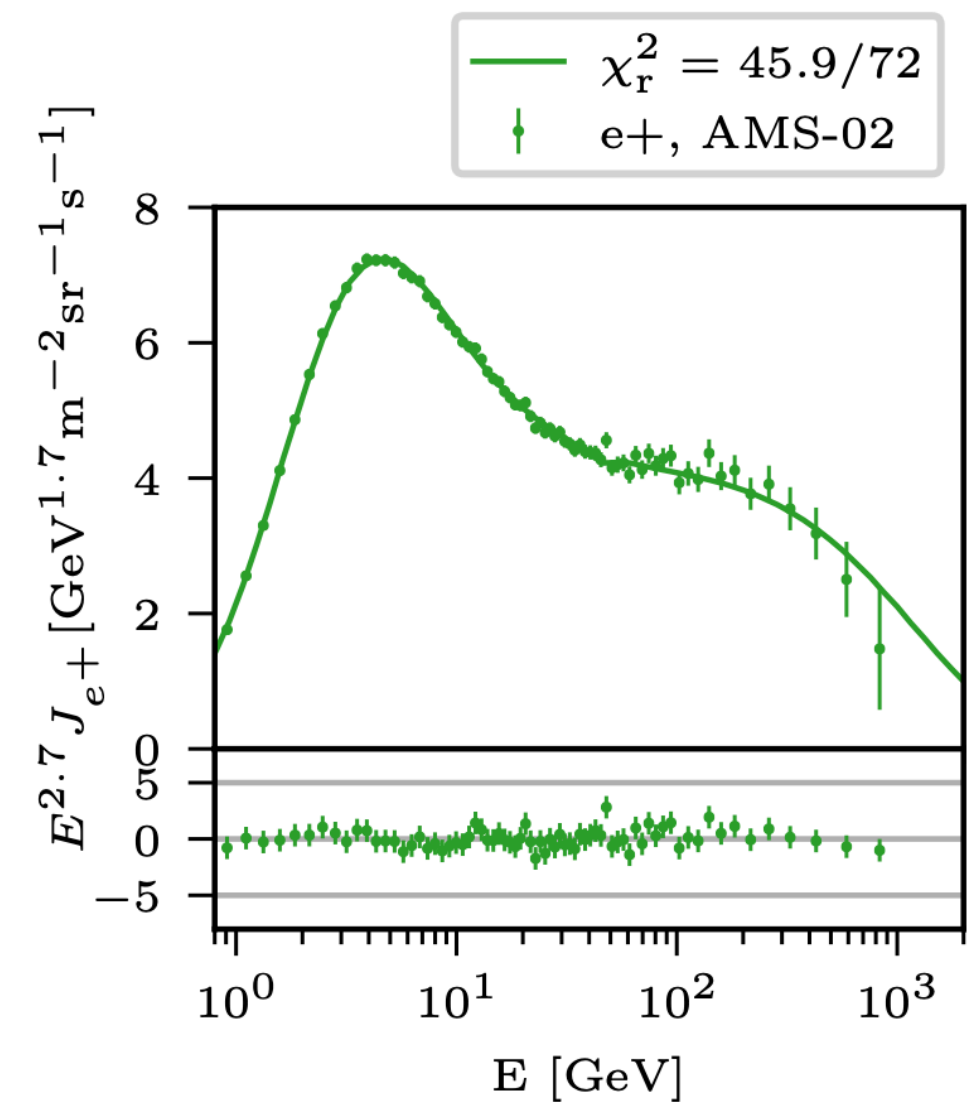
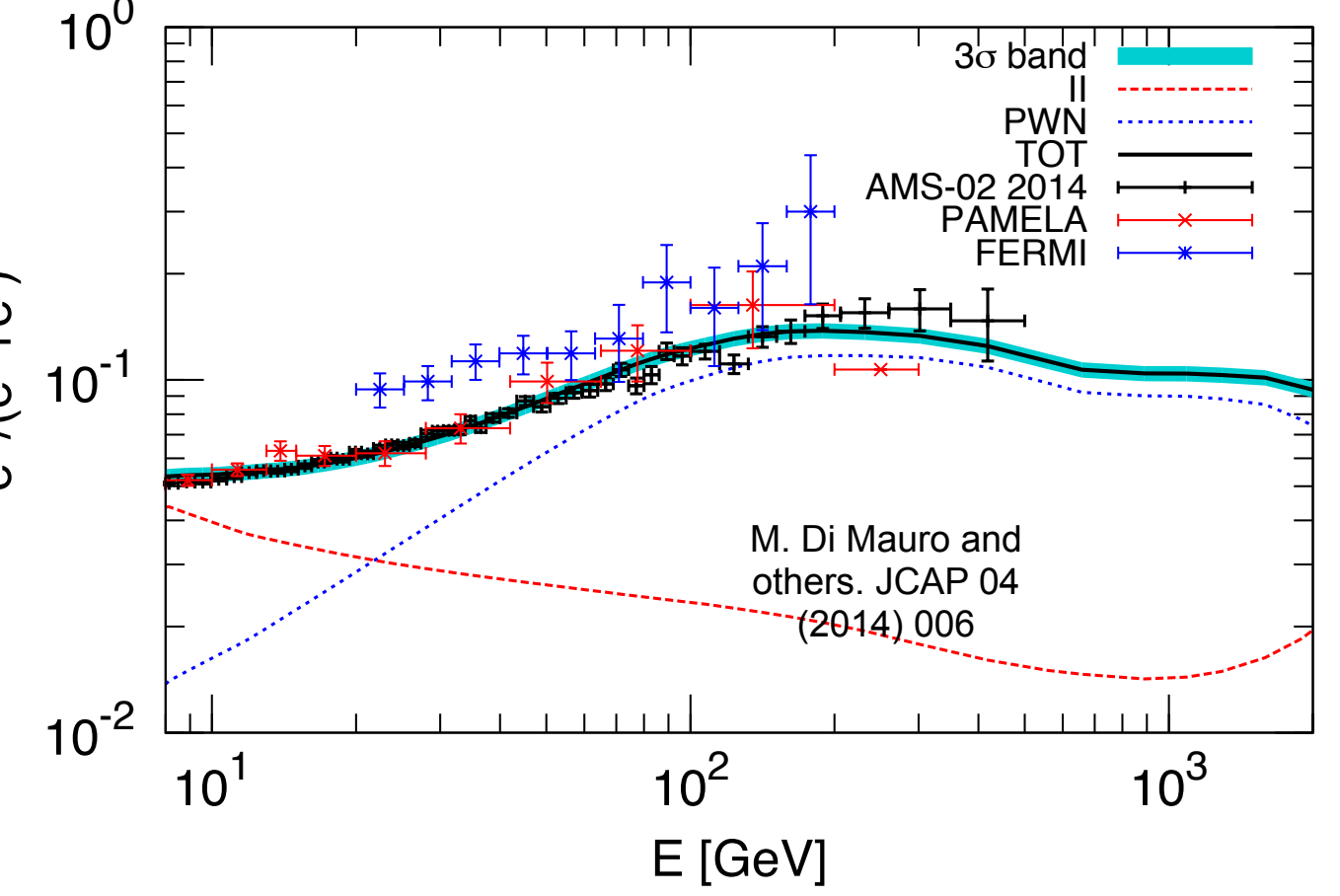
Positron excess interpretations



Dark matter



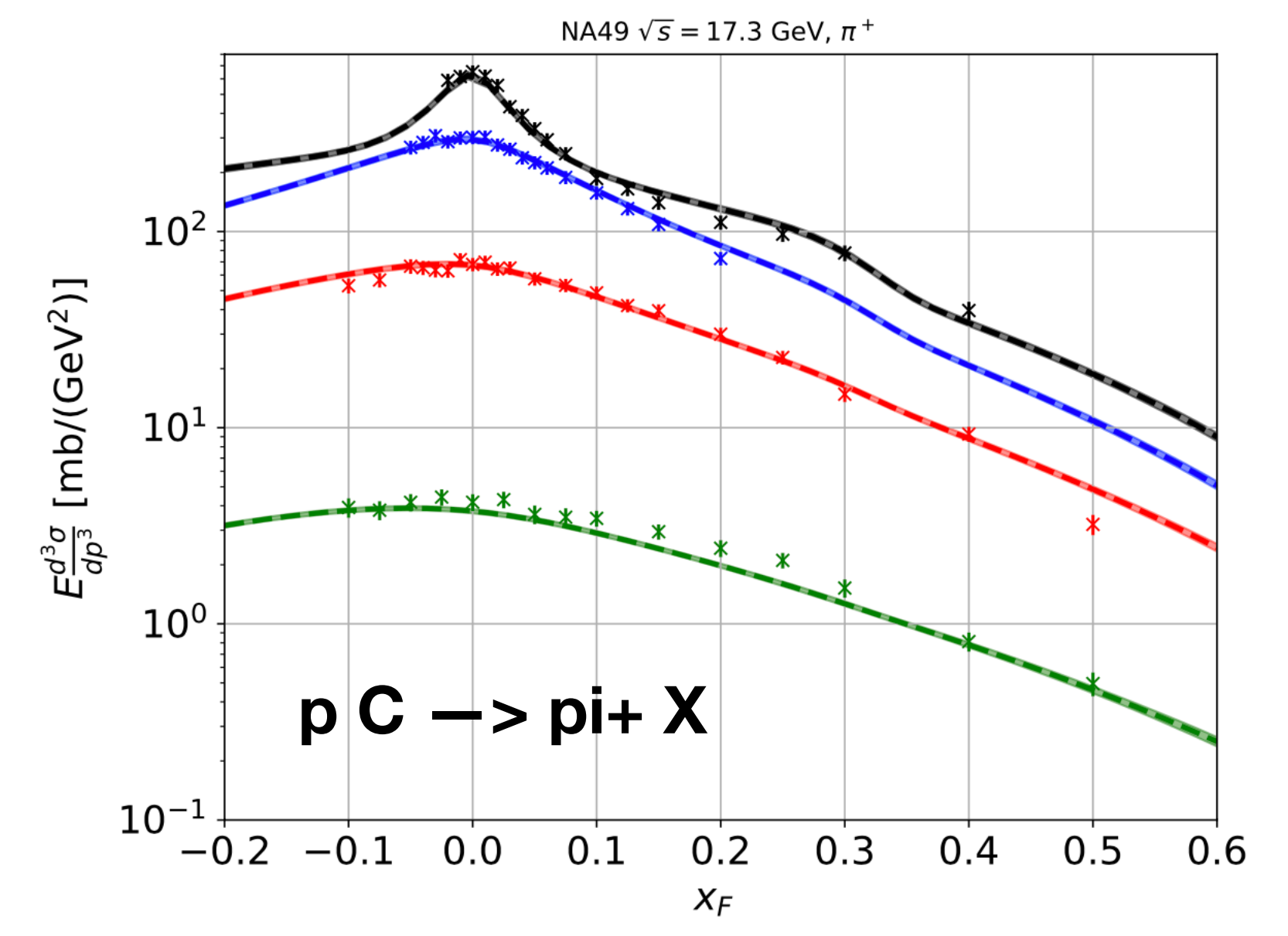
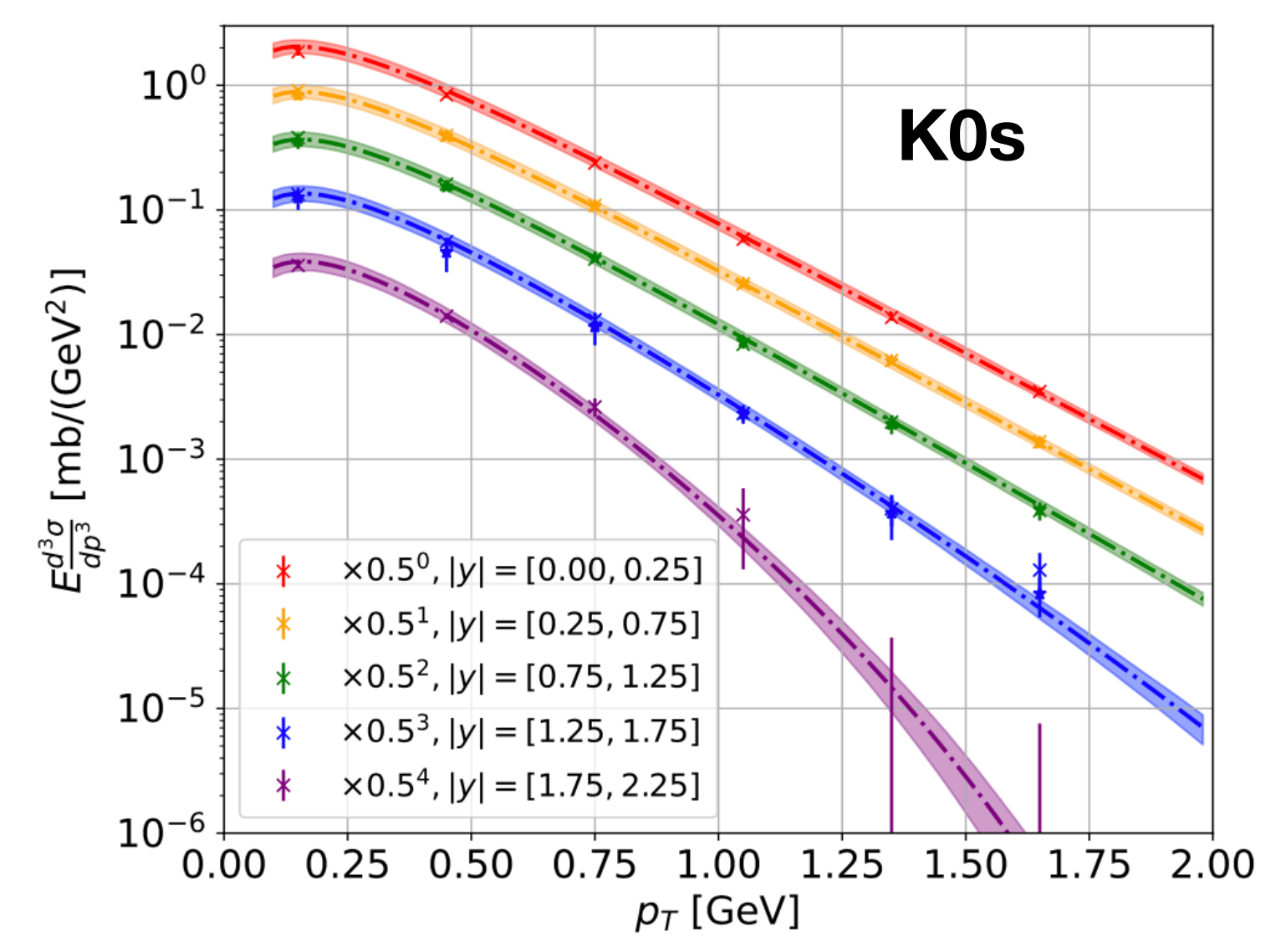
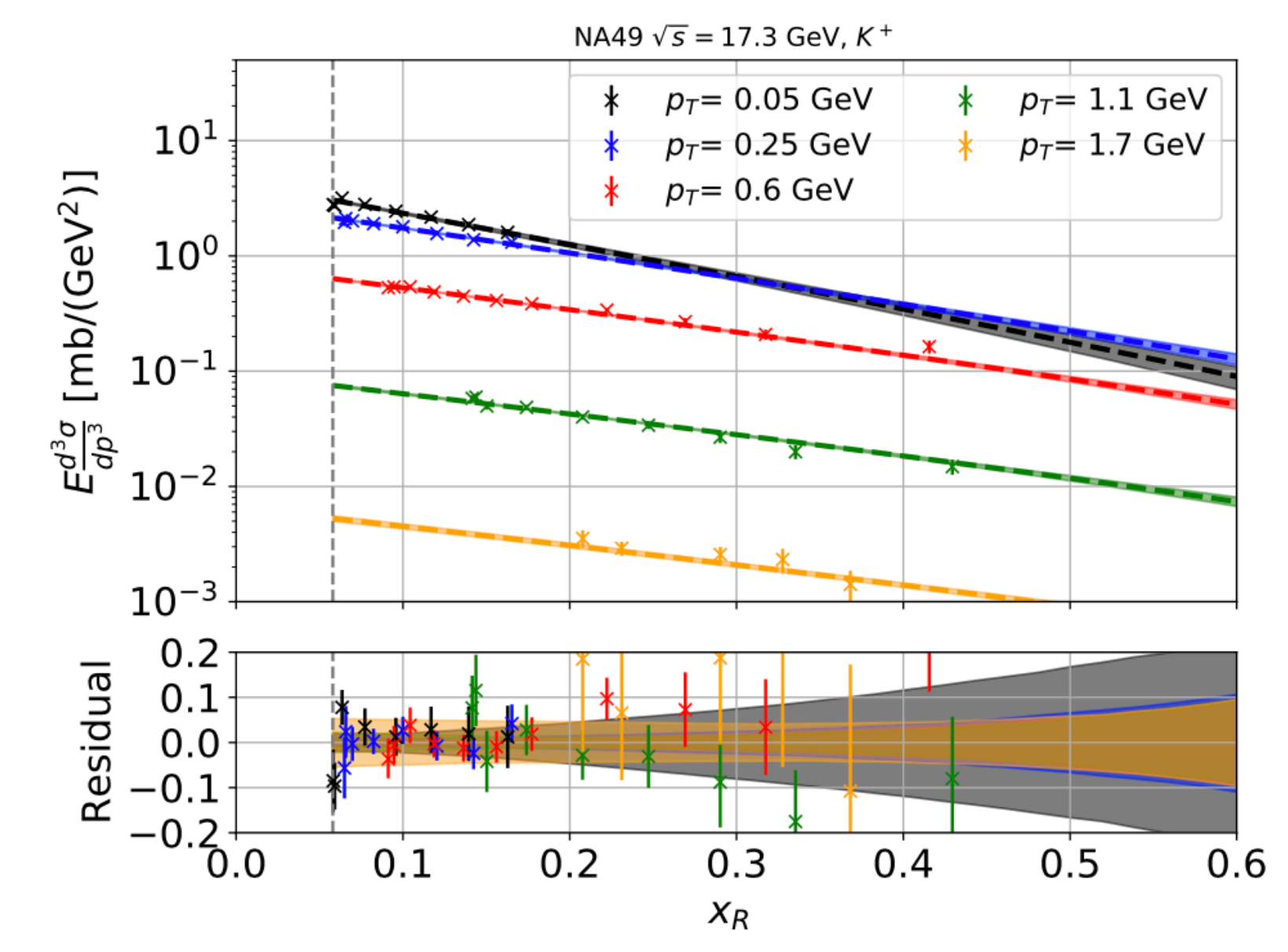
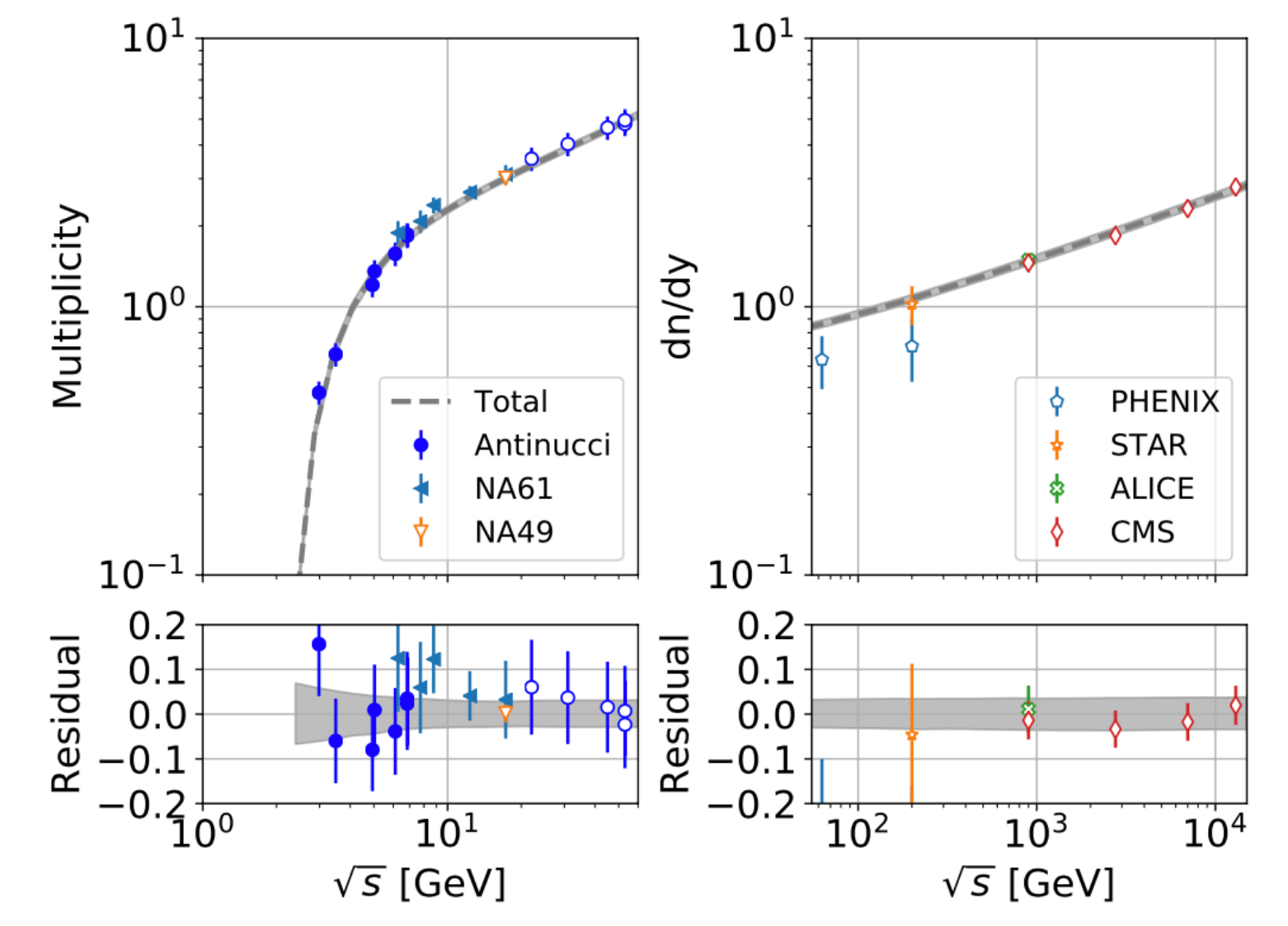
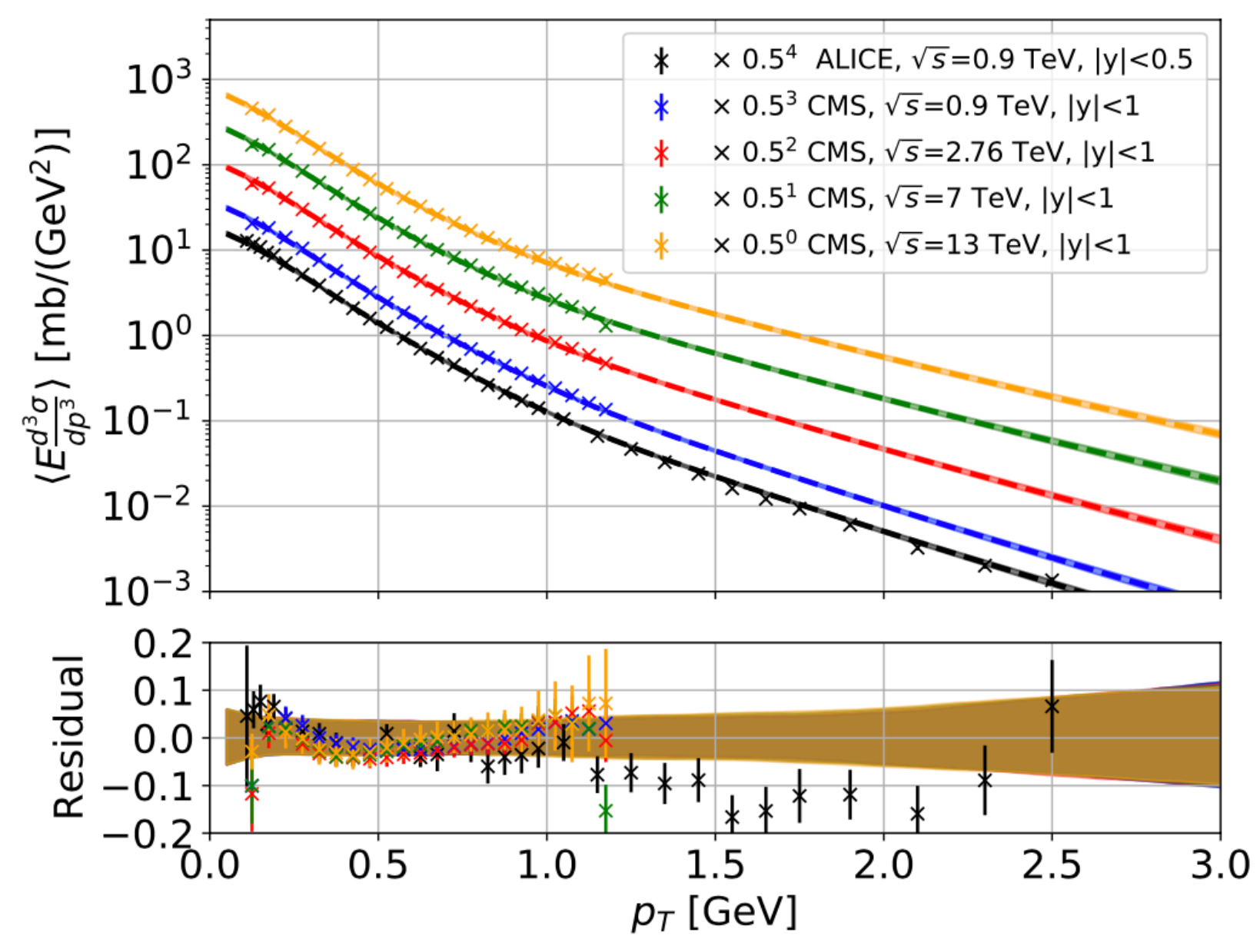
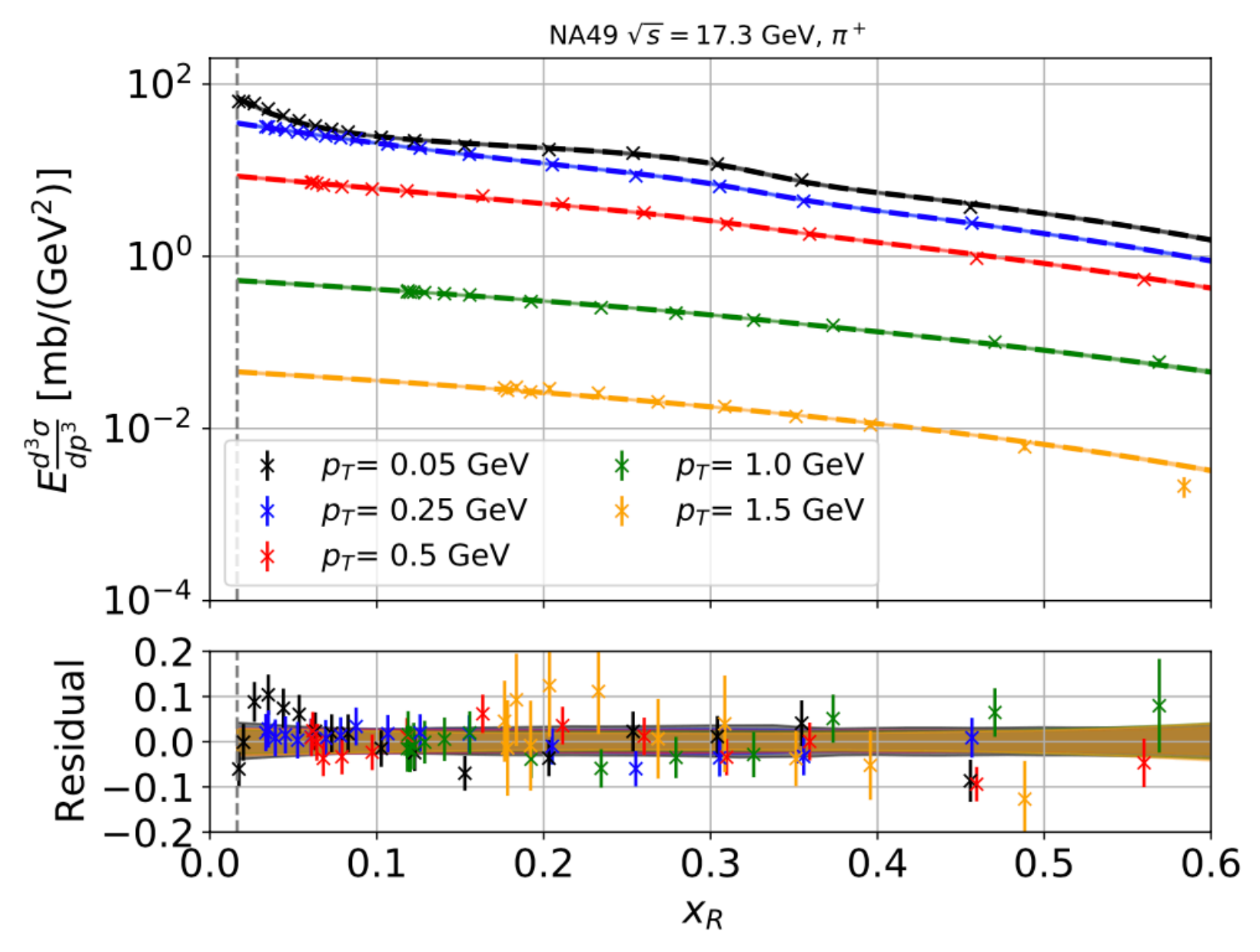
PWNe



Supernova remnants

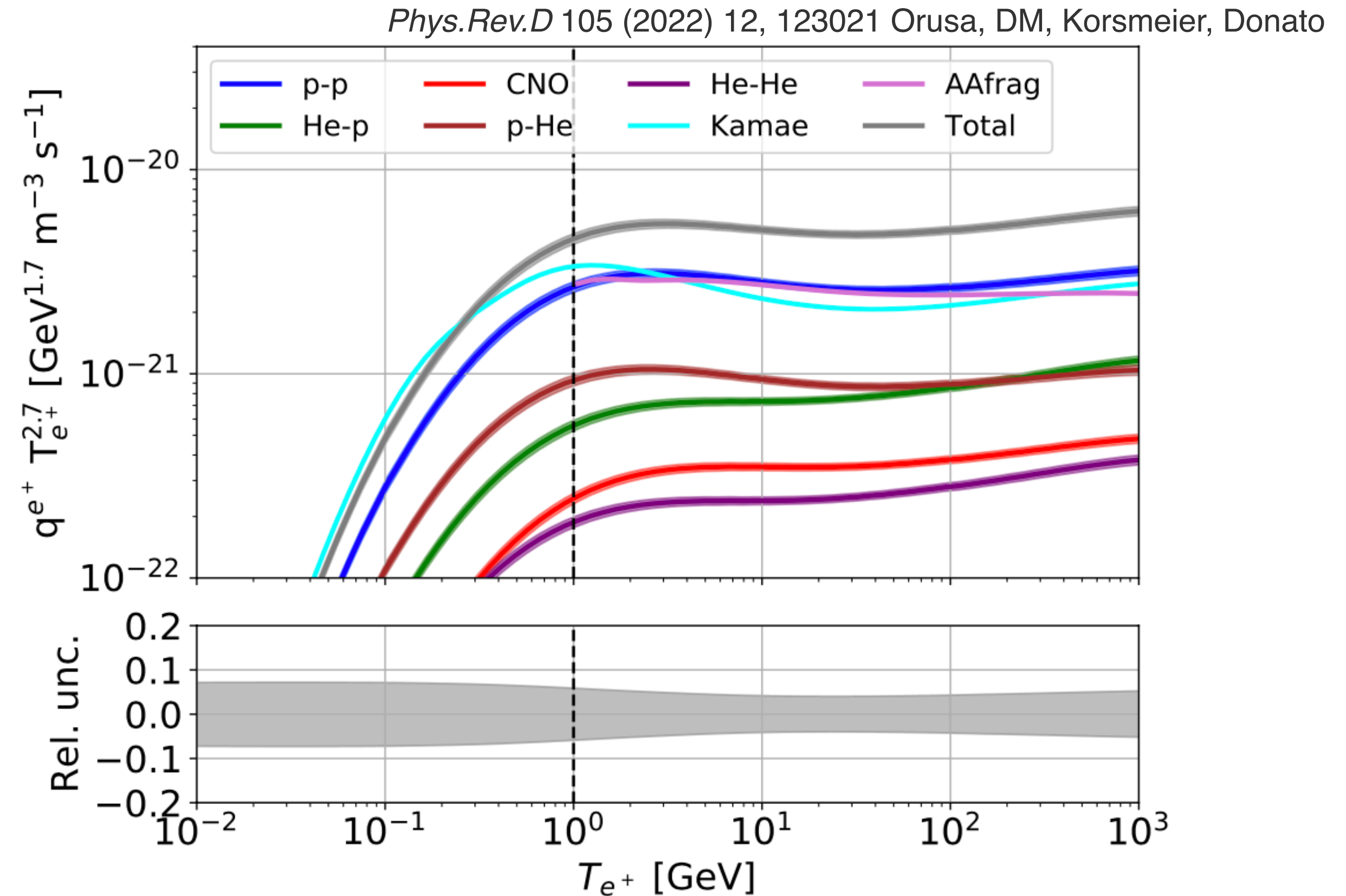
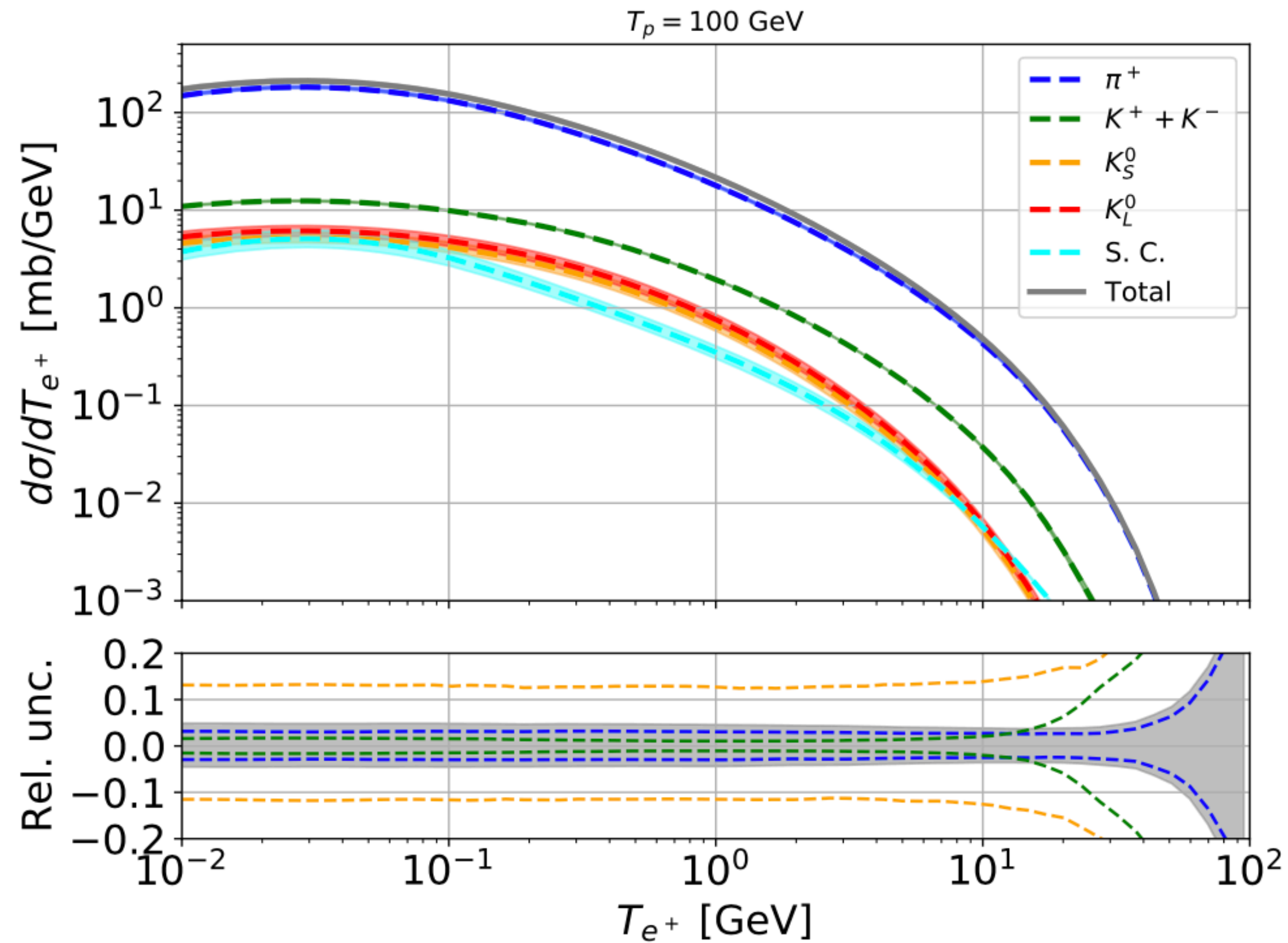
Exact origin of positron excess is still very debated!!

Fit to the data

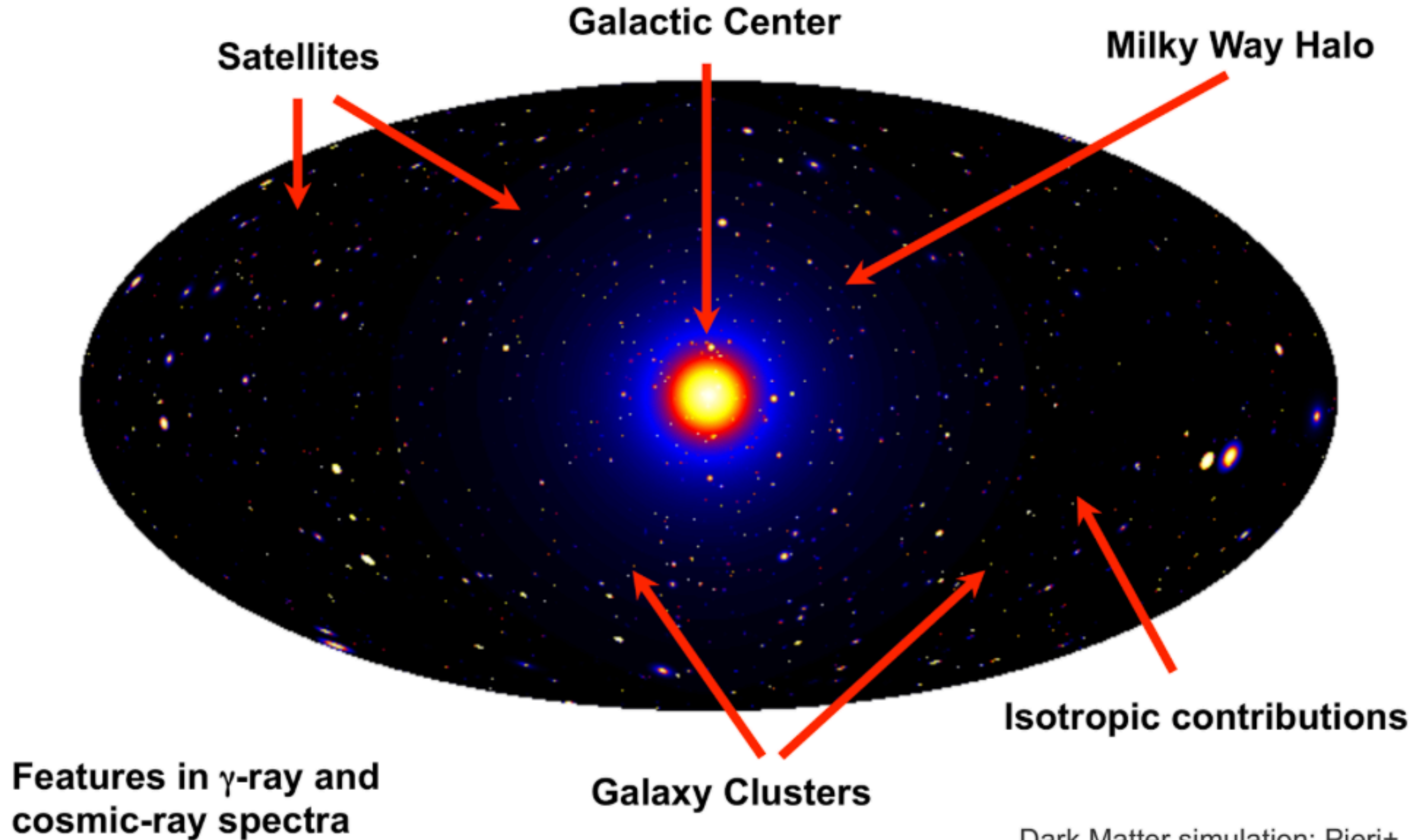


Final uncertainty

- Cross section is predicted from 10 MeV to 10 TeV with an uncertainty of about 5-7% at the energies relevant for AMS-02 positron flux.
- This is currently NOT the main limiting factor for the dark matter search with cosmic-ray positrons.
- The theoretical uncertainties related to the possible pulsar interpretation is much larger.

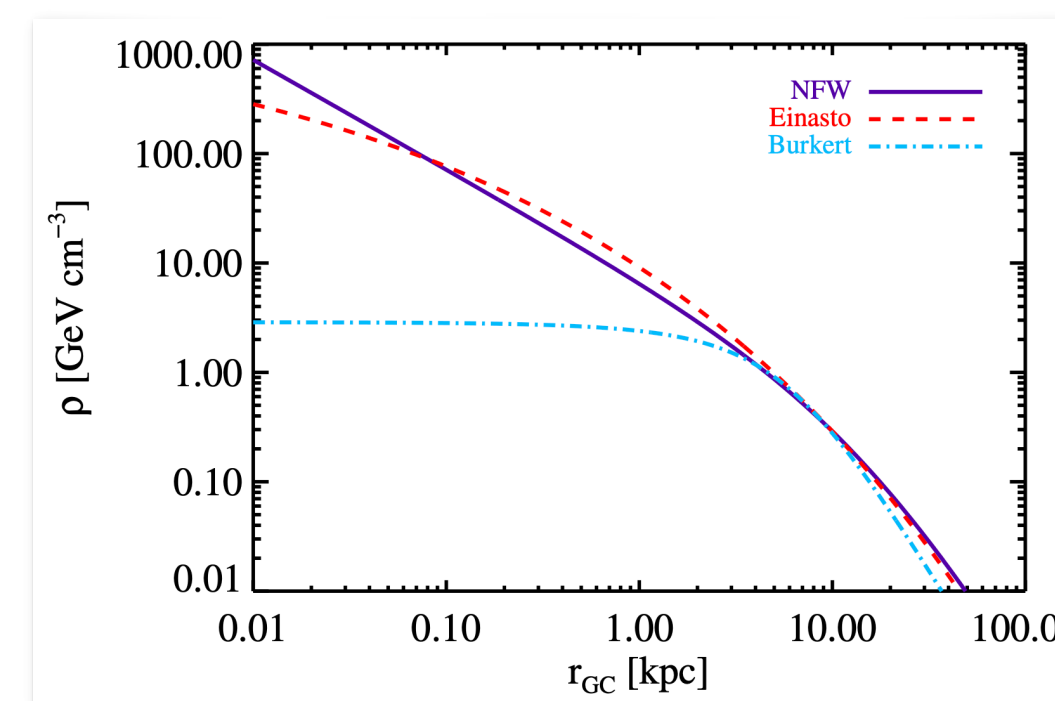
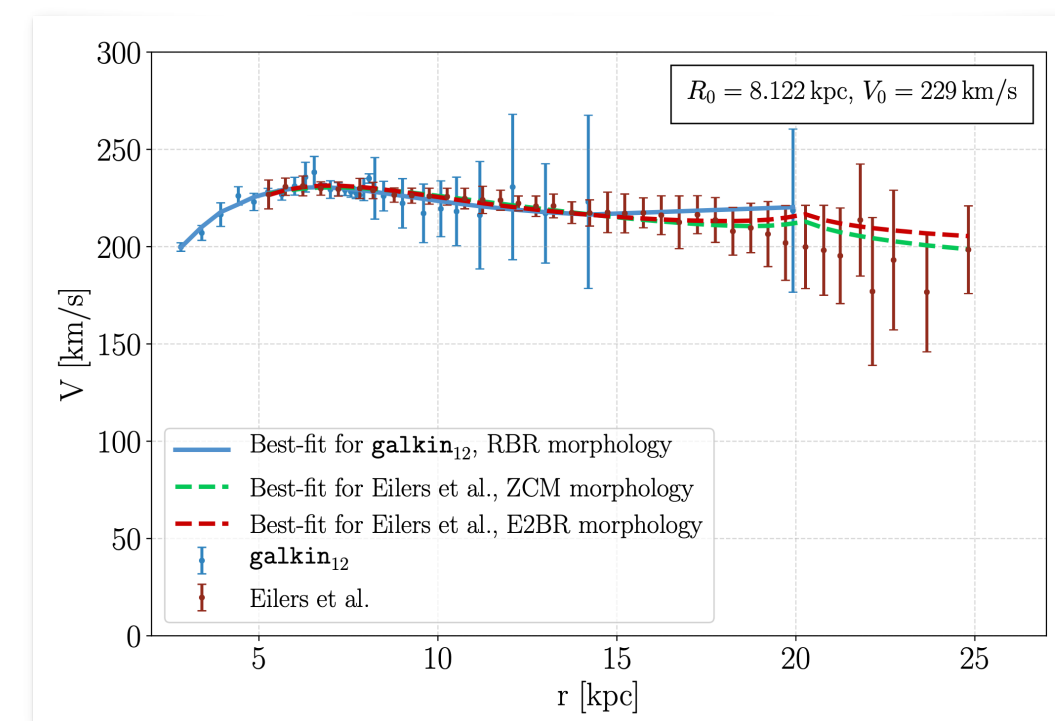
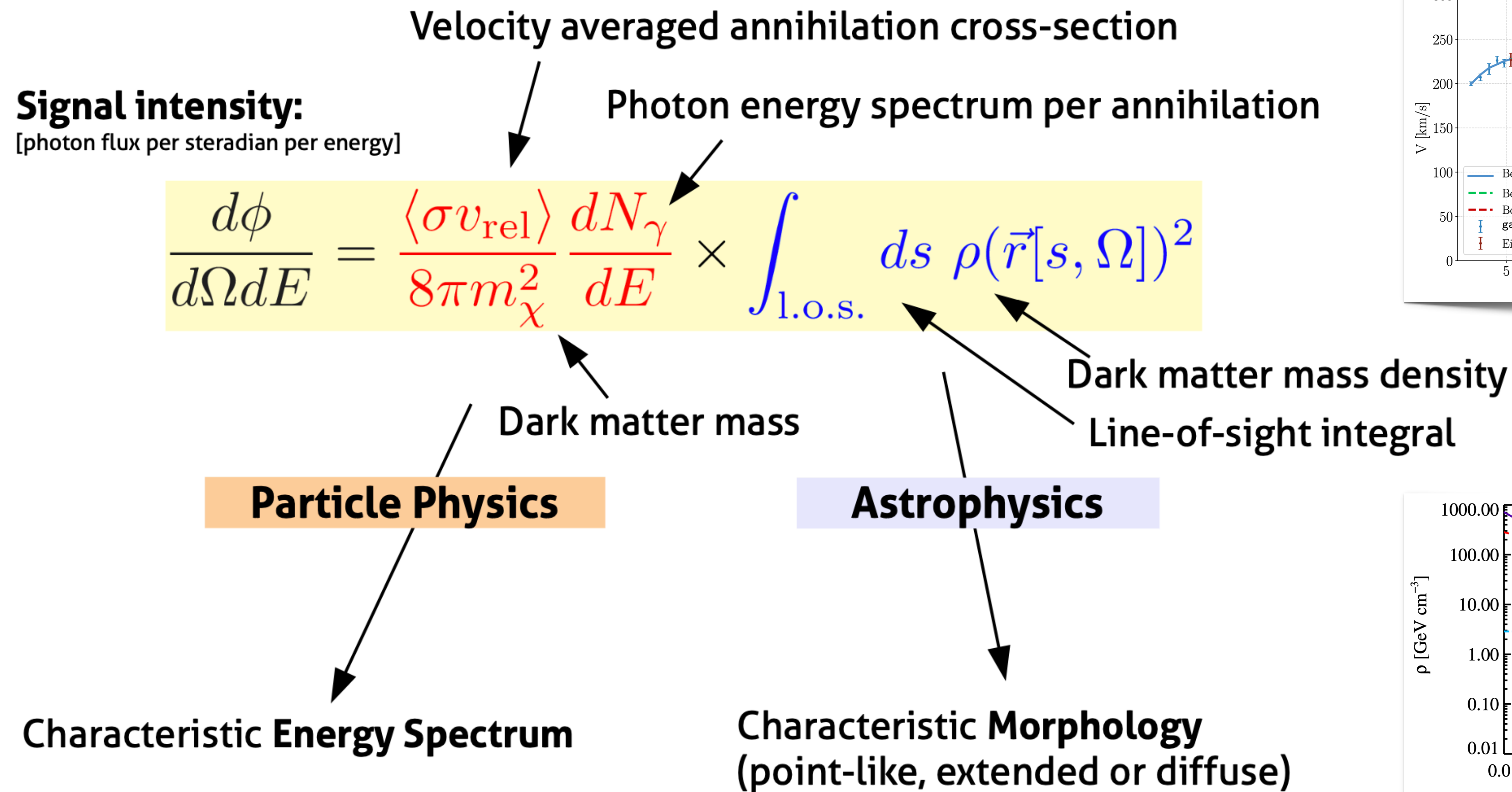


Gamma rays from dark matter annihilation



Dark Matter simulation: Pieri+
[2011PhRvD..83b3518P](#)

Gamma-ray spectrum



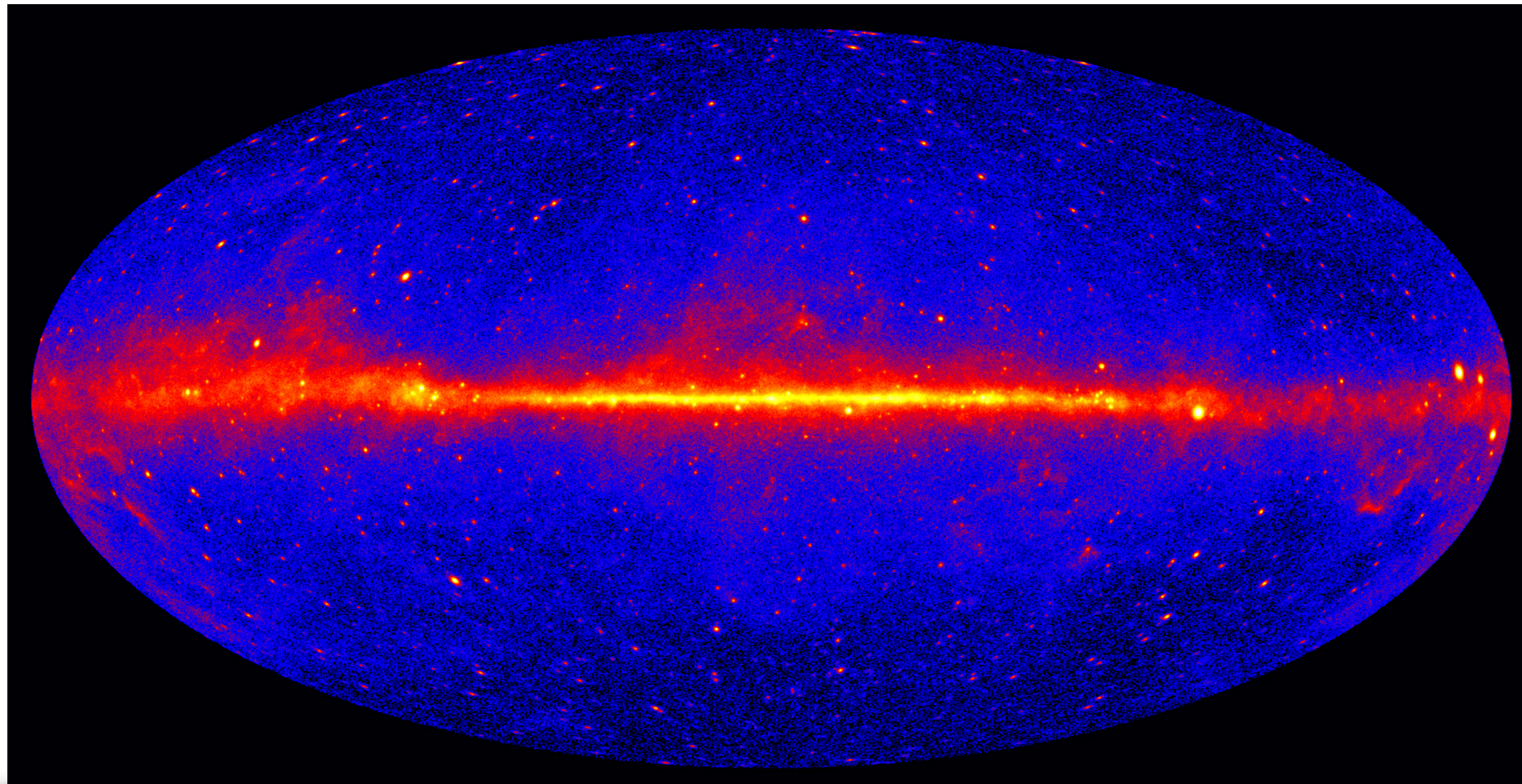
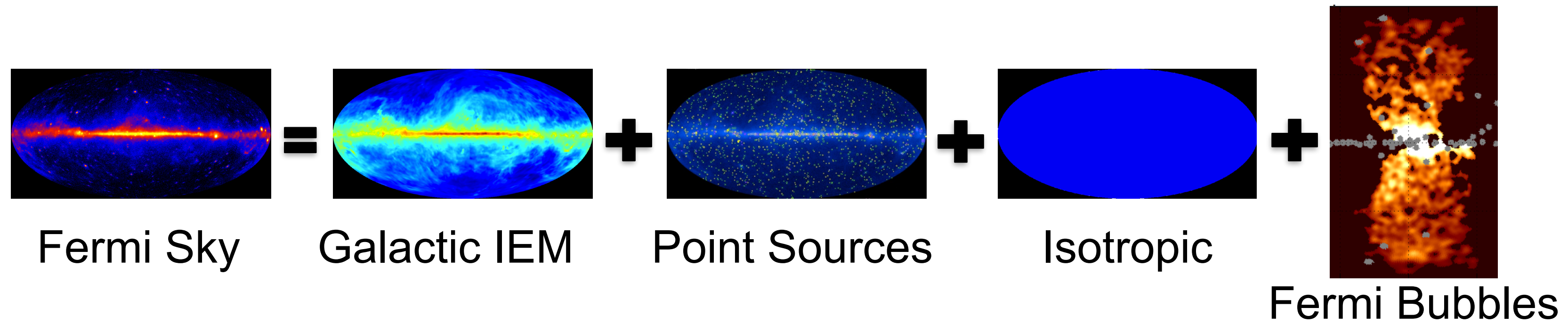
[review DM searches with gamma rays: Bringmann & Weniger (2012)]

It is convenient to define a "J-value":

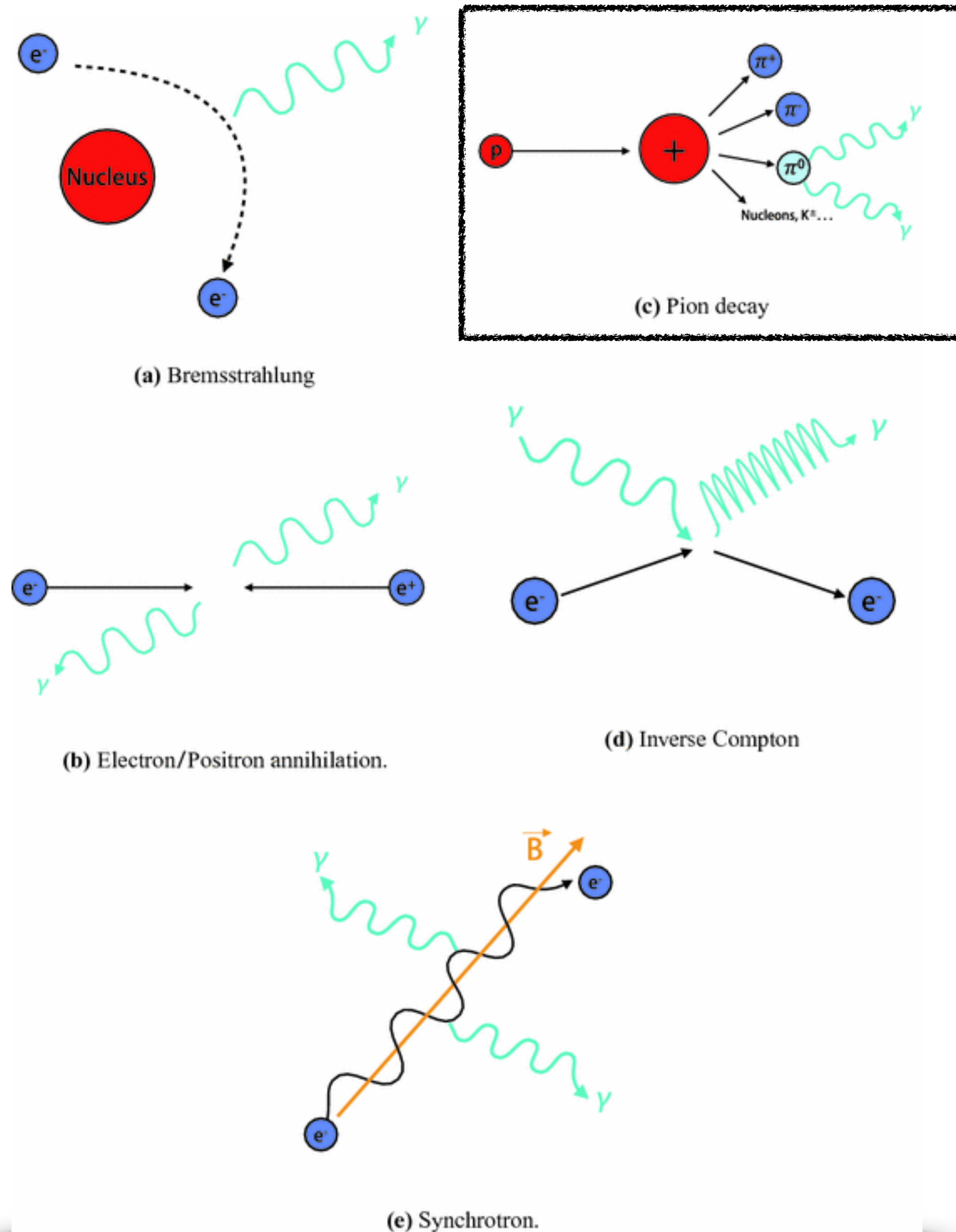
$$J_{\Delta\Omega} \equiv \int_{\Delta\Omega} d\Omega \int_{\text{l.o.s.}} ds \rho(r[s, \vec{\Omega}])^2$$

<https://github.com/ajueid/CosmiXs> DM spectra

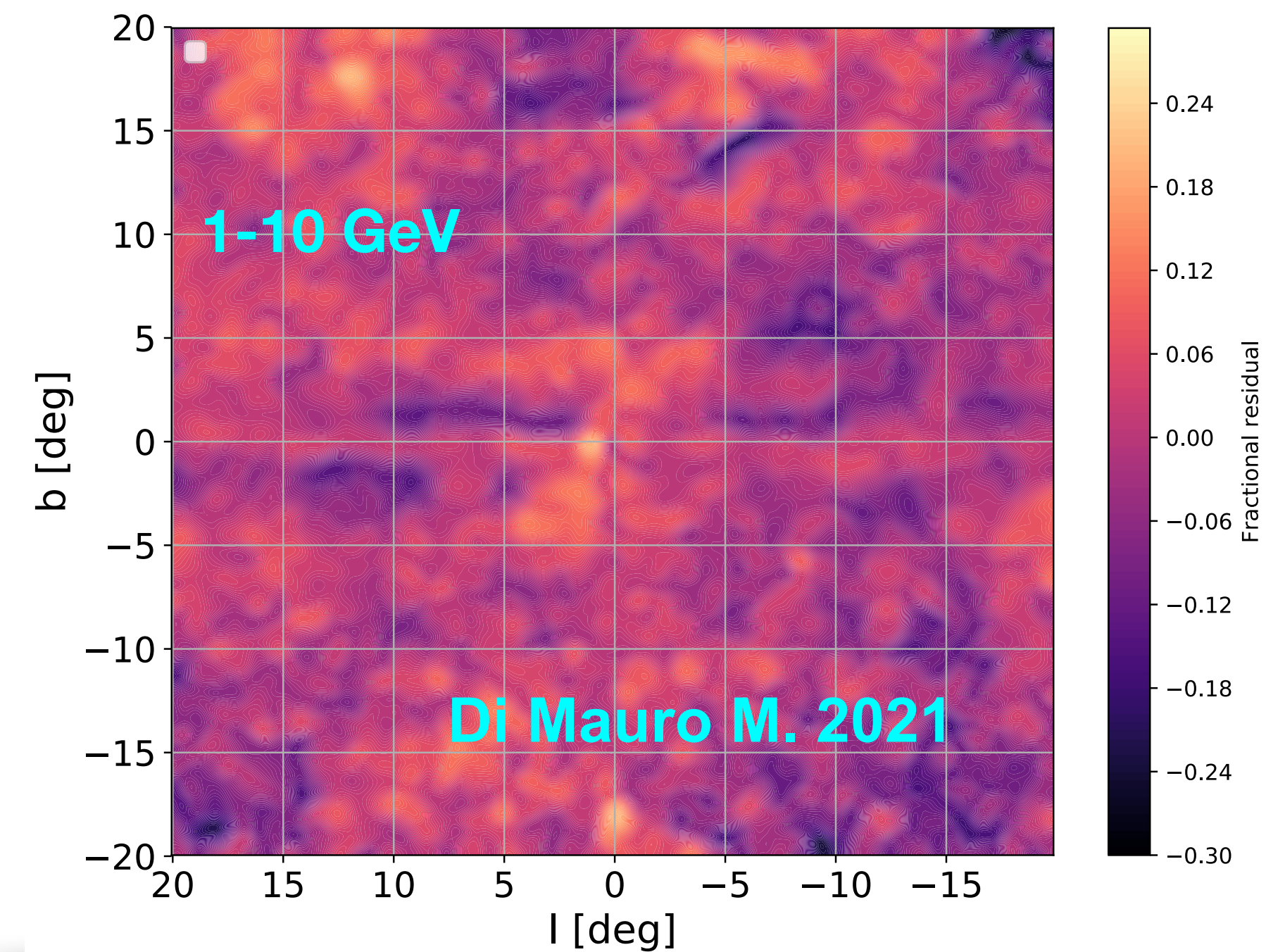
Standard picture for gamma-ray analysis



Galactic interstellar emission



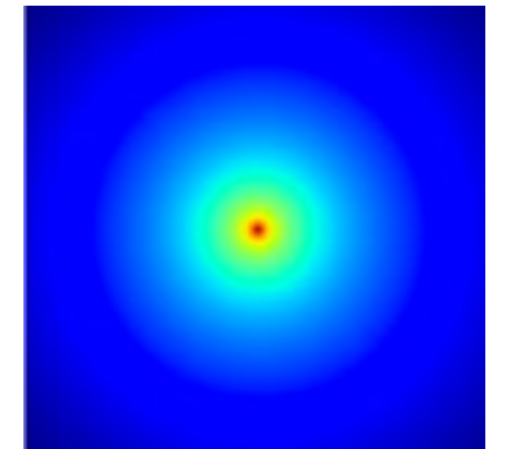
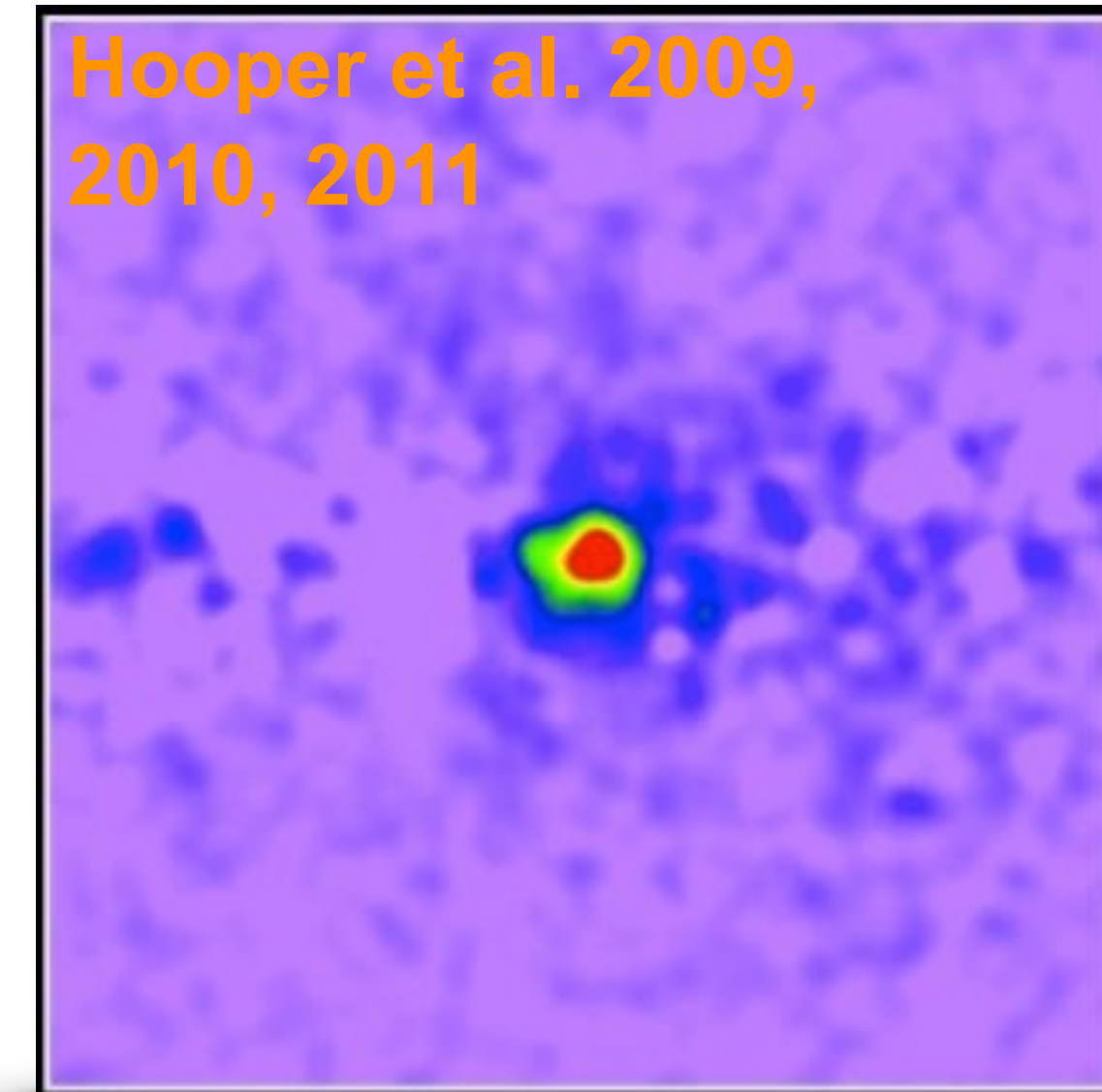
- The models usually used are divided into:
 - Bremsstrahlung*, π^0 , *ICS*, *isotropic component*, *Sun/Moon/Loop I* and the *Fermi bubbles*.
- The residuals are roughly at the level of 20-25% of the data.



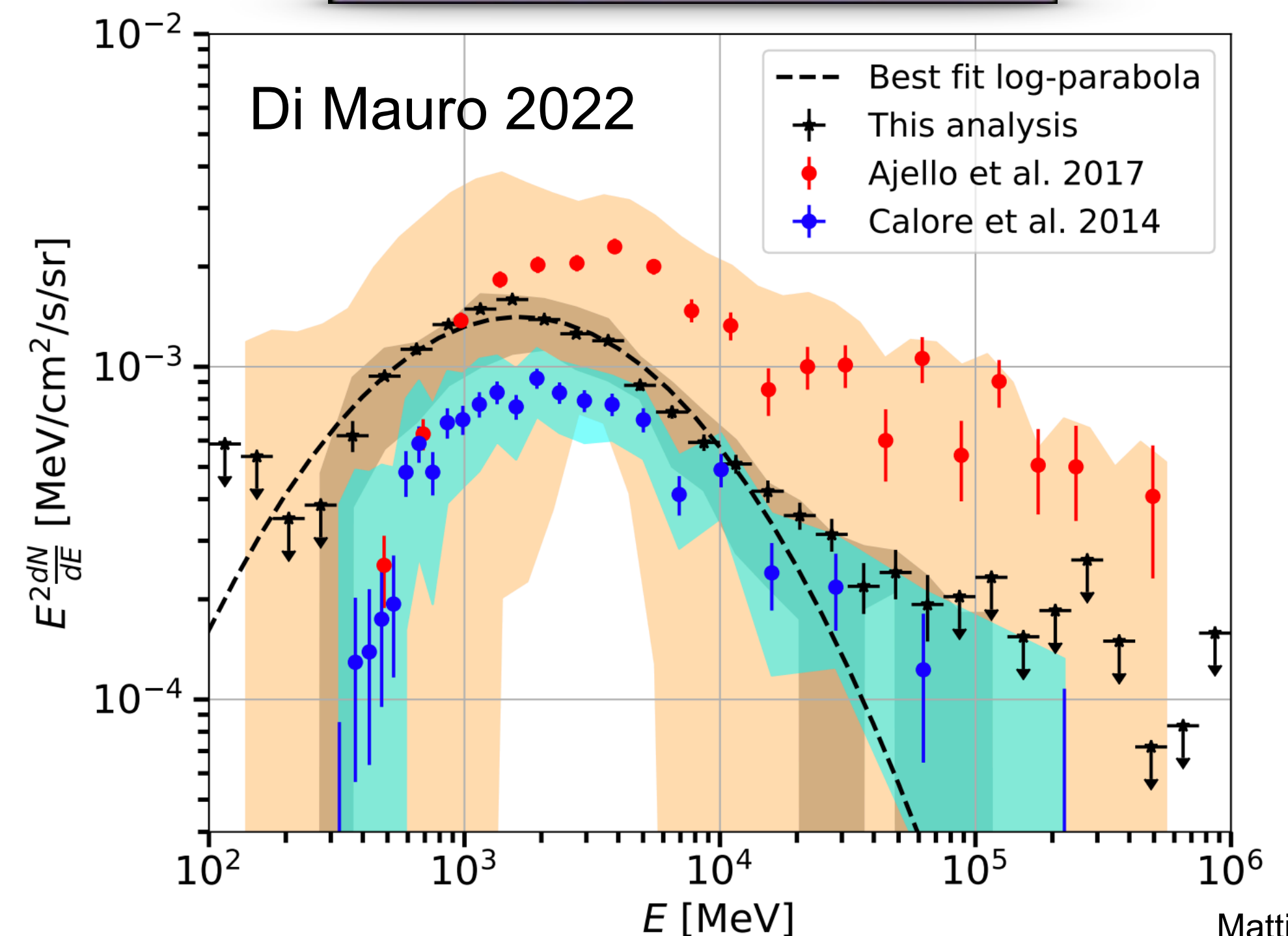
The GeV Excess in the Galactic Center (GCE)

- **Bright** and highly significant.
- **Spatially symmetric** around the Galactic center: $dN/dV \propto r^{-2.5} \rightarrow$ compatible with a gNFW profile.
- **Energy spectrum peaked at a few GeV** \rightarrow DM annihilating into a bottom-anti-bottom ($b\bar{b}$) $M_{DM}=40$ GeV.
- **Annihilation cross section** roughly equal to the thermal cross section is needed.

The properties of the GCE depend on the choice of the interstellar emission model.

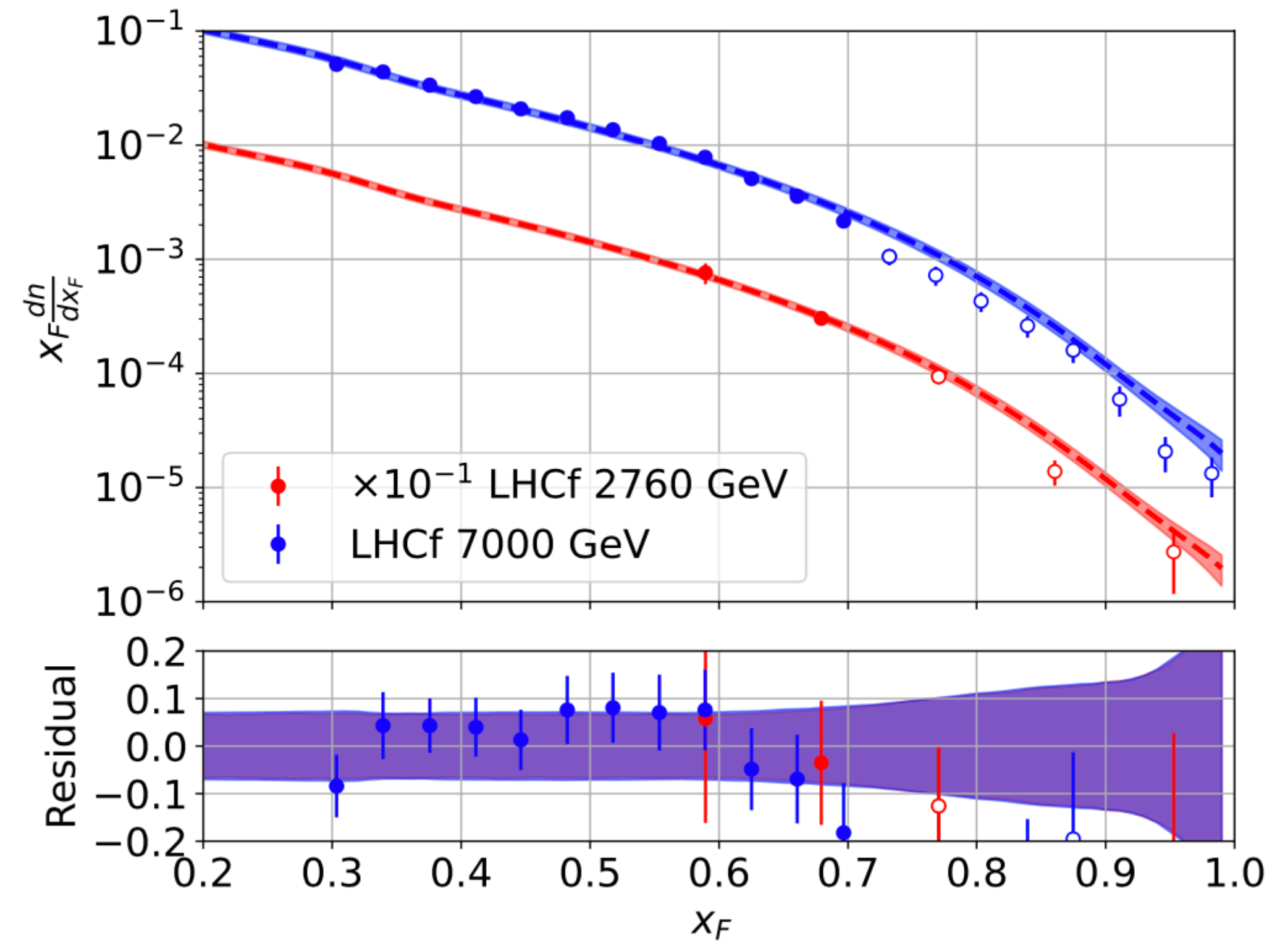
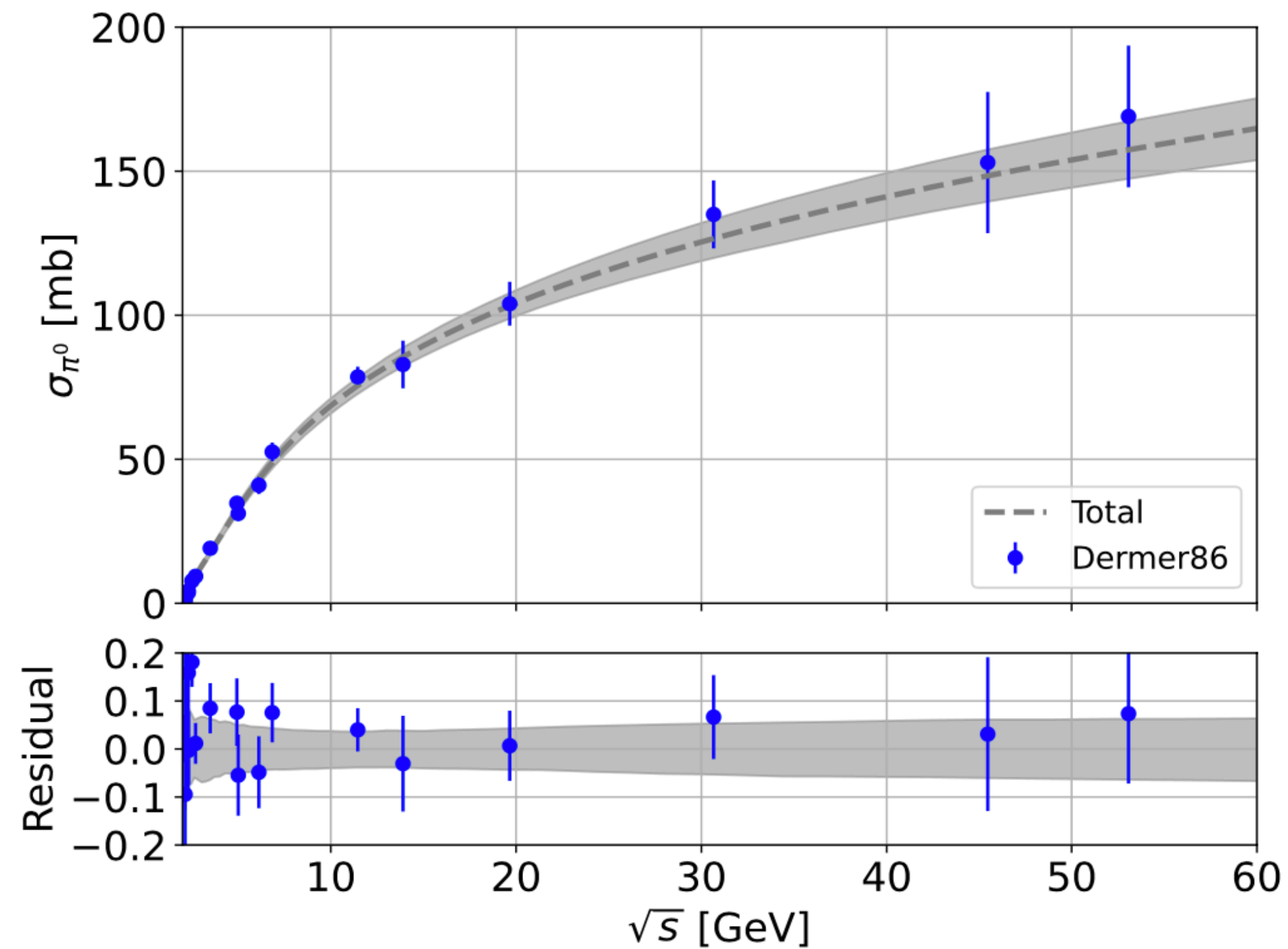


DM



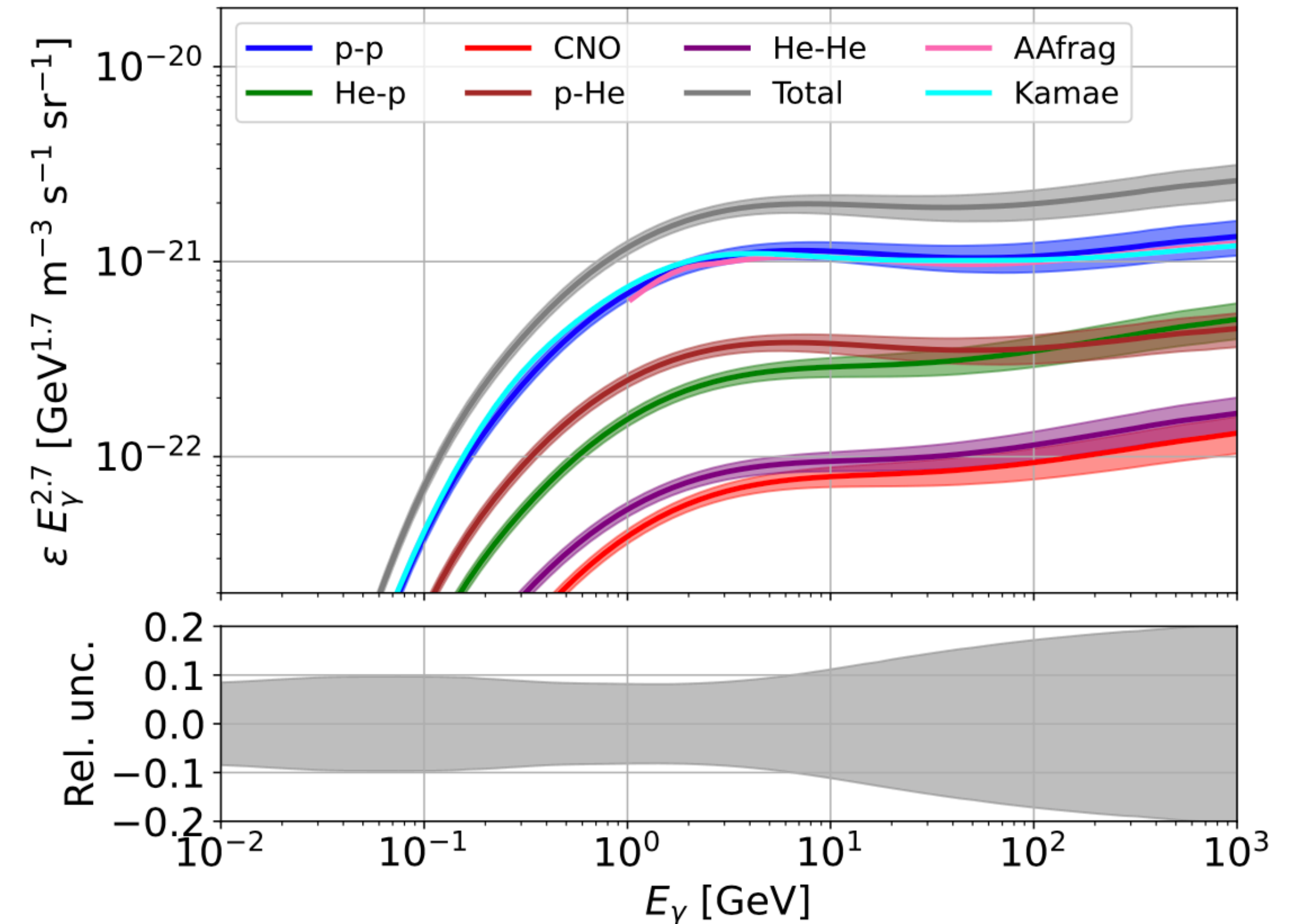
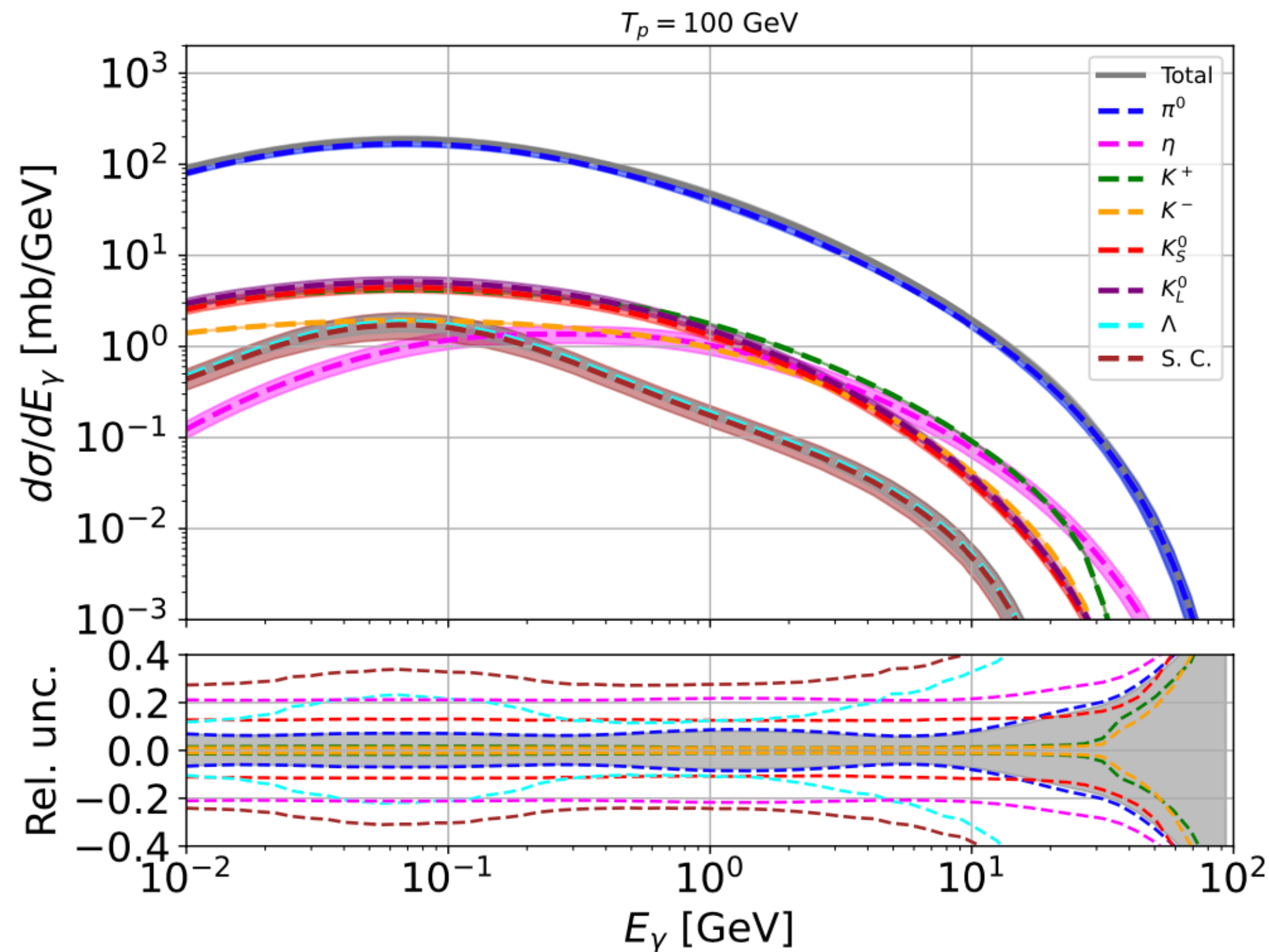
Fit to existing data

- We use an average of the production cross section of charged pions.
- We fit this average to multiplicity and LHCf data.
- *Future measurements on the double differential cross section are needed to confirm our findings.*



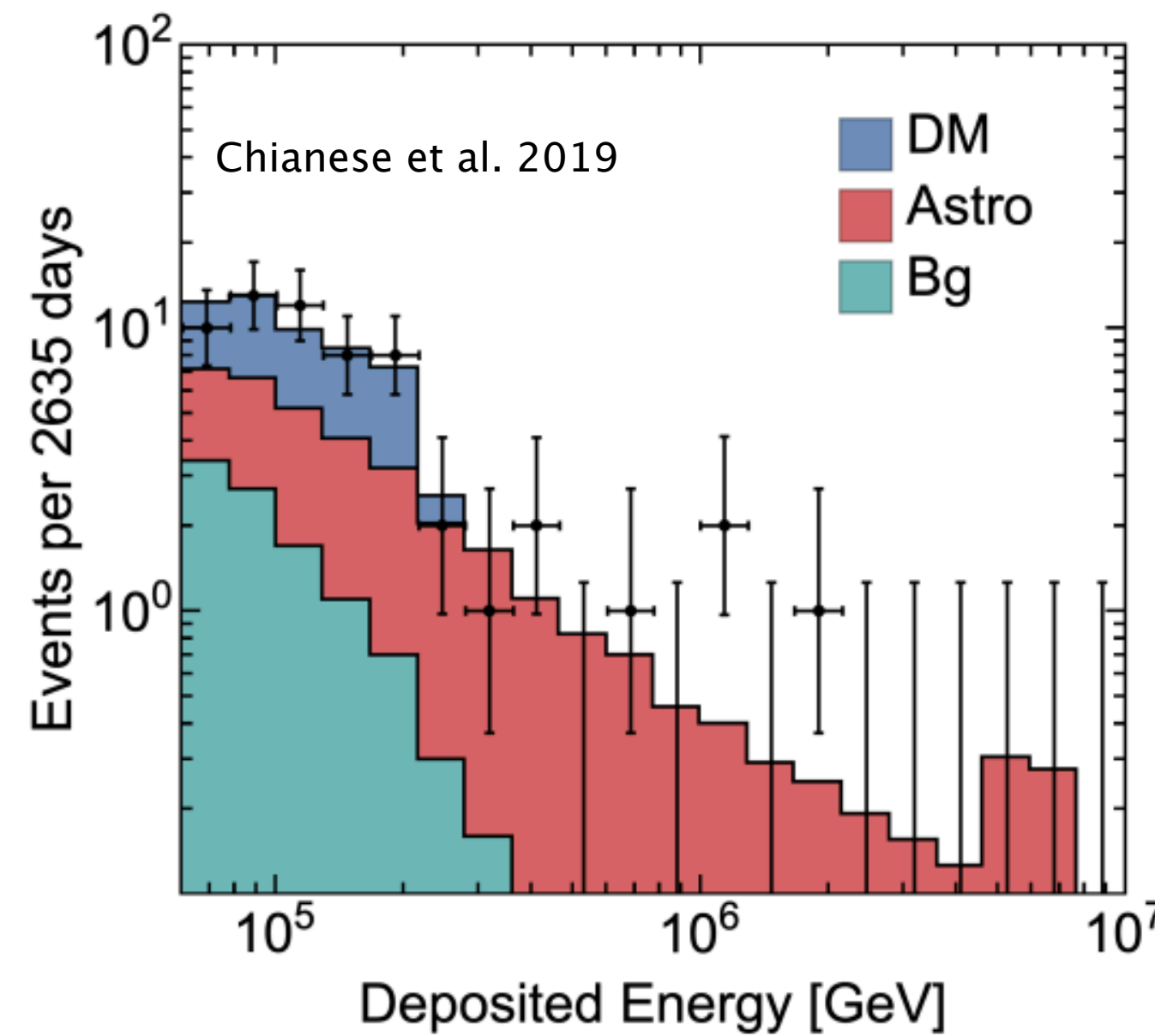
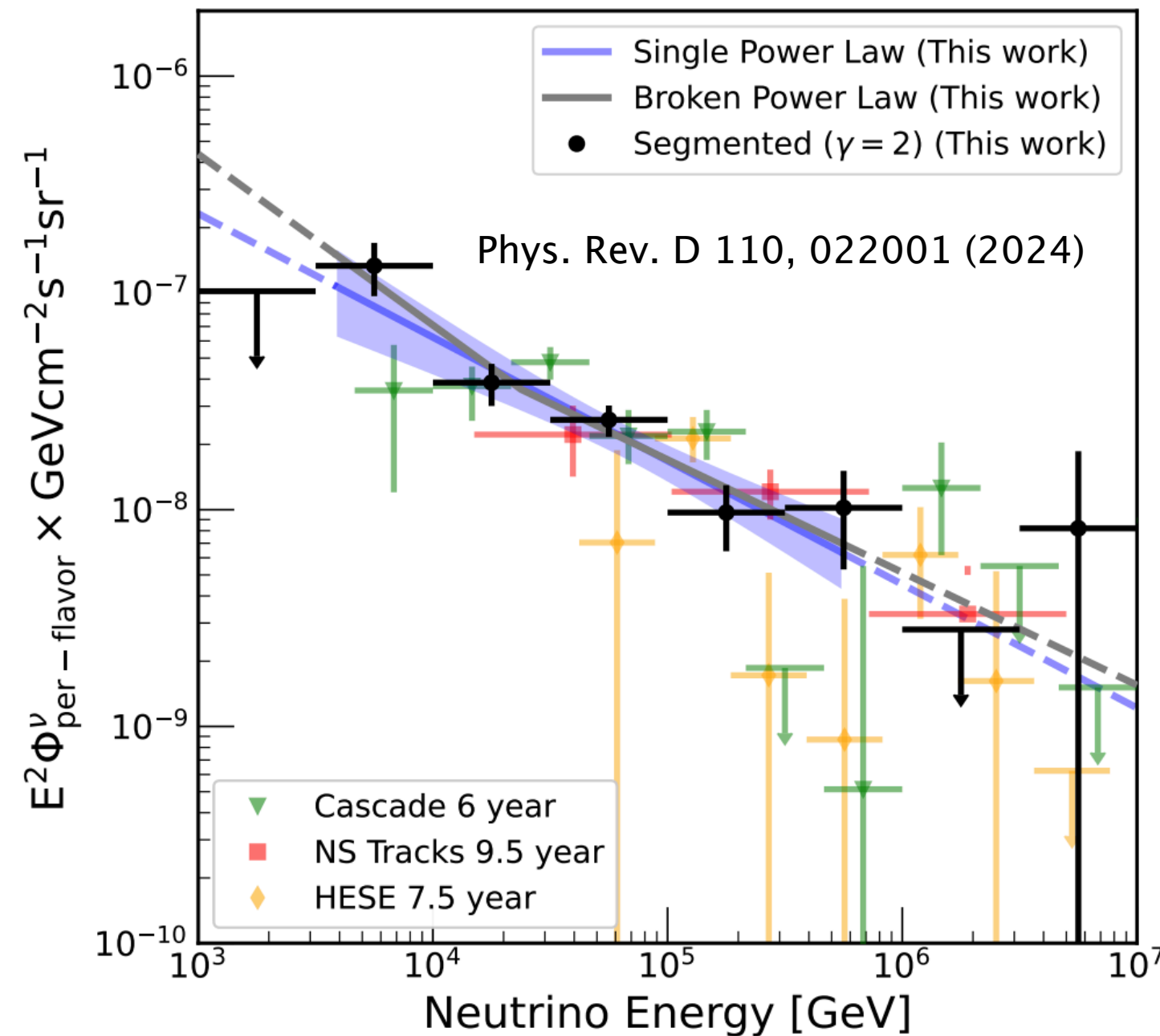
Results for the gamma-ray emissivity

- The final uncertainty is at the level of 10-20%.
- We provide predictions for the XS from 10 MeV to 100 TeV as tables.
- Future data for the invariant cross sections are needed.
- Uncertainties related to the other aspects of the interstellar emission are likely larger than XS ones.



Dark Matter search with VHE/UHE Neutrinos

- IceCube has measured an astrophysical flux of neutrinos whose origin is still not clear.
- There is very likely a Galactic and extragalactic contribution but the exact composition is debated.
- Production cross sections can be calculated in analogy to gamma/e+.
- XS will affect the ATM background component.

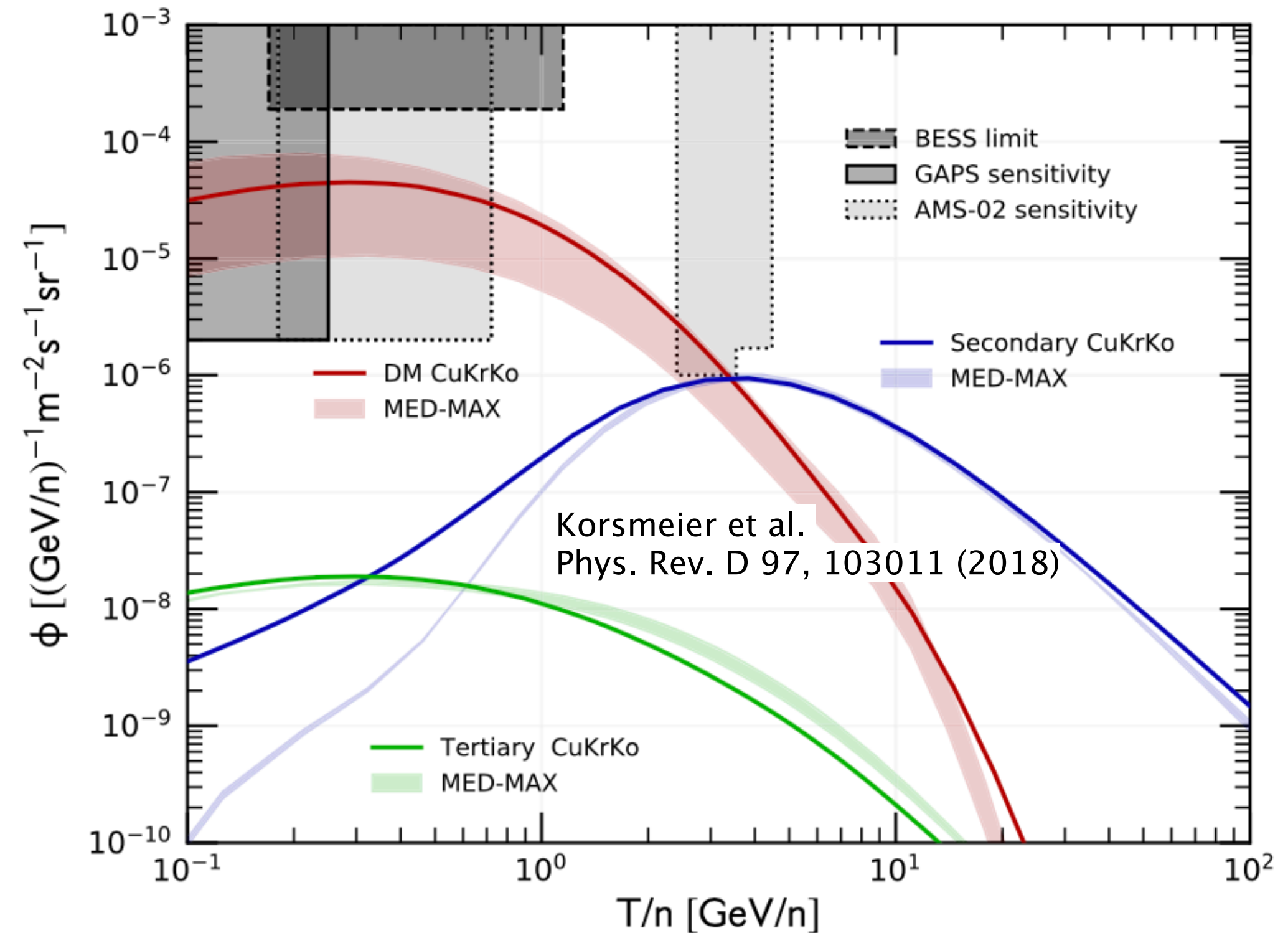
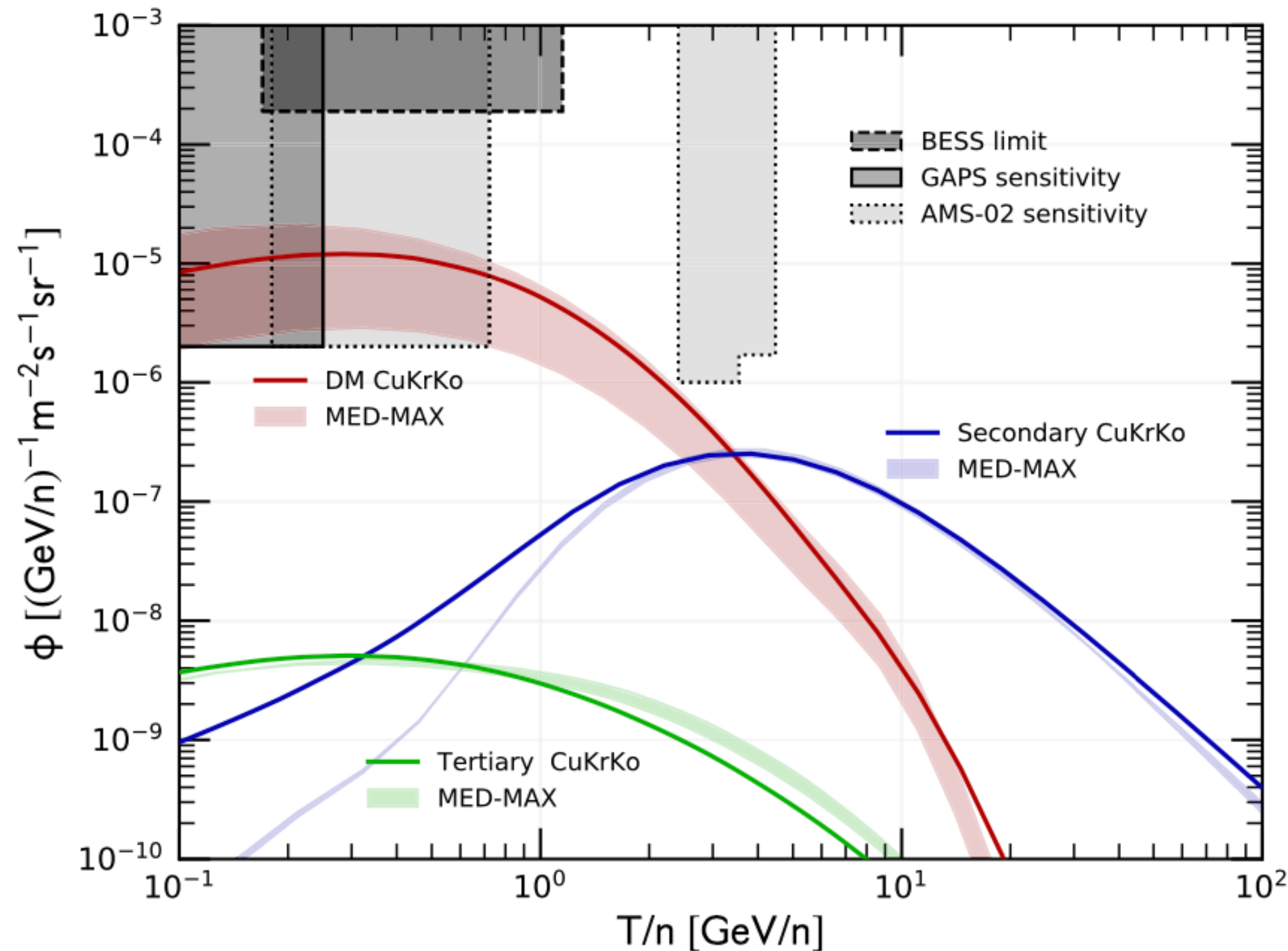


| Channel | $\phi_0^{\text{best}} (\times 10^{-15} \text{f.u.})$ | γ^{best} | $\tau^{\text{best}} (\times 10^{28} \text{s})$ | $m_{\text{DM}}^{\text{best}} (\text{TeV})$ |
|-----------------|--|------------------------|--|--|
| $\nu_e \nu_e$ | 0.88 | 2.43 | 6.92 | 501.19 |
| $\tau^+ \tau^-$ | 0.77 | 2.42 | 1.91 | 569.17 |
| $W^+ W^-$ | 0.77 | 2.42 | 0.63 | 575.44 |
| $b\bar{b}$ | 0.86 | 2.43 | 0.14 | 776.25 |
| $t\bar{t}$ | 0.83 | 2.43 | 0.30 | 676.08 |

(c) Channel W , no prior distribution

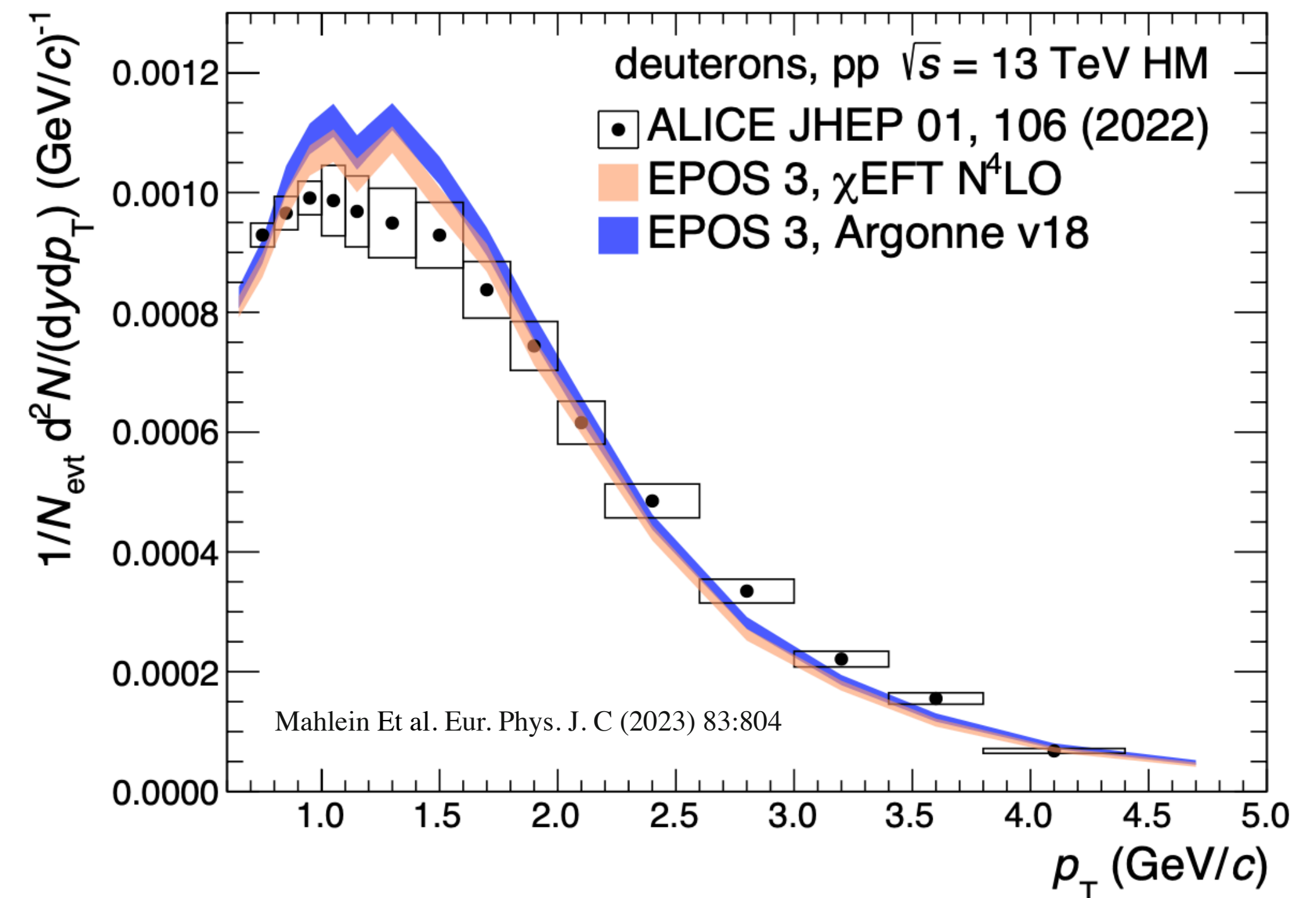
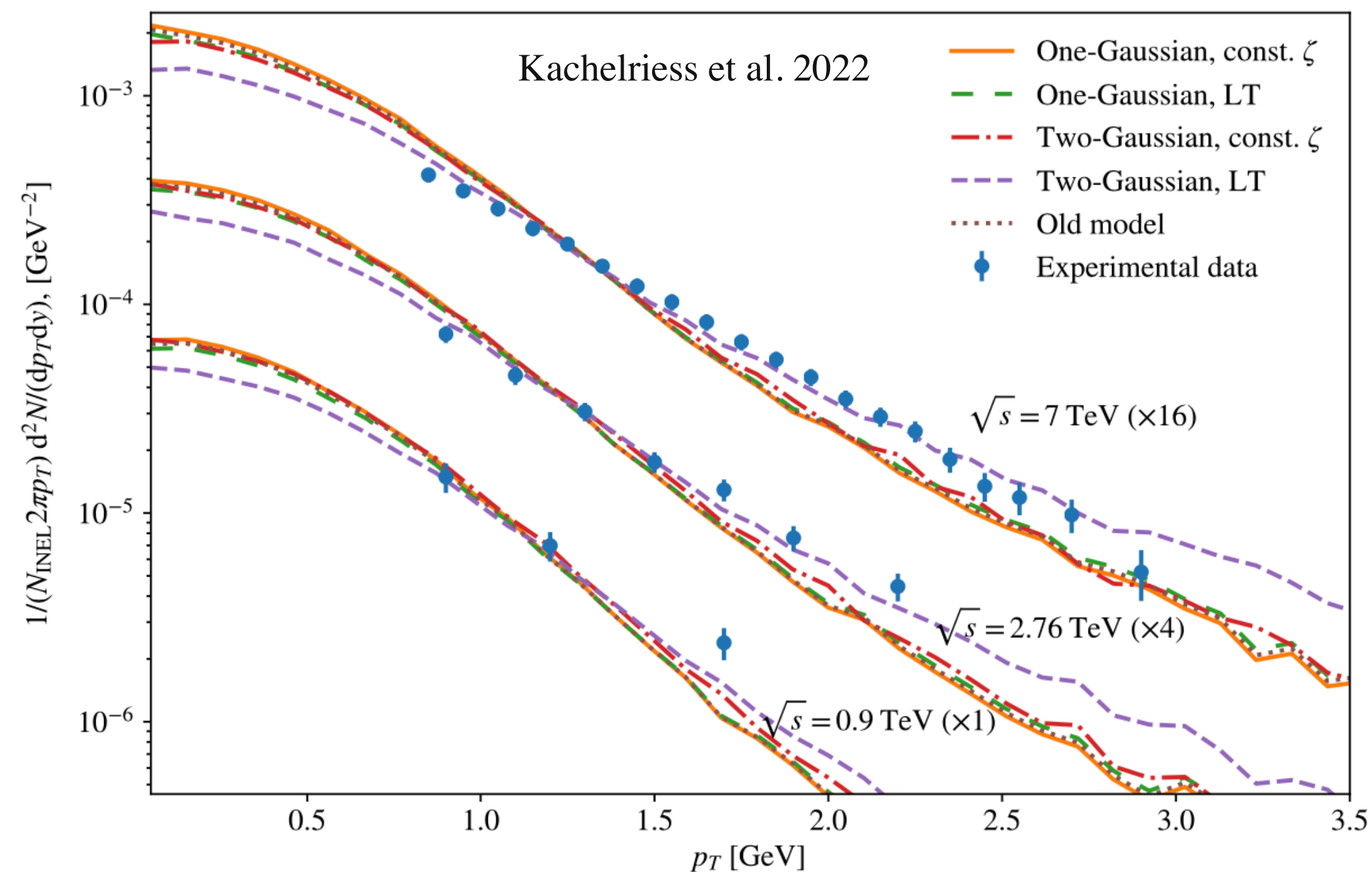
Indirect detection of DM with antinuclei

- First theorised by Donato, Fornengo, Salati (*Phys.Rev.D* 62 (2000) 043003).
- Dark matter signal much larger than secondary production for $K < 1 \text{ GeV/n}$.
- The main reason is the conservation of baryonic number for astro contribution.



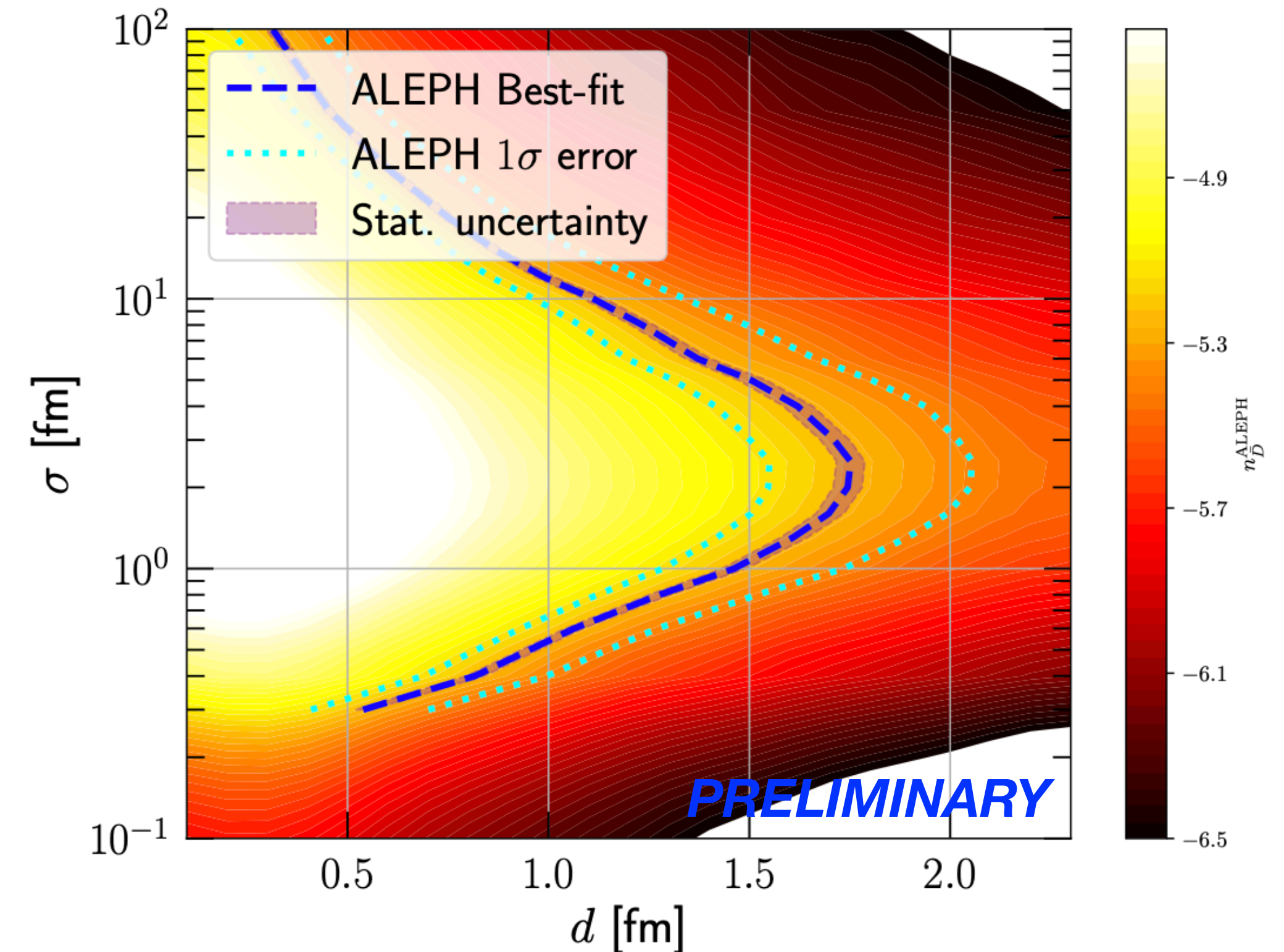
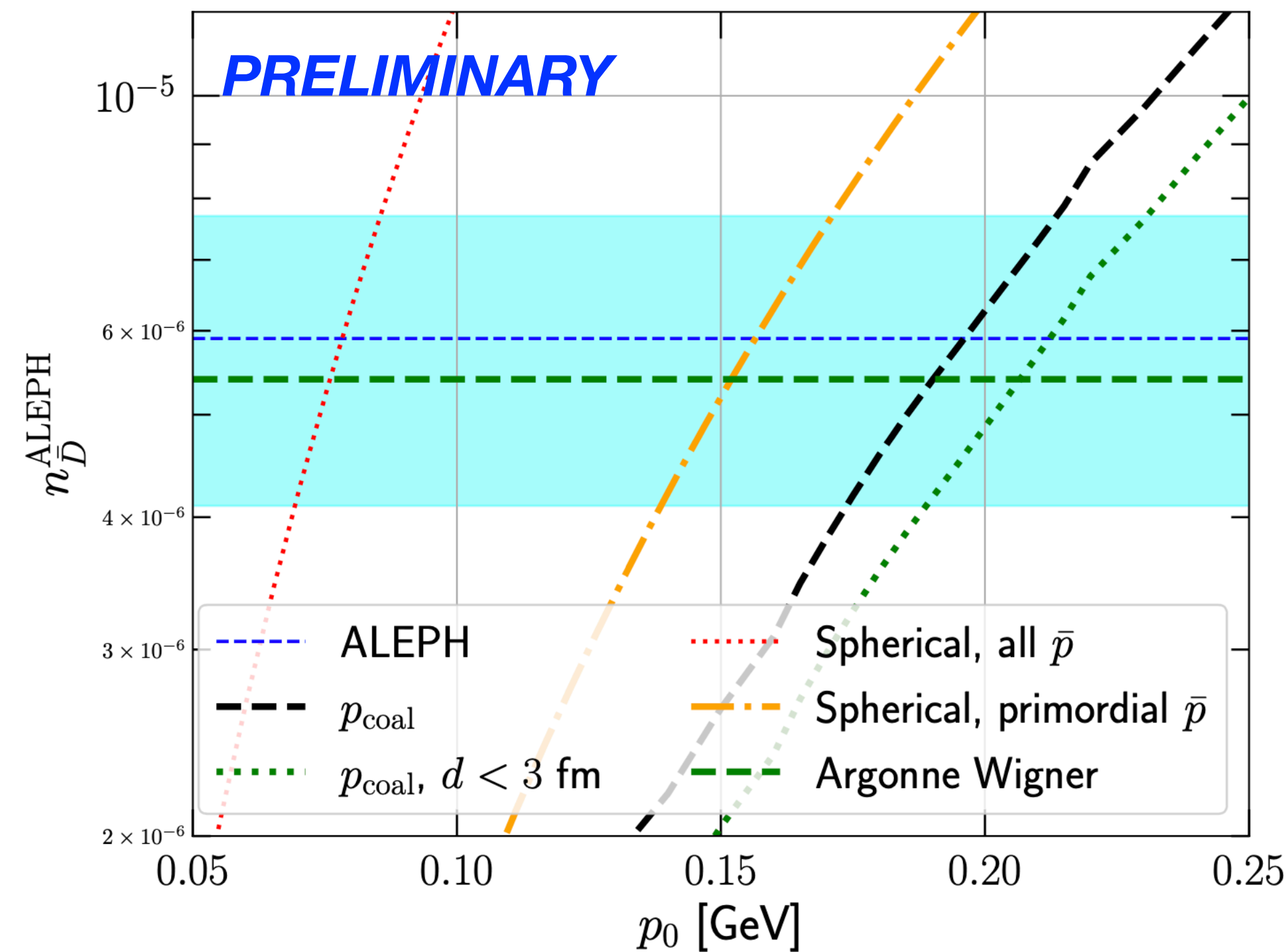
Production of antiD and antiHe3

- Predictions for the production of antiD and antiHe3 are typically based on coalescence models.
- These models assume that antinuclei are produced if anti-nucleons are close enough in momentum and coordinate space.
- Recently models based on a Wigner formalisms have been introduced.

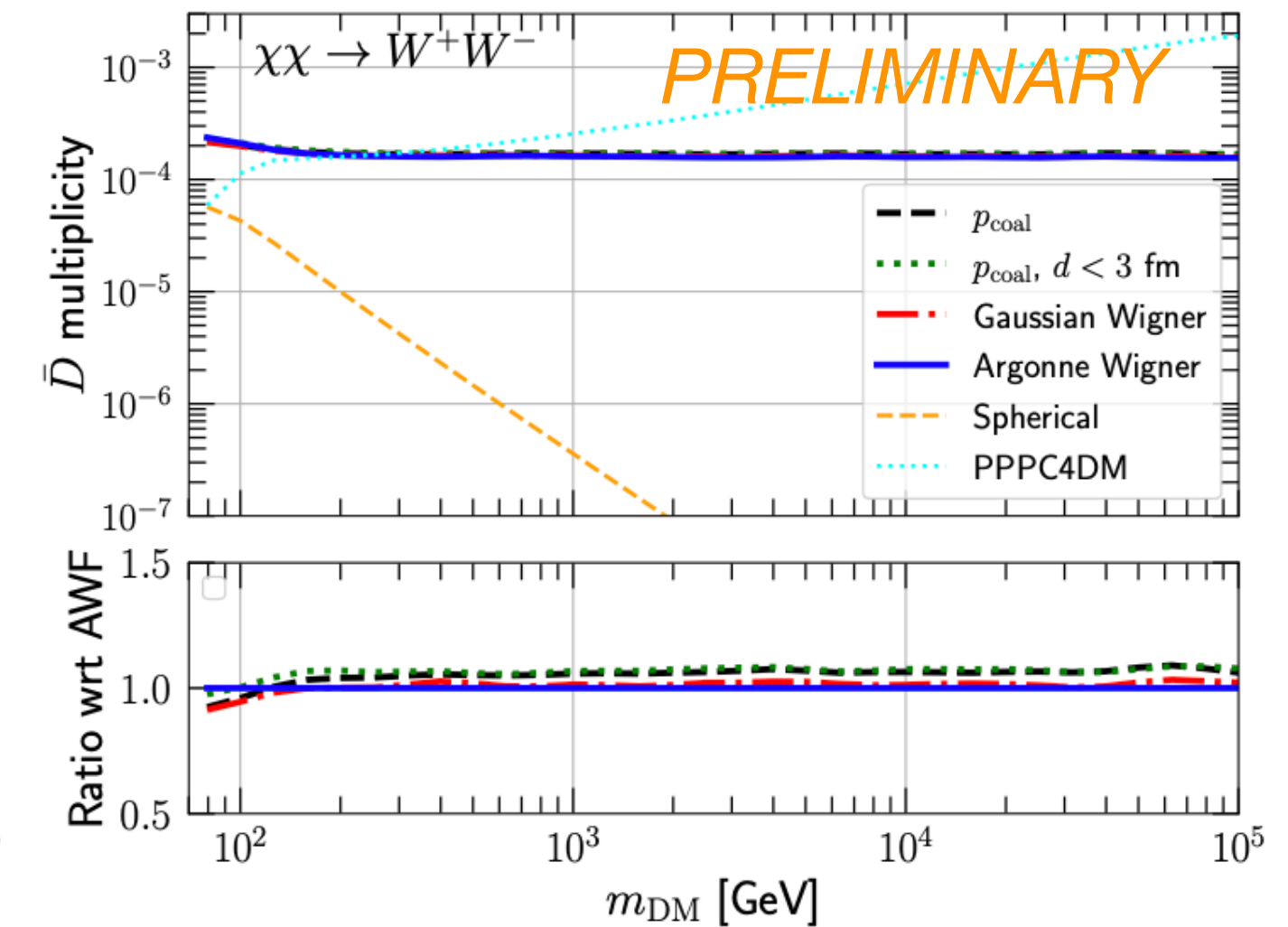
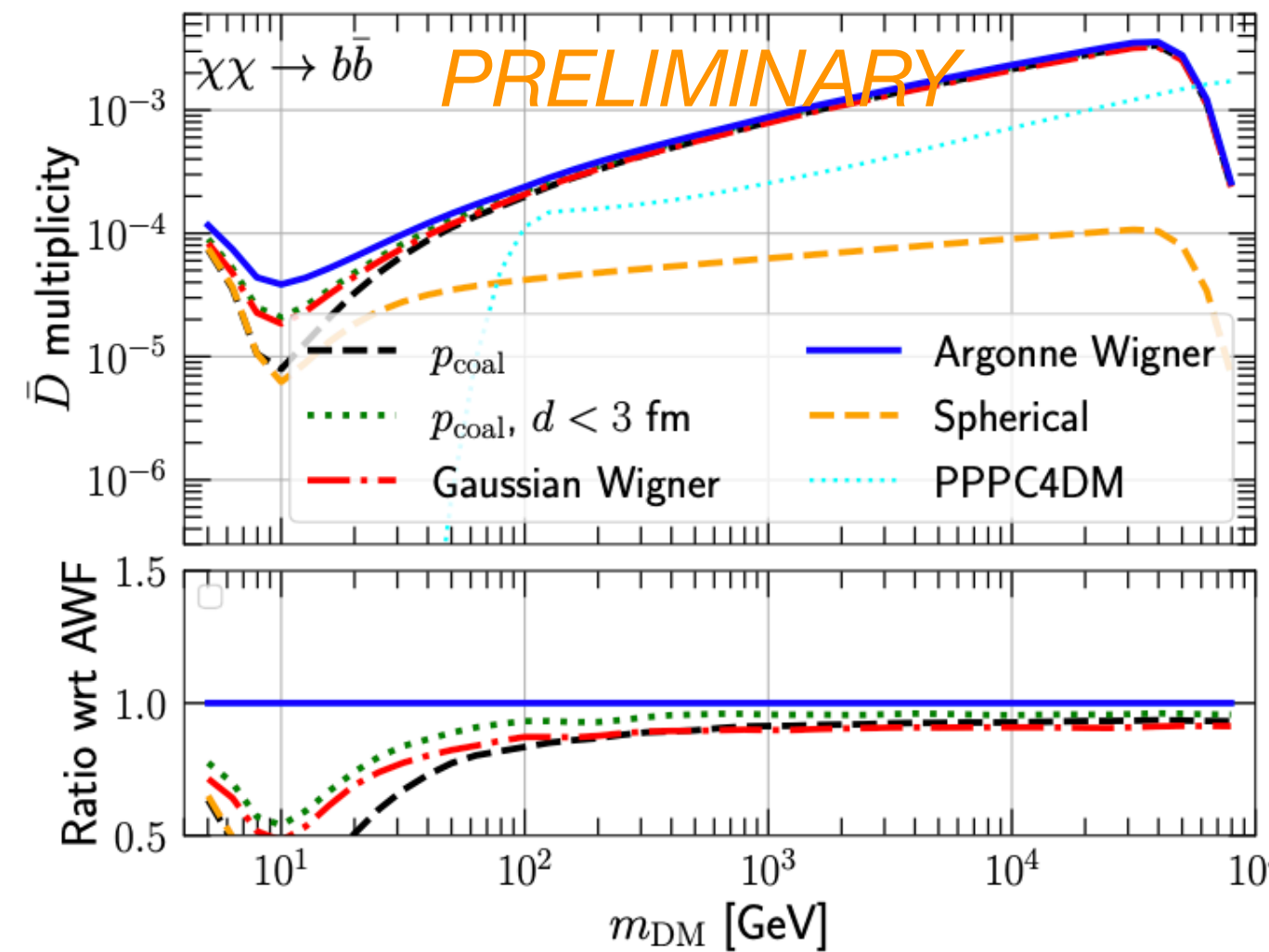
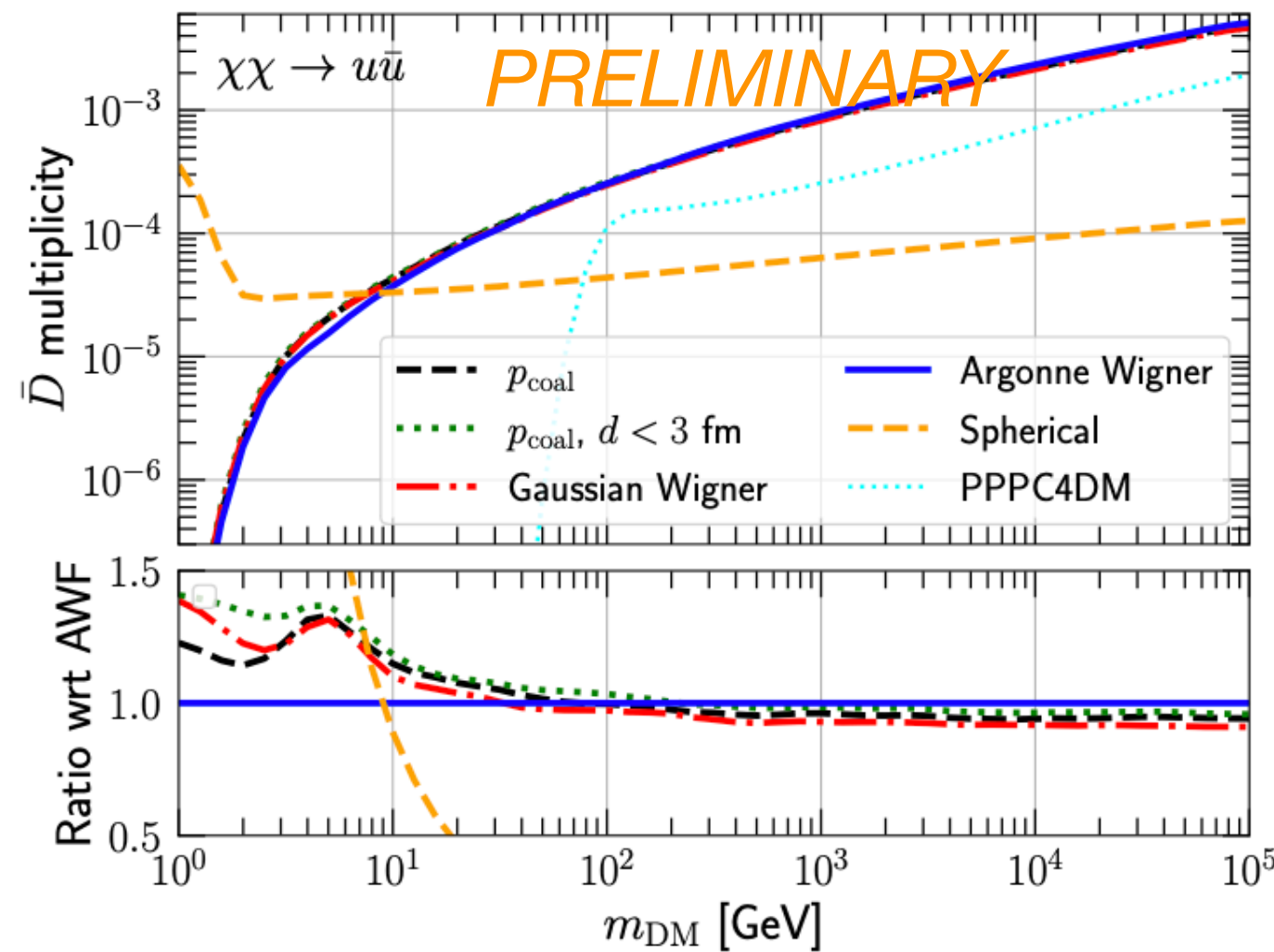
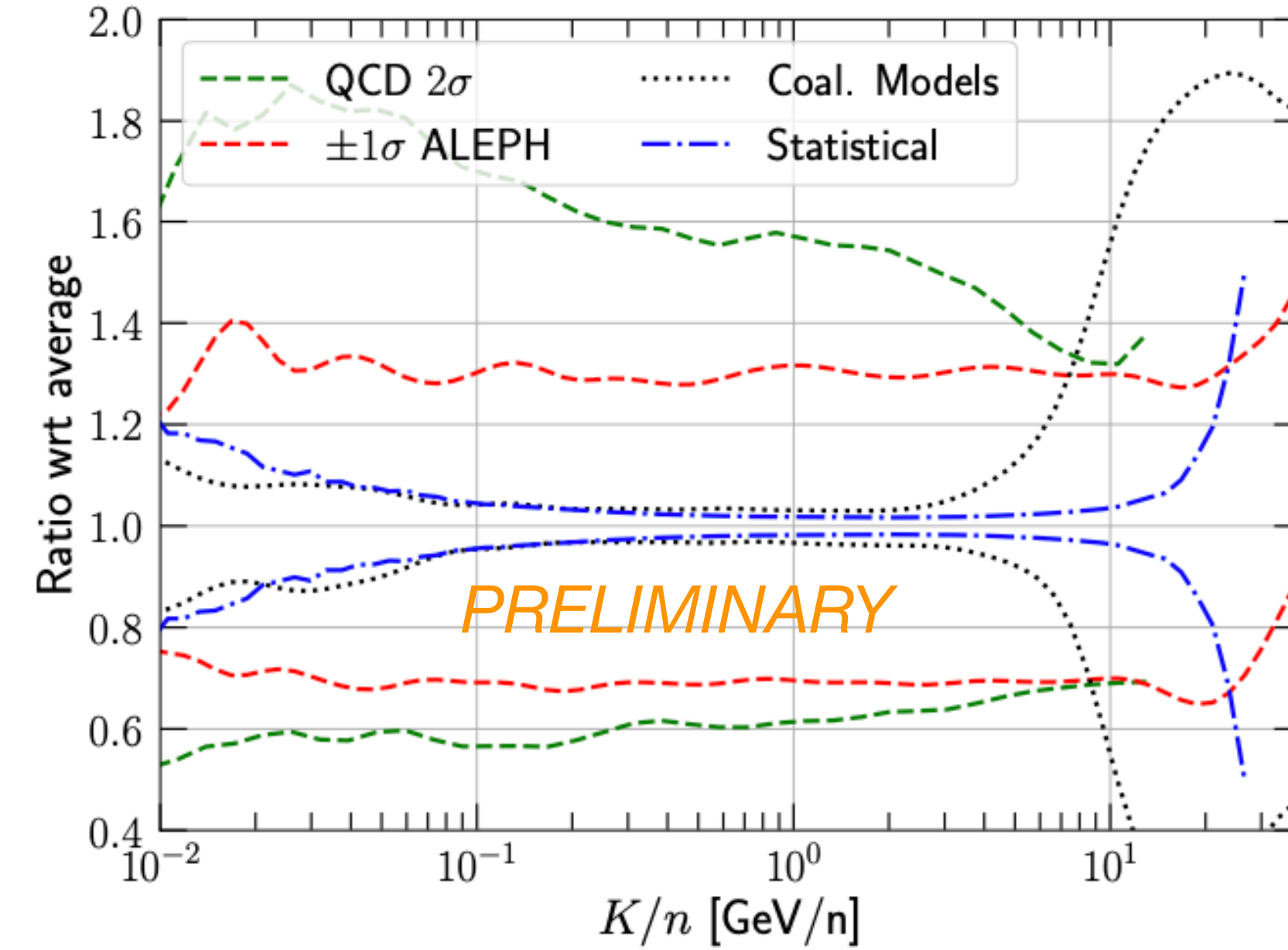
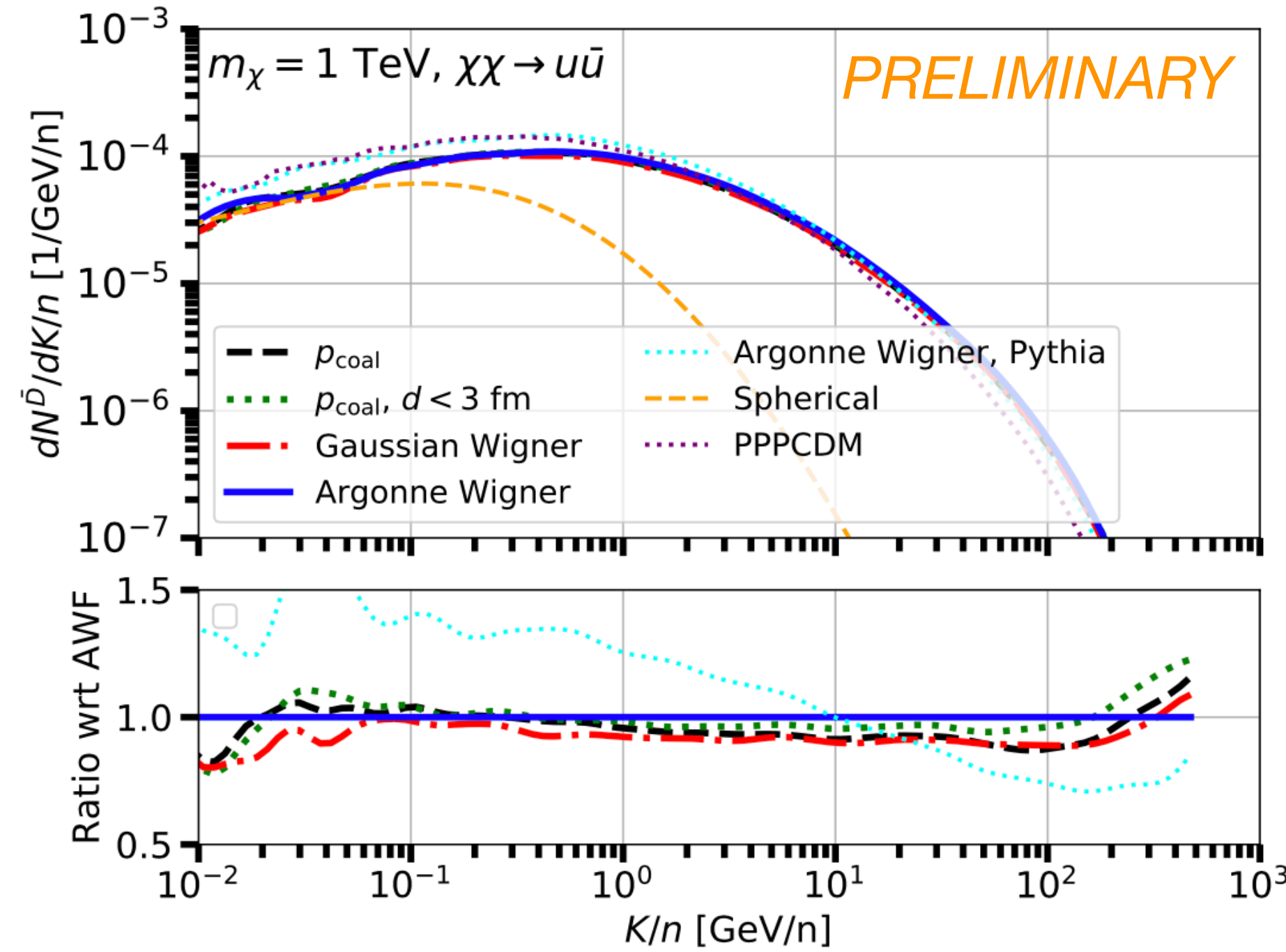


Tuning the models

- We tune the parameters of the coalescence models on the ALEPH datapoint for D bar production.
- We use simple coalescence models and Wigner formalism.
- In particular we also use the Argonne function which is completely fixed on scattering data and deuteron properties.



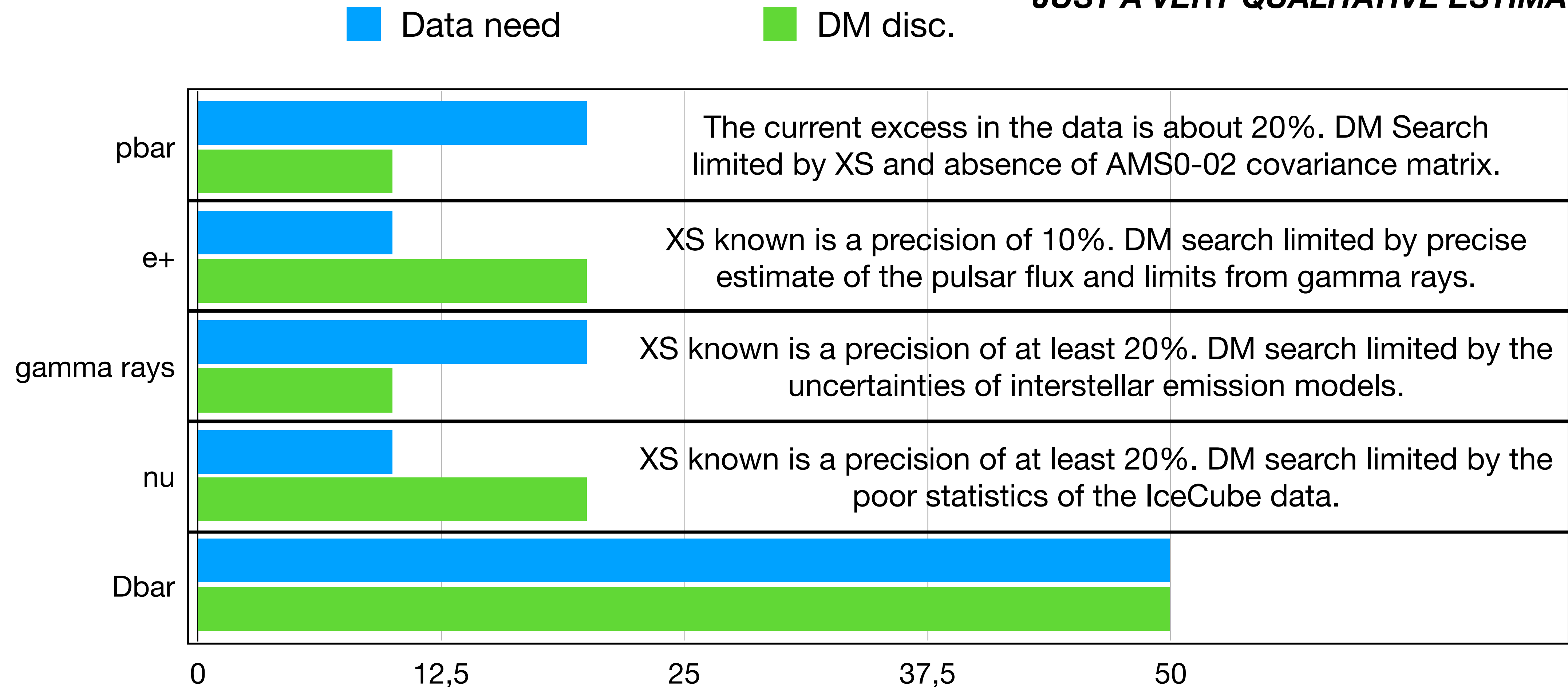
New predictions for antiD from DM



Conclusions about data precision vs DM discovery potential

- **DATA NEED** (current theory uncertainties)
- **DARK MATTER DISCOVERY POTENTIAL** (relative difference between astro background and DM signal)

JUST A VERY QUALITATIVE ESTIMATE!!



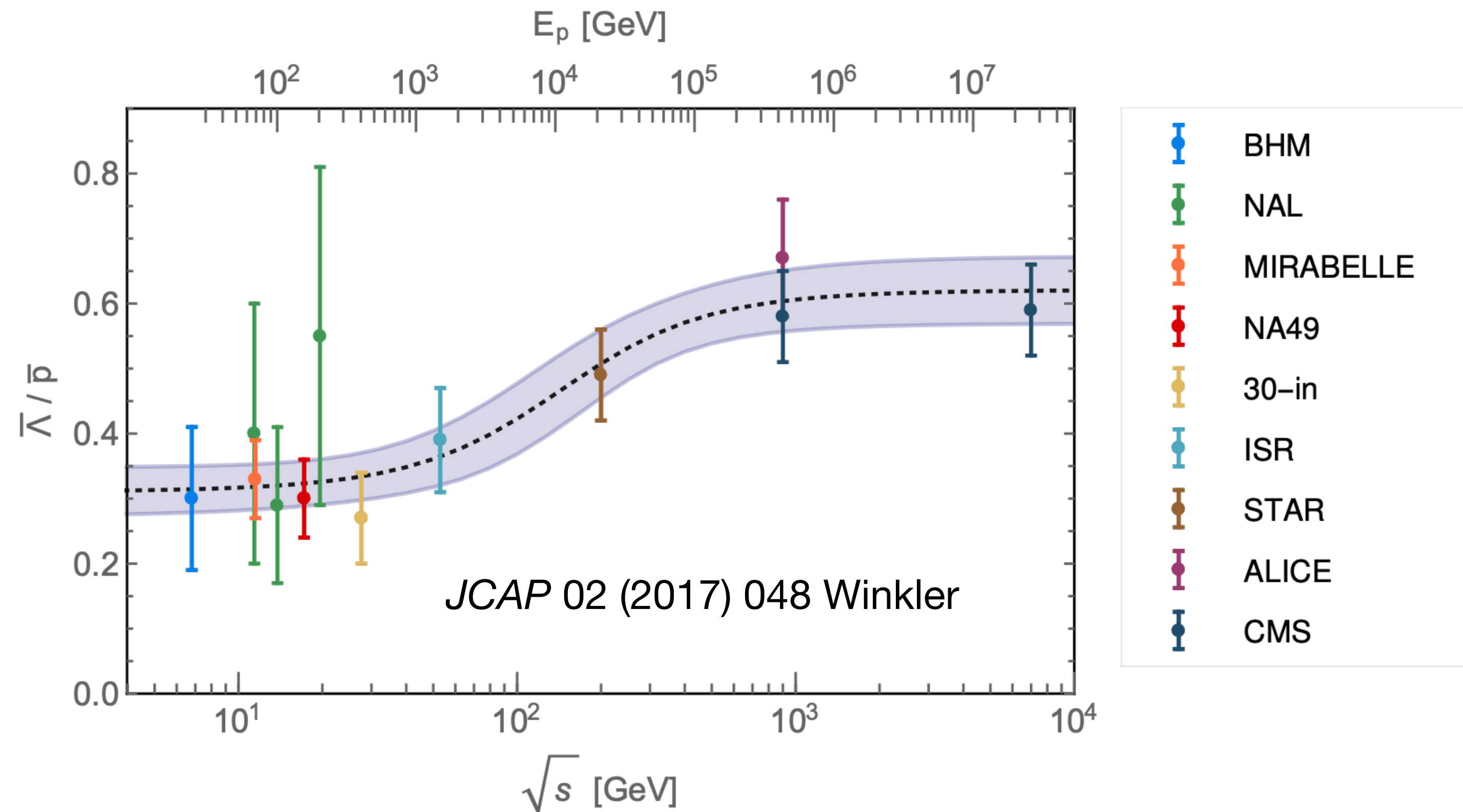
XS data need: suggested priorities

1. Measuring **$D\bar{b}$ XS** or multiplicities at \sqrt{s} between 5 to 100 GeV (NA61, AMBER,...).
2. Measuring the **$p\bar{b}$** Lorentz-invariant XS from **$n\bar{b}$ decay with at most 5% uncert..**
3. Measuring the **$p\bar{b}$** Lorentz-invariant XS from **p -He** for $\sqrt{s} = 5$ -100 GeV **with at most 5% uncert.**
4. Measuring the **π^0** Lorentz-invariant XS from **p -p and p He** for $\sqrt{s} = 5$ -1000 GeV.
5. Measuring the **$p\bar{b}$** Lorentz-invariant XS from **Hyperon** decay for **p -p and p -He** for $\sqrt{s} = 5$ -100 GeV **with at most 5% uncert.**

Backup slides

Hyperon production channel

- The contribution of hyperons is usually taken as a rescaling of the pp.
- Hyperons contribute about 30-40% of the prompt pp channel.
- This contribution has an uncertainty of about 10-20%.
- This is probably a subdominant uncertainty of about 5-10%.



Wigner formalism

$$\frac{d^3 N_d}{dp_d^3} = S \int \frac{d^3 r_d d^3 r d^3 q}{(2\pi)^6} \cdot \mathcal{D}(\vec{r}, \vec{q}) \cdot W_{pn}(\vec{p}_d/2 + \vec{q}, \vec{p}_d/2 - \vec{q}, \vec{r}_p, \vec{r}_n)$$

$$\mathcal{D}(\vec{r}, \vec{q}) = \int d^3 \xi e^{-i\vec{q} \cdot \vec{\xi}} \varphi_d(\vec{r} + \vec{\xi}/2) \varphi_d^*(\vec{r} - \vec{\xi}/2)$$

$$W_{pn} = H_{pn}(\vec{r}_p, \vec{r}_n) G_{pn}(\vec{p}_d/2 + \vec{q}, \vec{p}_d/2 - \vec{q})$$

$$\varphi_d(\Delta r) = (\pi d^2)^{-3/4} e^{-\Delta r^2 / (2d^2)}$$

$$H_{pn}(\vec{r}_p, \vec{r}_n) = h(\vec{r}_p) h(\vec{r}_n)$$

$$\mathcal{D}(\Delta r, q = \Delta p/2) = 8e^{-r^2/d^2} e^{-q^2 d^2}$$

$$\frac{d^3 N_d}{dp_d^3} = \frac{3}{(2\pi)^6} \left(\frac{d^2}{d^2 + 4\sigma^2} \right)^{3/2} \int d^3 q e^{-q^2 d^2} G_{np}(\vec{p}_d, \vec{q})$$

XS Parameterizations

Phys.Rev.D 97 (2018) 10, 103019 Korsmeier, Donato, DM

$$\sigma_{\text{inv}}^{\text{Galaxy}} = \sigma_{\text{inv}}(2 + \Delta_{\text{IS}} + 2\Delta_{\Lambda})$$

$$\Delta_{\text{IS}} = \frac{c_1^{\text{IS}}}{1 + (s/c_2^{\text{IS}})^{c_3^{\text{IS}}}} \quad \Delta_{\Lambda} = 0.81 \left(c_1^{\Lambda} + \frac{c_2^{\Lambda}}{1 + (c_3^{\Lambda}/s)^{c_4^{\Lambda}}} \right)$$

$$\sigma_{\text{inv}}(\sqrt{s}, x_R, p_T) = \sigma_{\text{in}}(1 - x_R)^{c_1} \exp(-C_2 x_R) \times [C_3(\sqrt{s})^{c_4} \exp(-C_5 p_T) + C_6(\sqrt{s})^{c_7} \exp(-C_8 p_T^2)].$$

$$\sigma_{\text{inv}}(\sqrt{s}, x_R, p_T) = \sigma_{\text{in}} R C_1 (1 - x_R)^{c_2} \times \left[1 + \frac{X}{\text{GeV}} (m_T - m_p) \right]^{\frac{-1}{c_3 X}},$$

$$R = \begin{cases} 1 & \sqrt{s} \geq 10 \text{ GeV} \\ \left[1 + C_5 \left(10 - \frac{\sqrt{s}}{\text{GeV}} \right)^5 \right] & \text{elsewhere} \\ \times \exp \left[C_6 \left(10 - \frac{\sqrt{s}}{\text{GeV}} \right)^2 \right] \\ \times (x_R - x_{R,\text{min}})^2 \end{cases}$$

$$f^{pA} = A^{D_1} \left[A^{D_2} \left(1 + \frac{N}{A} \Delta_{\text{IS}} \right) F_{\text{pro}}(x_f) + F_{\text{tar}}(x_f) \right]$$

$$\sigma_{\text{in}} = c_{\text{in},1} + c_{\text{in},2} \log(\sqrt{s}) + c_{\text{in},3} \log^2(\sqrt{s})$$

Phys.Rev.D 105 (2022) 12, 123021 Orusa, DM, Korsmeier, Donato

$$\sigma_{\text{inv}} = \sigma_0(s) c_1 \left[F_p(s, p_T, x_R) + F_r(p_T, x_R) \right] A(s).$$

$$F_p(s, p_T, x_R) = (1 - x_R)^{c_2} \exp(-c_3 x_R) p_T^{c_4} \quad (\xi)$$

$$\times \exp \left[-c_5 \sqrt{s/s_0}^{c_6} \left(\sqrt{p_T^2 + m_\pi^2} - m_\pi \right)^{c_7 \sqrt{s/s_0}^{c_6}} \right]$$

$$F_r(p_T, x_R) = (1 - x_R)^{c_8}$$

$$\times \exp \left[-c_9 p_T - \left(\frac{|p_T - c_{10}|}{c_{11}} \right)^{c_{12}} \right]$$

$$\times \left[c_{13} \exp(-c_{14} p_T^{c_{15}} x_R) + c_{16} \exp \left(- \left(\frac{|x_R - c_{17}|}{c_{18}} \right)^{c_{19}} \right) \right].$$

$$A(s) = \frac{1 + \left(\sqrt{s/c_{20}} \right)^{c_{21} - c_{22}}}{1 + \left(\sqrt{s_0/c_{20}} \right)^{c_{21} - c_{22}}} \left(\sqrt{\frac{s}{s_0}} \right)^{c_{22}}$$

XS from heavier nuclei

- In the Galaxy, nuclei interactions ($p + A$, $A + p$, and $A + A$) give a significant contribution to the production of secondary particles.
- We used the data of NA49 for the production of π^+ in $p+C$ collisions at $E_p = 158$ GeV and K^+ in $p+C$ collisions at $E_p = 30$ GeV.

We model the inclusive Lorentz invariant cross section of the $A_1 + A_2 \rightarrow \pi^+ + X$ scattering by:

$$\sigma_{\text{inv}}^{A_1 A_2}(\sqrt{s}, x_F, p_T) = f^{A_1 A_2}(A_1, A_2, x_F, D_1, D_2, D_3) \sigma_{\text{inv}}^{pp}(\sqrt{s}, x_F, p_T), \quad (25)$$

where A_1 and A_2 are the mass numbers of the projectile and target nucleus, respectively, and D_1 , D_2 , and D_3 are three fit parameters. Explicitly, the factor $f^{A_1 A_2}$ is defined by:

$$f^{A_1 A_2}(x_F) = A_1^{D_1} A_2^{D_1} \left[A_1^{D_2} F_{\text{pro}}(x_F) + A_2^{D_2} F_{\text{tar}}(x_F) \right], \quad (26)$$

with $F_{\text{pro}}(x_F)$ and $F_{\text{tar}}(x_F)$ given by

$$F_{\text{pro/tar}}(x_F) = \frac{1 \pm \tanh(D_3 x_F)}{2}. \quad (27)$$

In the above equations, the kinetic variables x_F and \sqrt{s} refer to the nucleon-nucleon CM frame. We do not claim

<https://arxiv.org/abs/2203.13143>

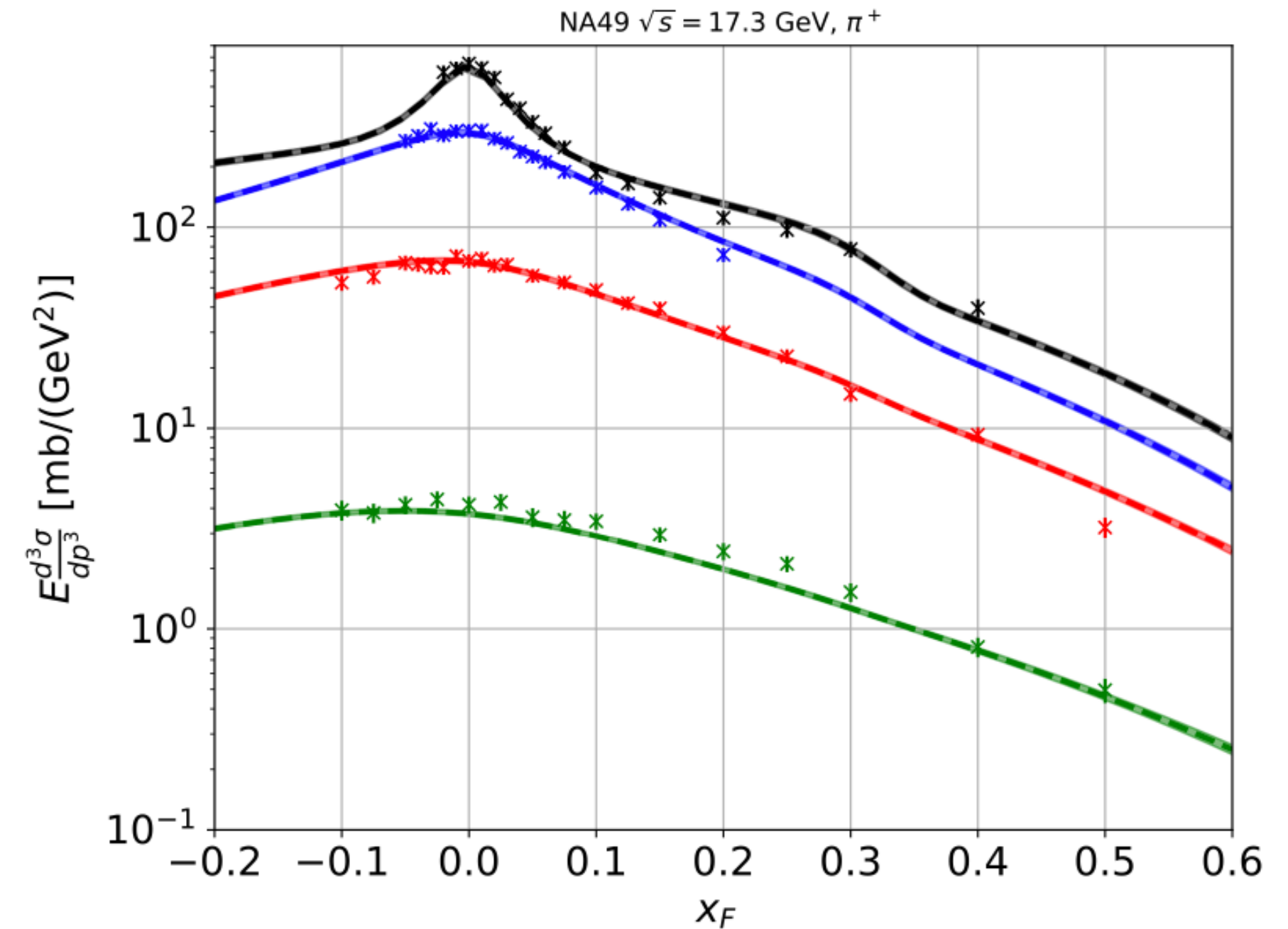
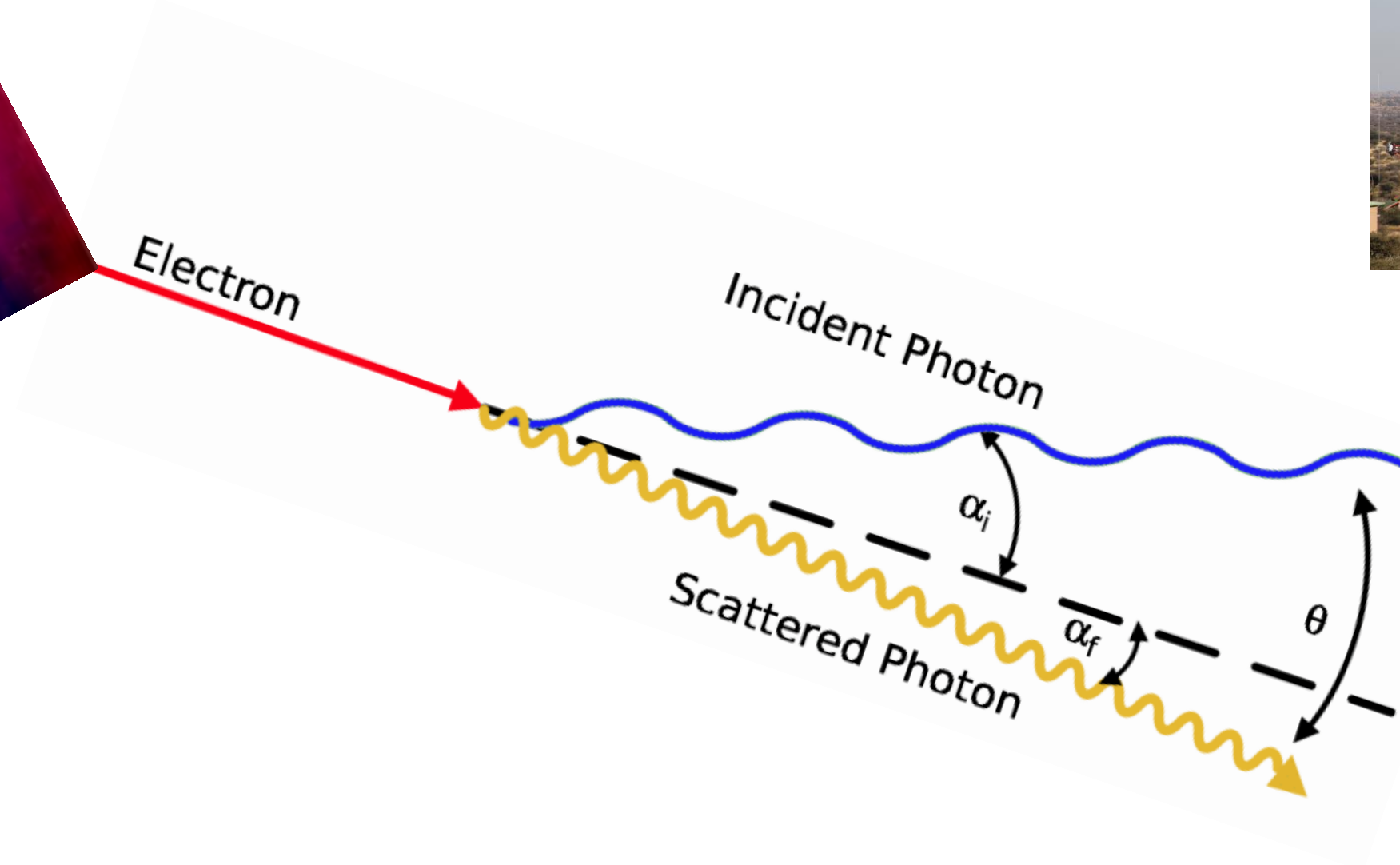


FIG. 11. Results of the fit on the NA49 data [89] invariant cross section for the inclusive π^+ production in $p+C$ collisions. We show the NA49 data together with our fit results as a function of x_F for some representative values of p_T . Shaded bands show the 1σ uncertainty band.

γ rays produced by inverse Compton scattering



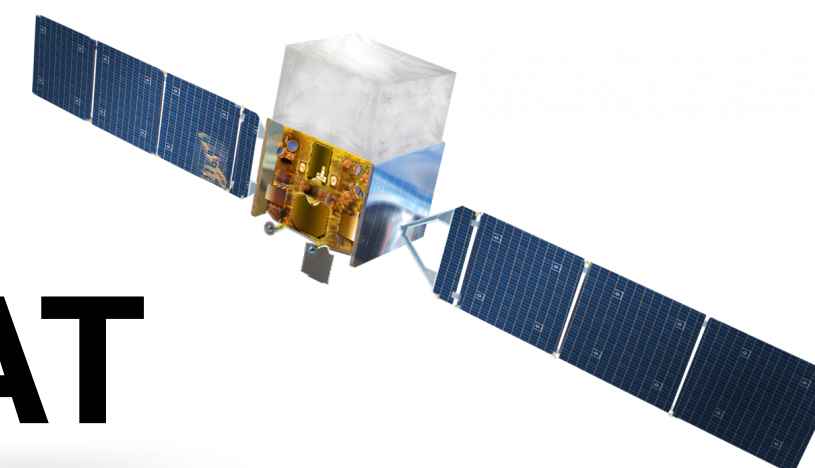
IACTs



HAWC

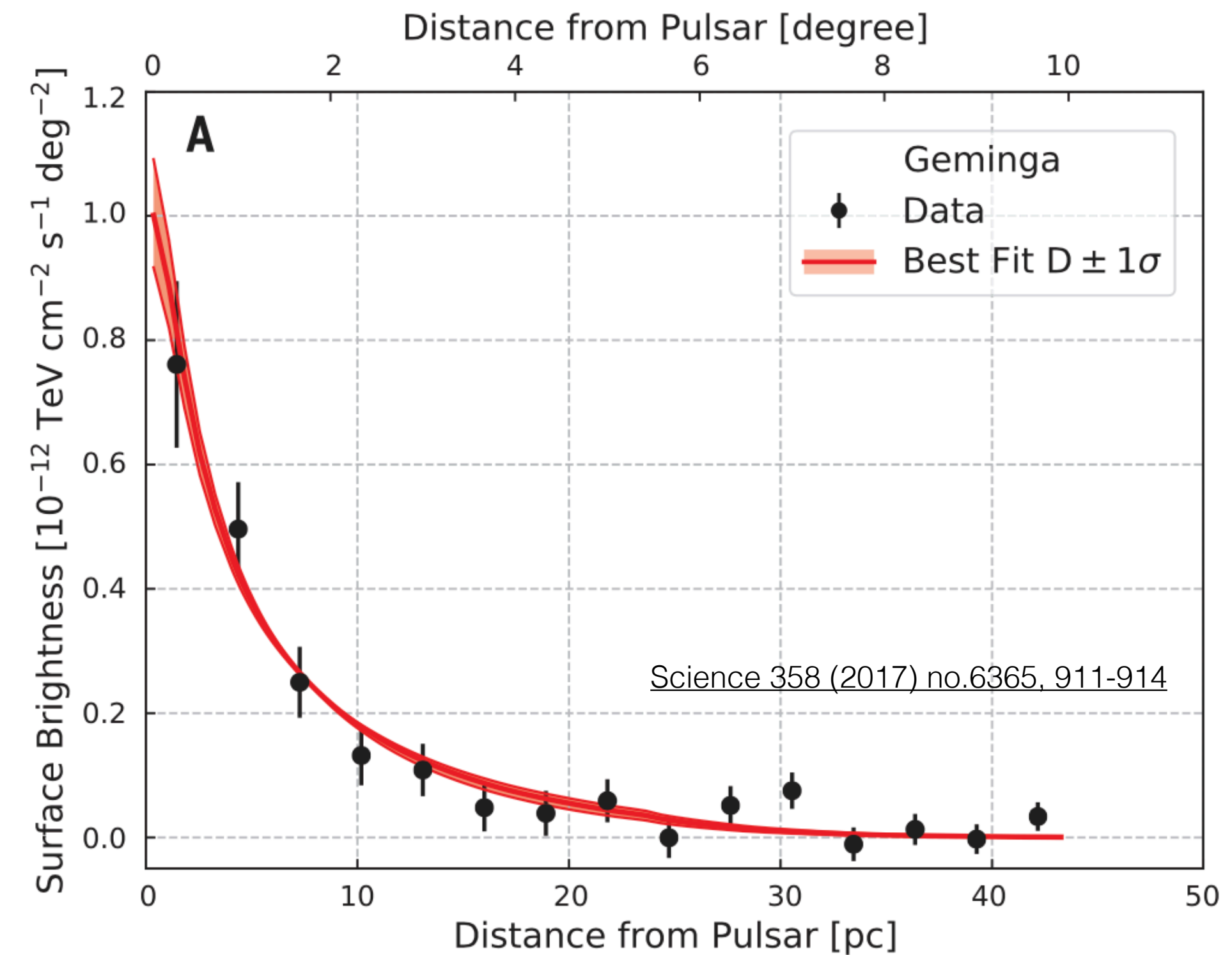
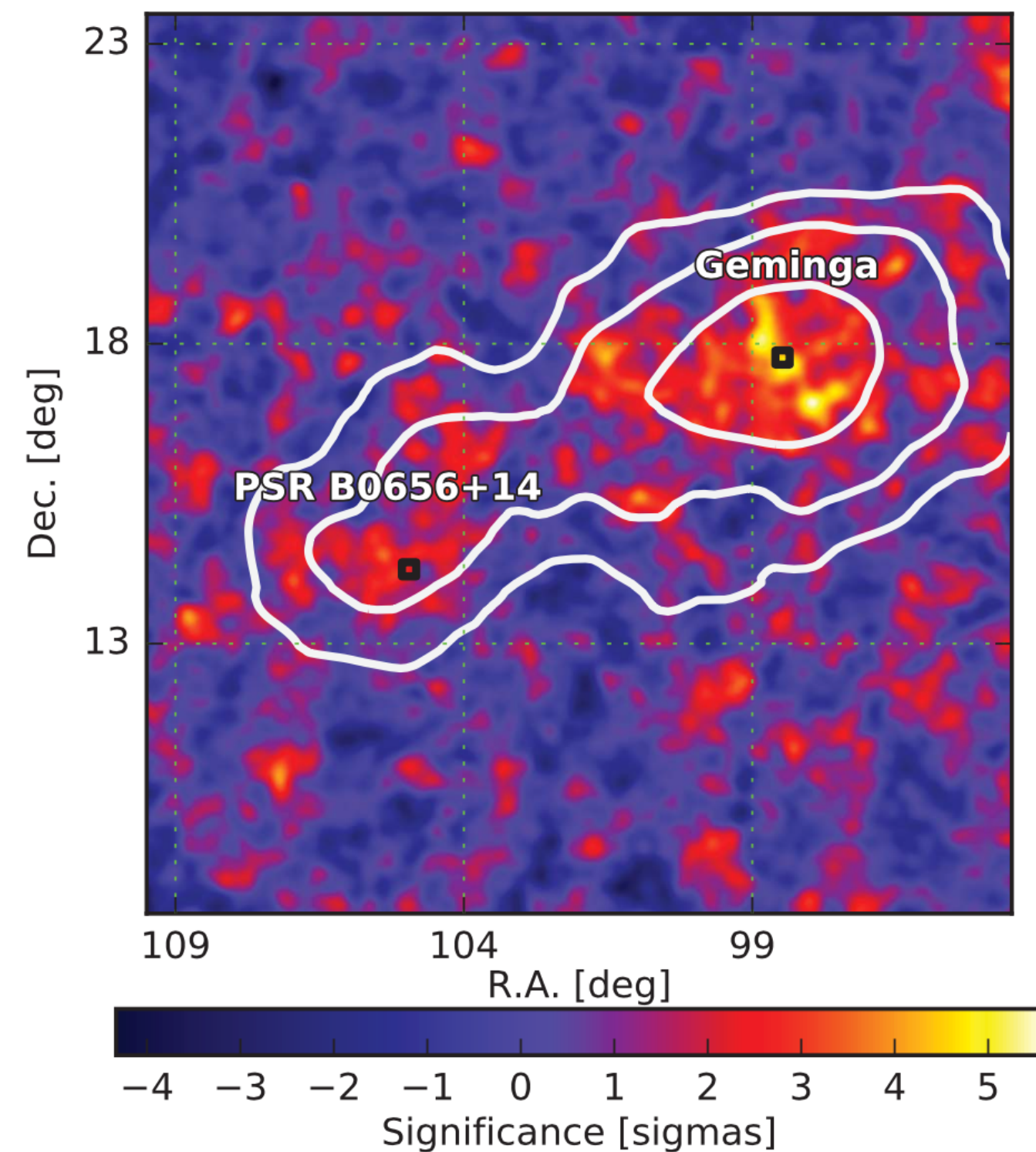


Fermi-LAT



HAWC results for Geminga and Monogem PWNe

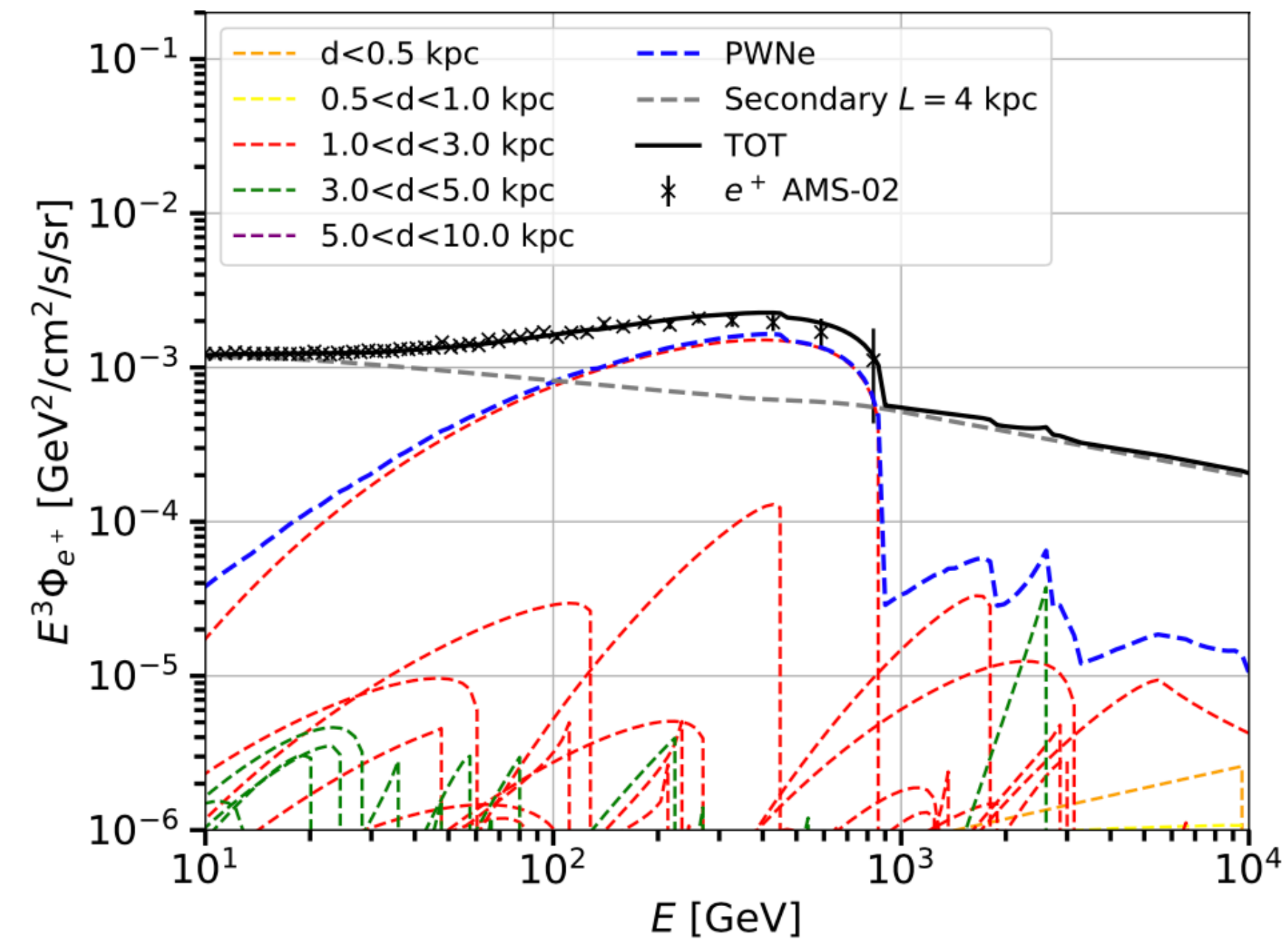
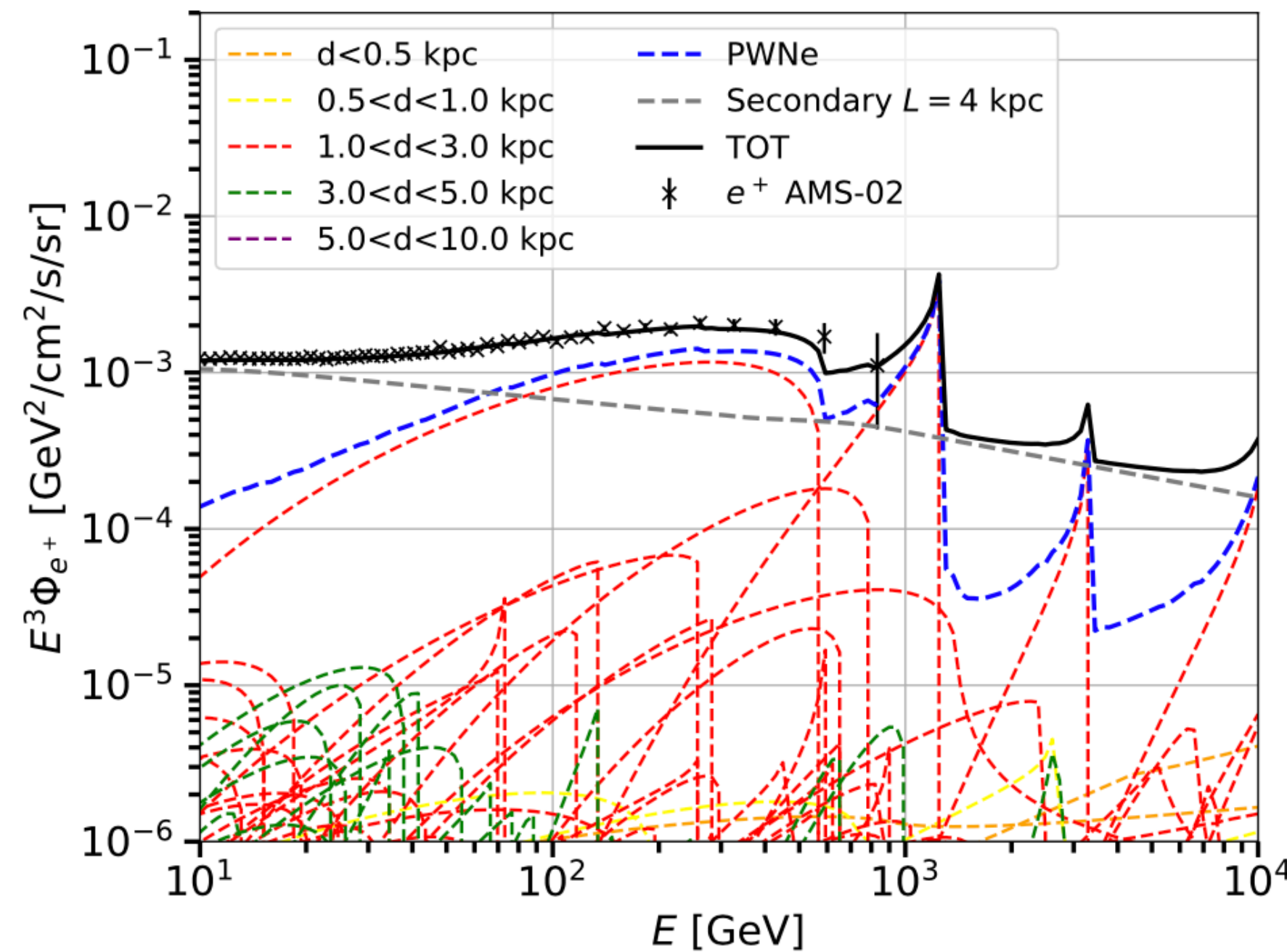
- HAWC detected an extended emission from Geminga and Monogem PWNe for $E > 5$ TeV.
- *In the vicinity of the PWN, the diffusion coefficient D must be about 500 times smaller than the average in the Galaxy.*



A few pulsars dominate the positron flux

| | AMS-02 errors | Total flux 1% |
|------|---------------|---------------|
| ModA | 1.3/2.9/3.3 | 1.0/1.8/2.2 |
| ModB | 3.5 | 1.9 |
| ModC | 3.9 | 3.0 |
| ModD | 5.4 | 3.5 |
| ModE | 1.0 | 1.0 |

Efficiencies between
1-10% are sufficient
to fit the data



Orusa et al. JCAP 12 (2021) 12, 014.

Cosmic-ray antiprotons

Diffusion

$$K = K_0 \beta^\eta \left(\frac{\mathcal{R}}{GV} \right)^\delta \left(1 + \left(\frac{\mathcal{R}}{\mathcal{R}_b} \right)^{\Delta\delta/s} \right)^{-s}$$

Energy losses

$$b_{\text{disc}} = b_{\text{coul}} + b_{\text{ion}} + b_{\text{brems}} + b_{\text{reac}}$$

Reacceleration

$$K_{EE} = \frac{4}{3} \frac{V_a^2}{K} \frac{p^2}{\delta(4-\delta)(4-\delta^2)}$$

Annihilation rate

$$-K \Delta \mathcal{N}_i + 2h\delta(z) \left[\partial_E (b_{\text{disc}} \mathcal{N}_i - K_{EE} \partial_E \mathcal{N}_i) + \Gamma_{\text{ann}} \mathcal{N}_i \right] + \partial_E (b_{\text{halo}} \mathcal{N}_i) = 2h\delta(z) \mathcal{Q}_i^{\text{sec}} + \mathcal{Q}_i^{\text{prim}}$$

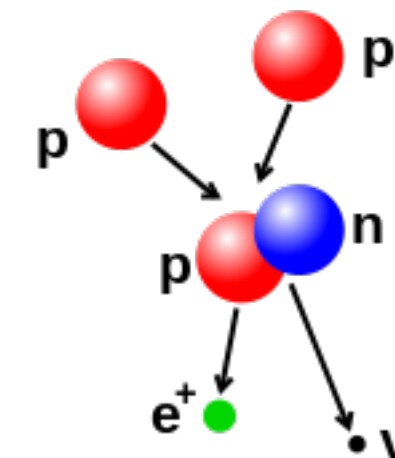
$$b_{\text{halo}} = b_{\text{ic}} + b_{\text{synch}}$$

Energy losses

$$\mathcal{Q}_i^{\text{sec}} = \sum_{j,k} 4\pi \int dE' \left(\frac{d\sigma_{jk \rightarrow i}}{dE} \right) n_k \Phi_j(E')$$

Secondary

Primary

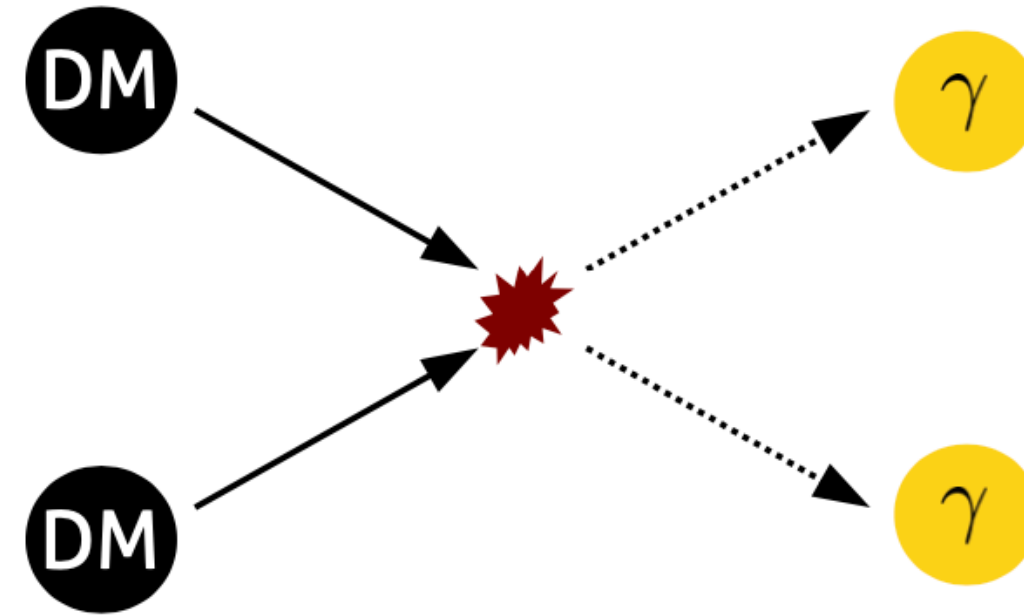


L vertical size of the diffusive halo

Gamma rays from dark matter annihilation

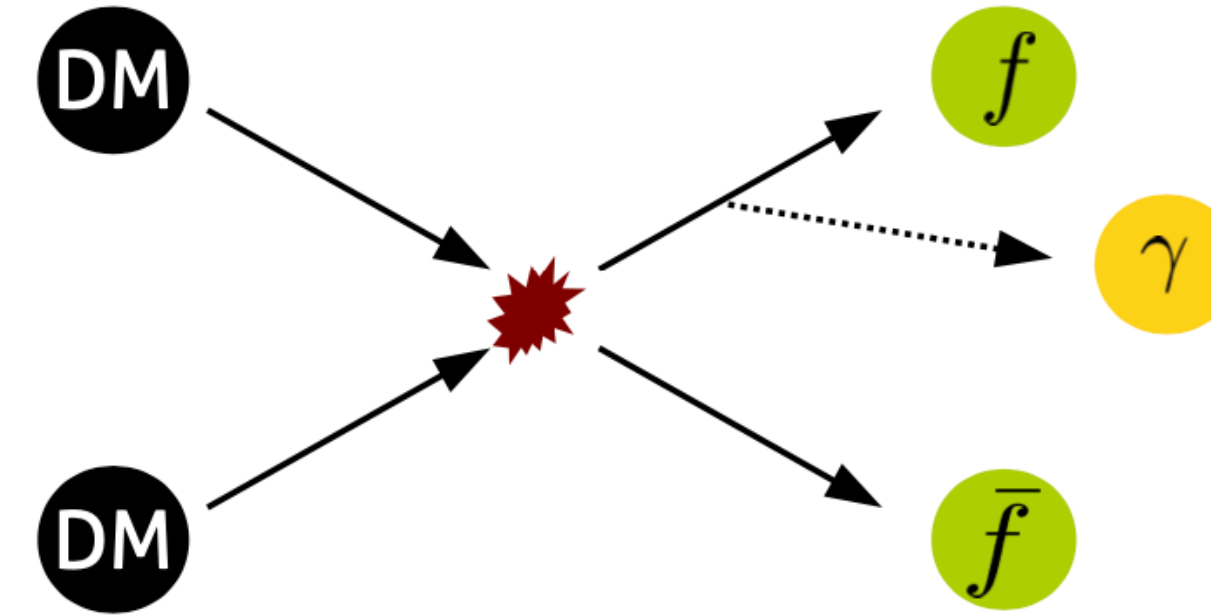
Gamma-ray lines:

Two-body annihilation into photons



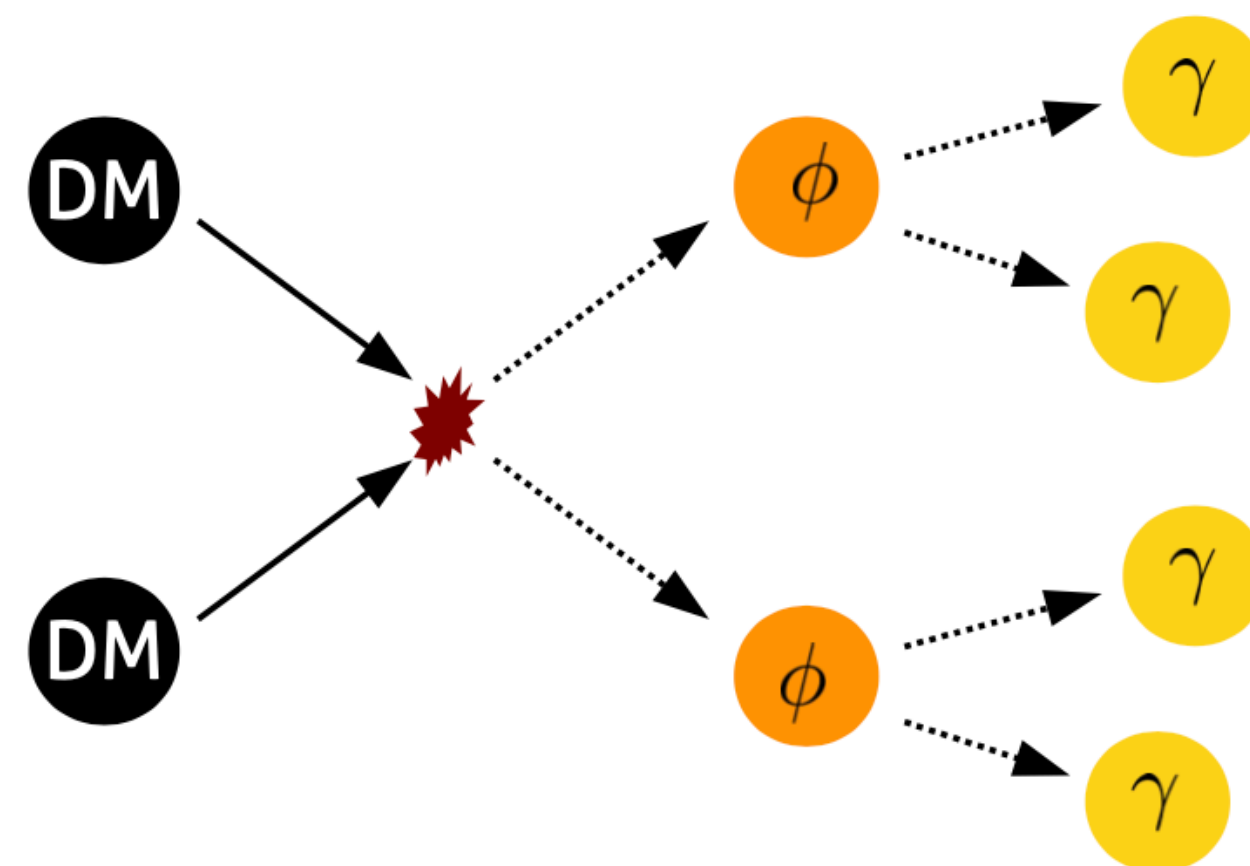
Bremsstrahlung:

Photon production in "hard process"



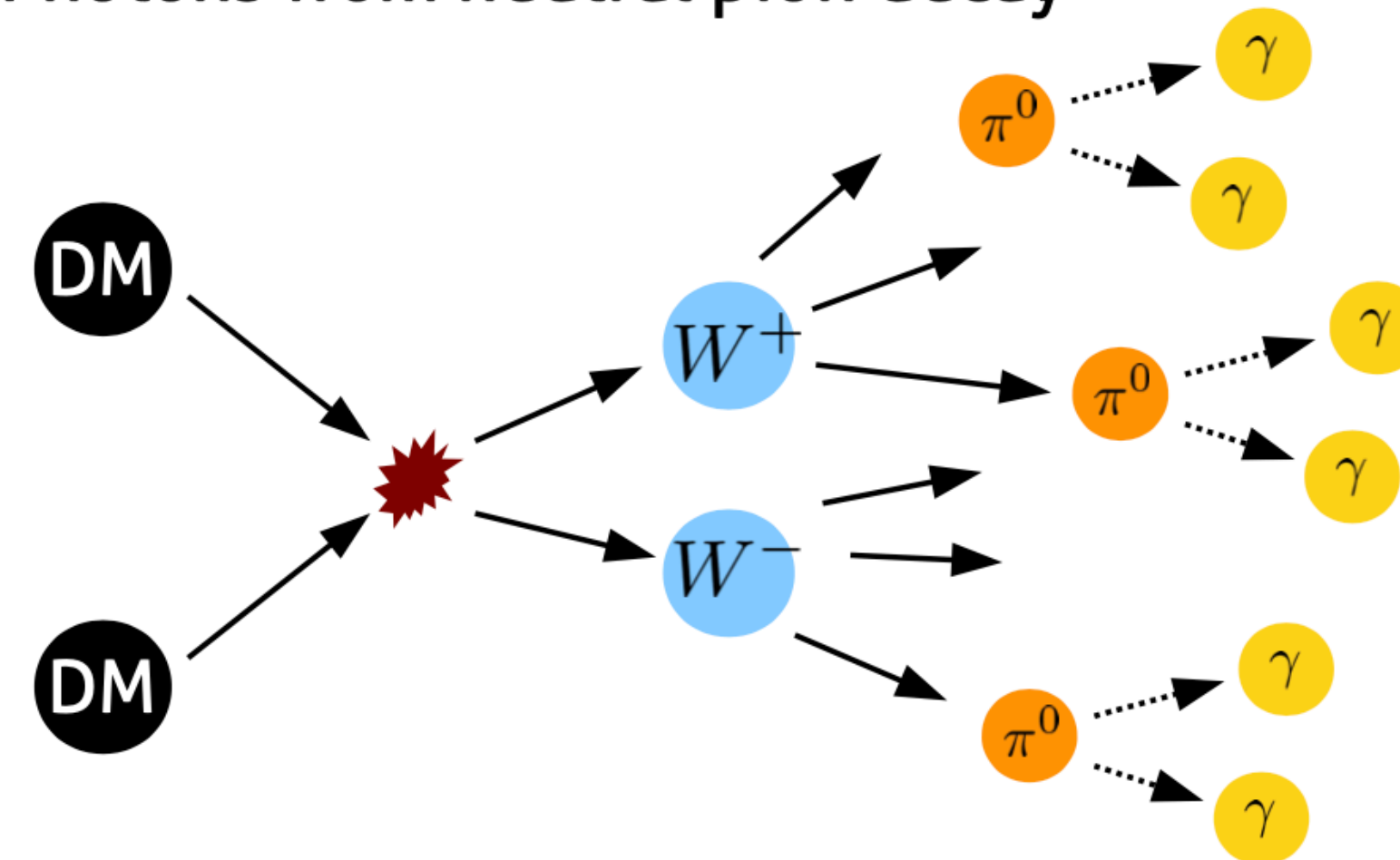
Box-shaped spectra:

Photons from cascade decay

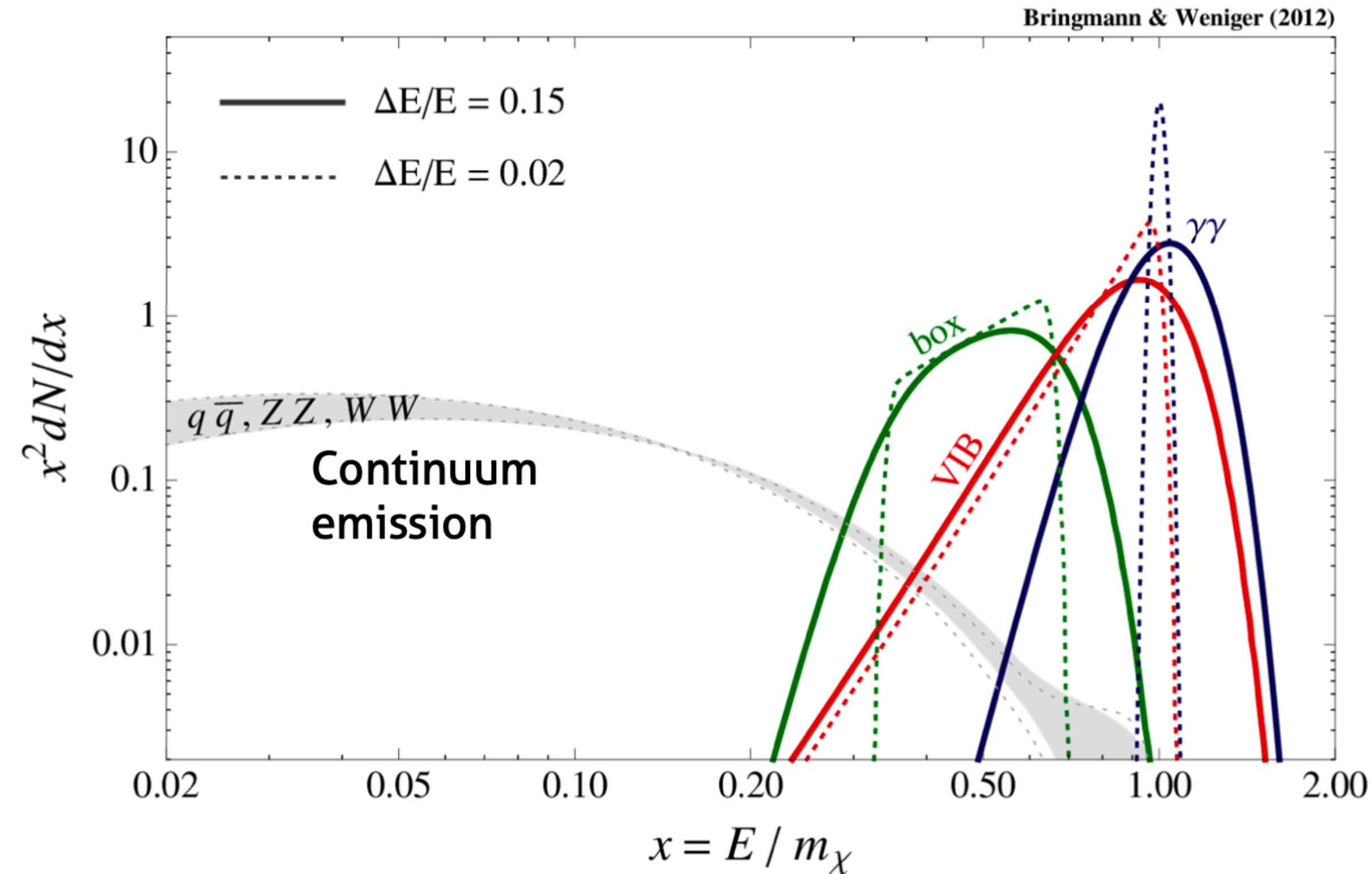


Continuum emission: (Prompt)

Photons from neutral pion decay



Gamma rays from dark matter annihilation



Box-shaped spectra

- Cascade-decay into monochromatic photons
- already at tree level

Internal Bremsstrahlung (IB)

- radiative correction to processes with charged final states
- Generically suppressed by $O(\alpha)$

$$\chi\chi \rightarrow \bar{f}f\gamma$$

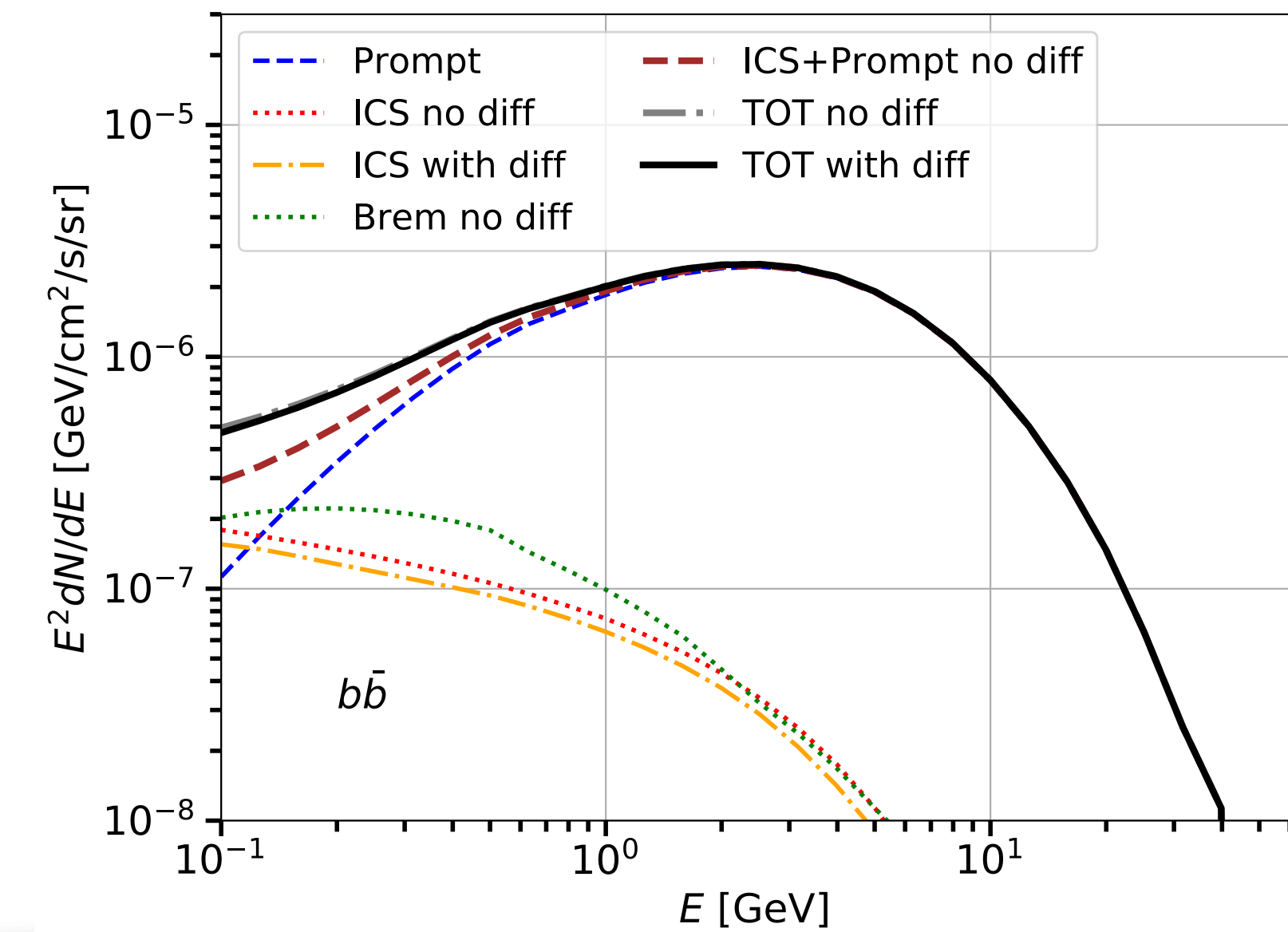
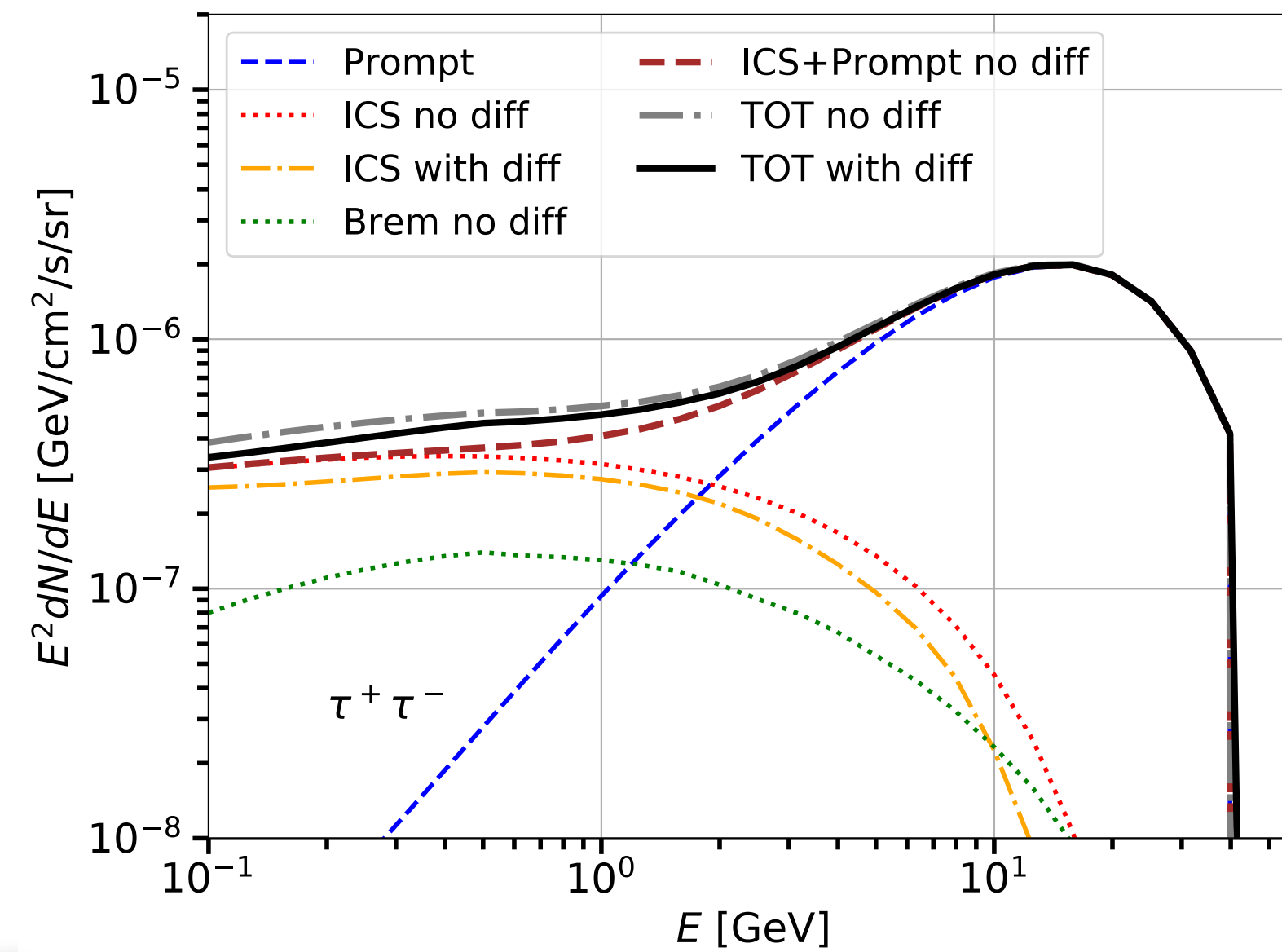
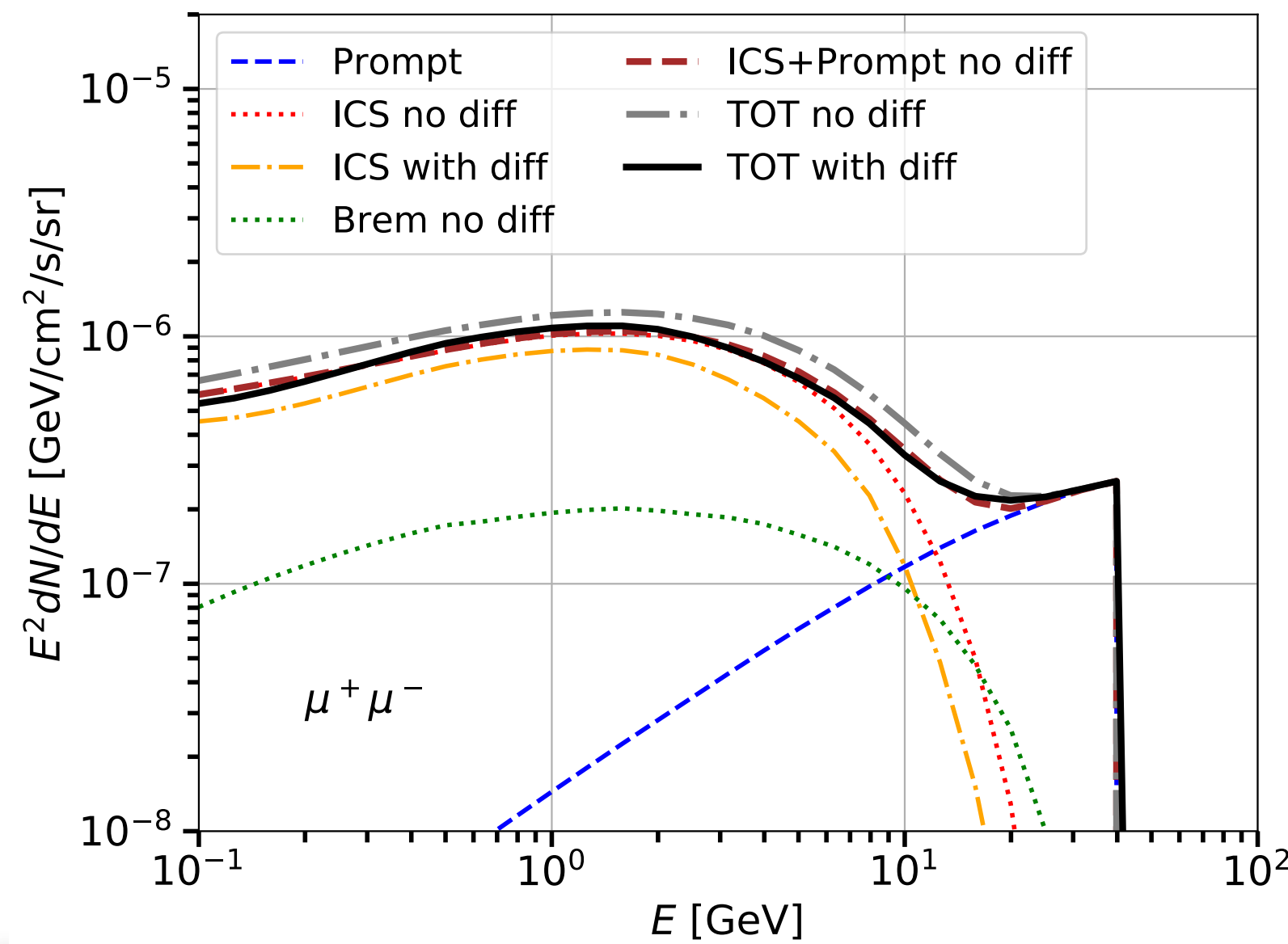
Gamma-ray lines

- from two-body annihilation into photons
- forbidden at tree-level, generically suppressed by $O(\alpha^2)$

$$\chi\chi \rightarrow \gamma\gamma$$

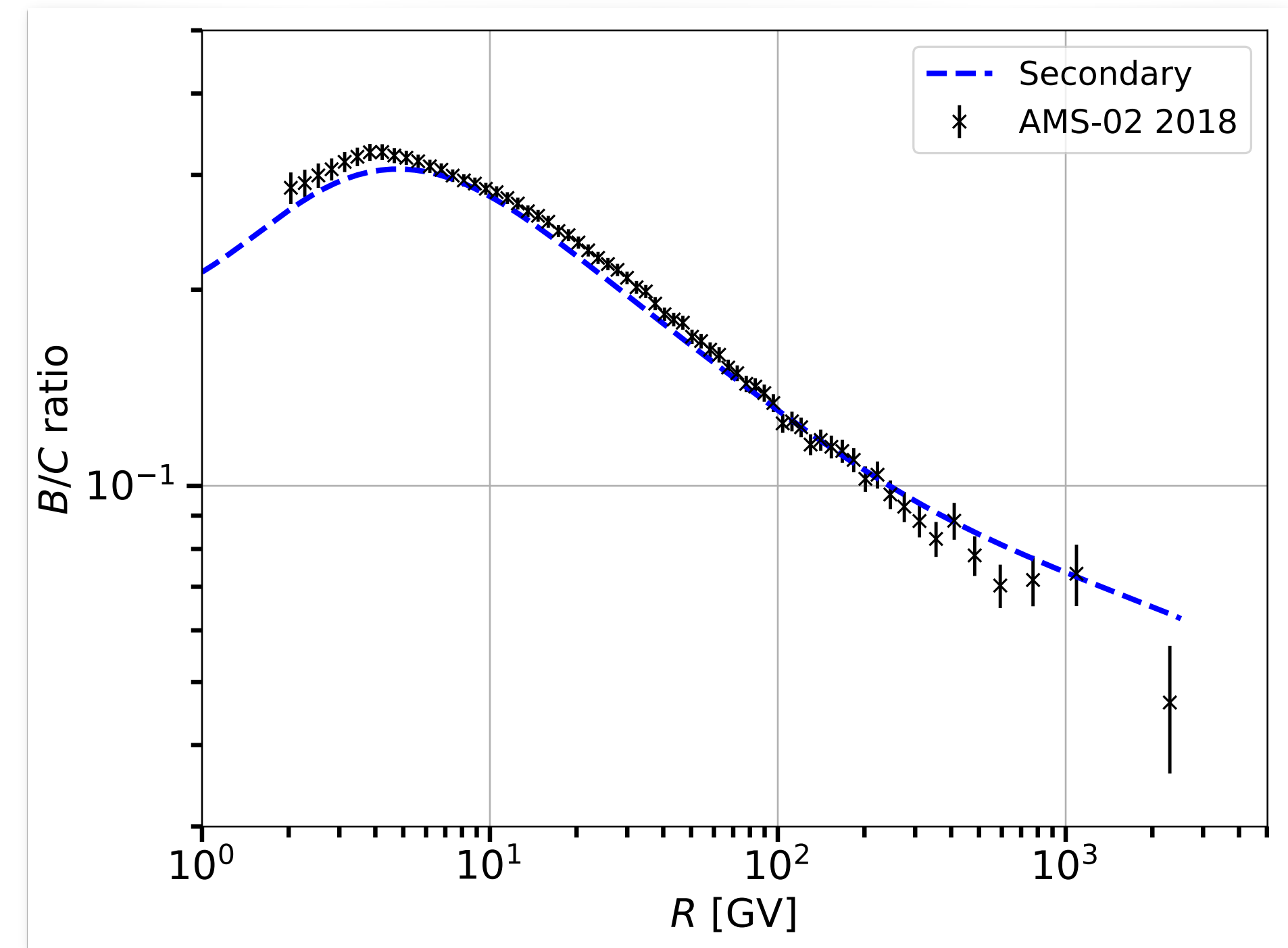
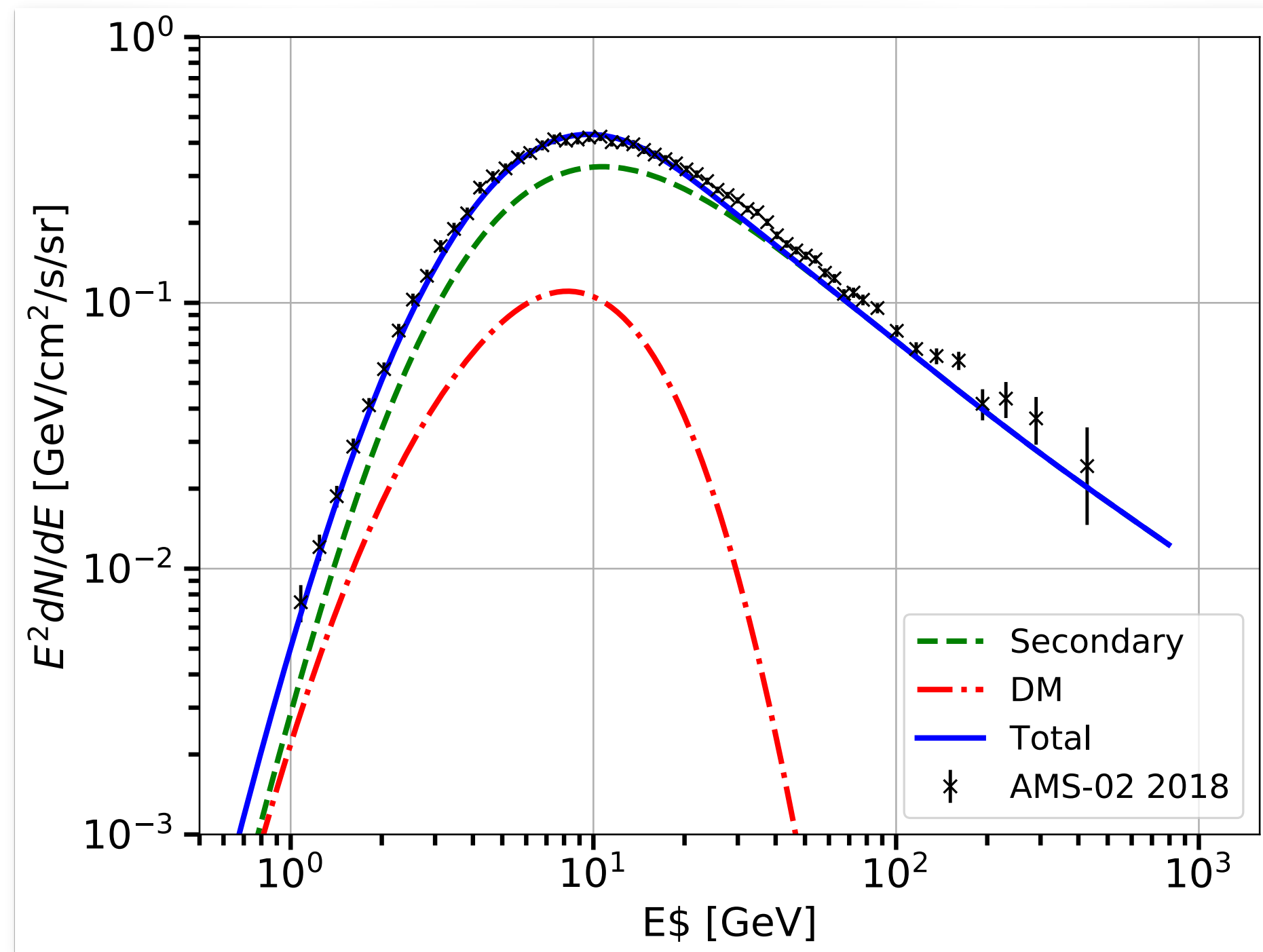
Theory for the gamma-ray flux from Dark matter

- We use a model that accounts for prompt and ICS emission from DM.
- The diffusion process has a much smaller effect than energy losses in the GC.
- The bremsstrahlung component is also negligible.



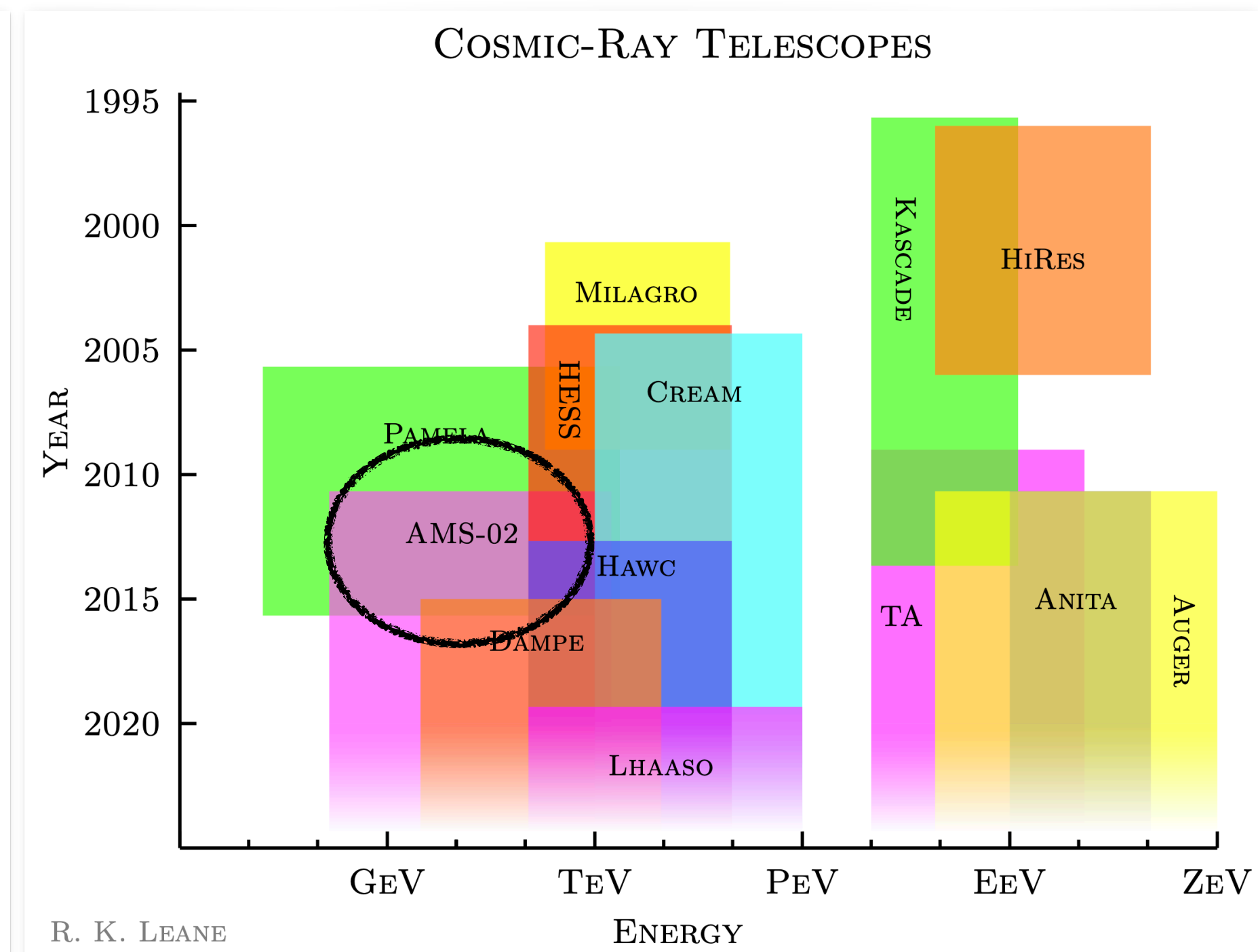
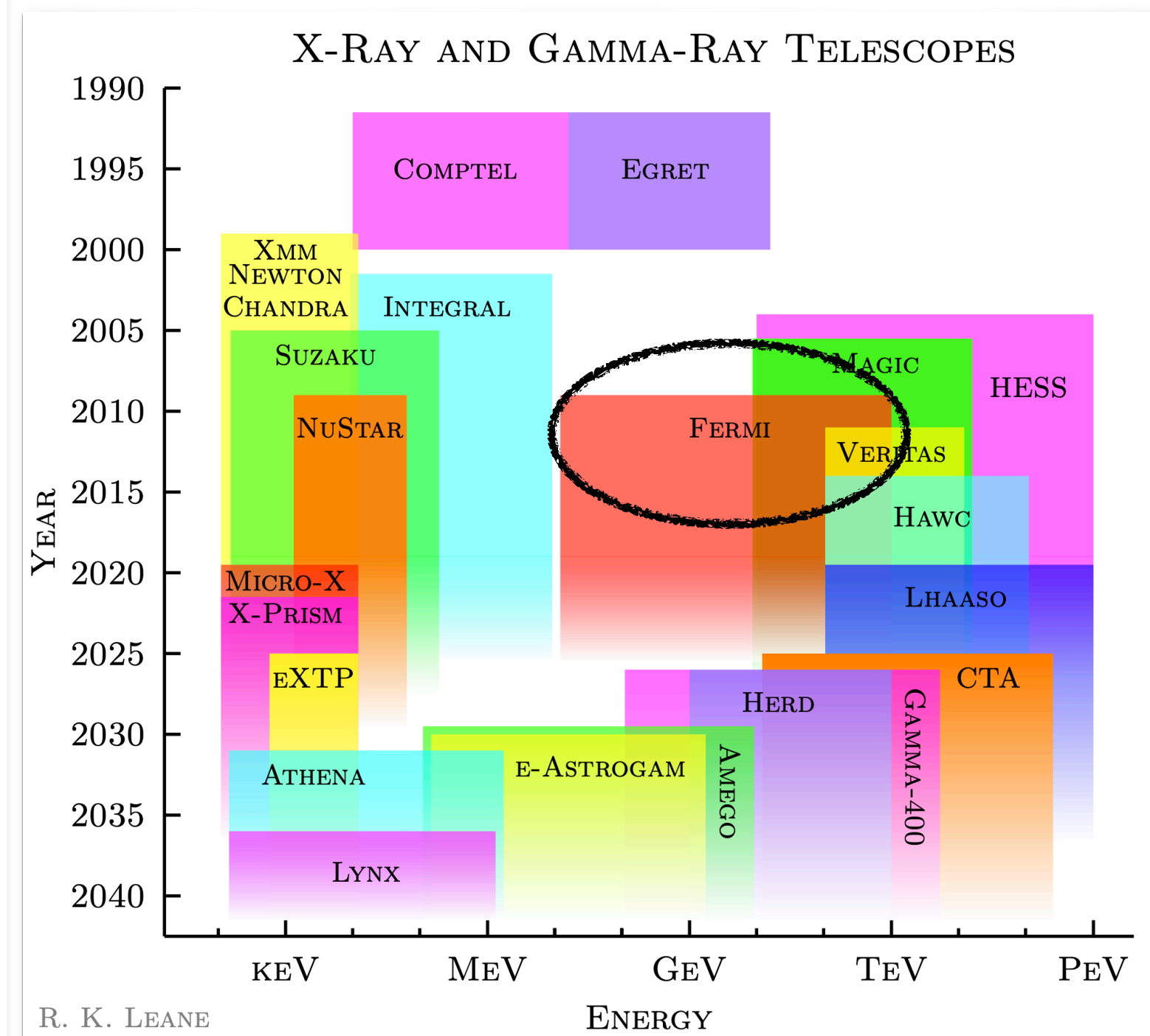
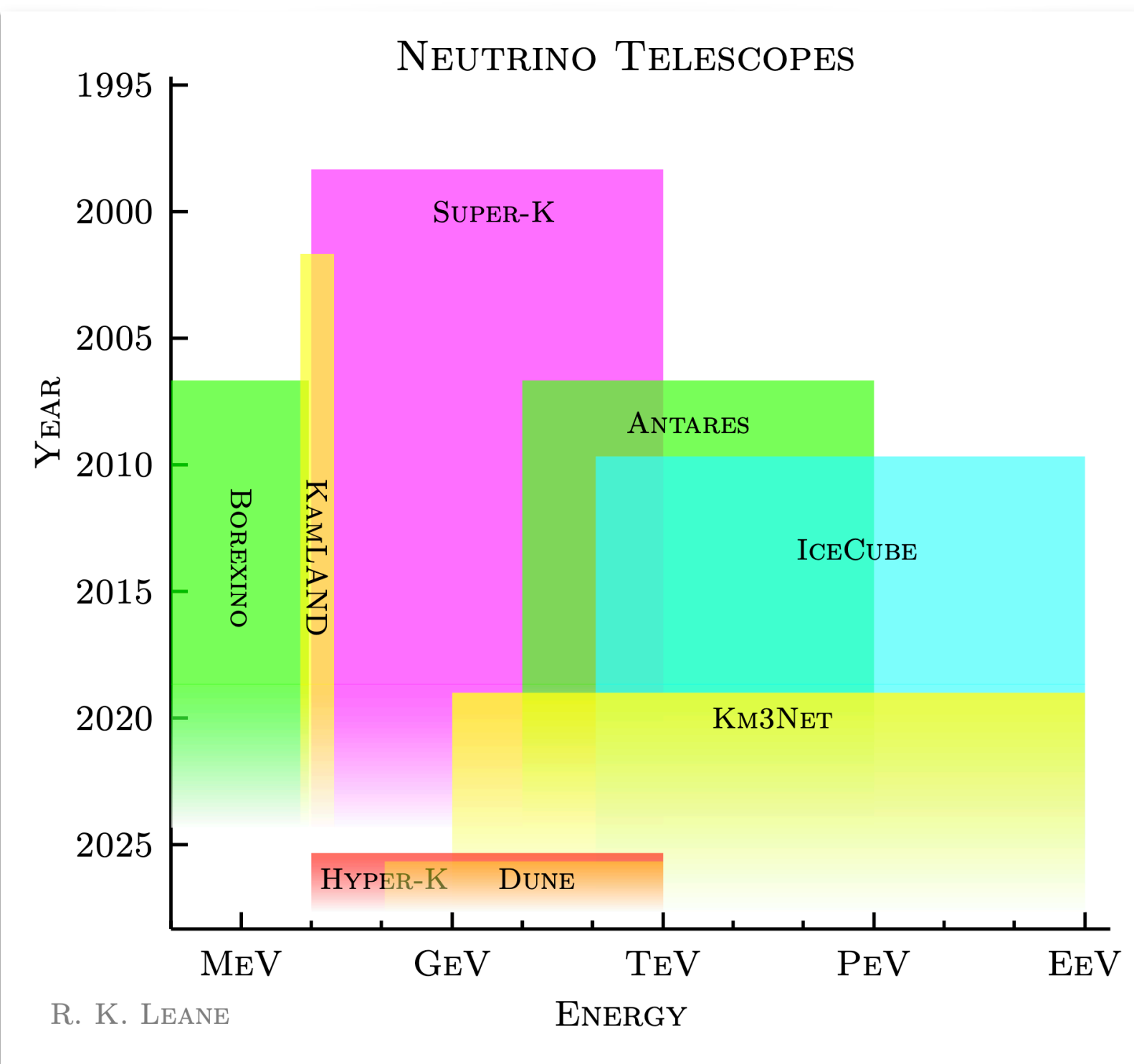
Antiprotons vs GCE

- We use the same analysis as in **Reinert and Winkler 2018**.
 - A combined fit to AMS-02 and Voyager p, AMS-02 and Pamela anti-p, AMS-02 B/C is performed.
- The addition of best-fit DM for the GCE with bottom channel worsens the fit with a delta chi-square of 44 (6σ worsening).
- We have used $L=3\text{kpc}$.

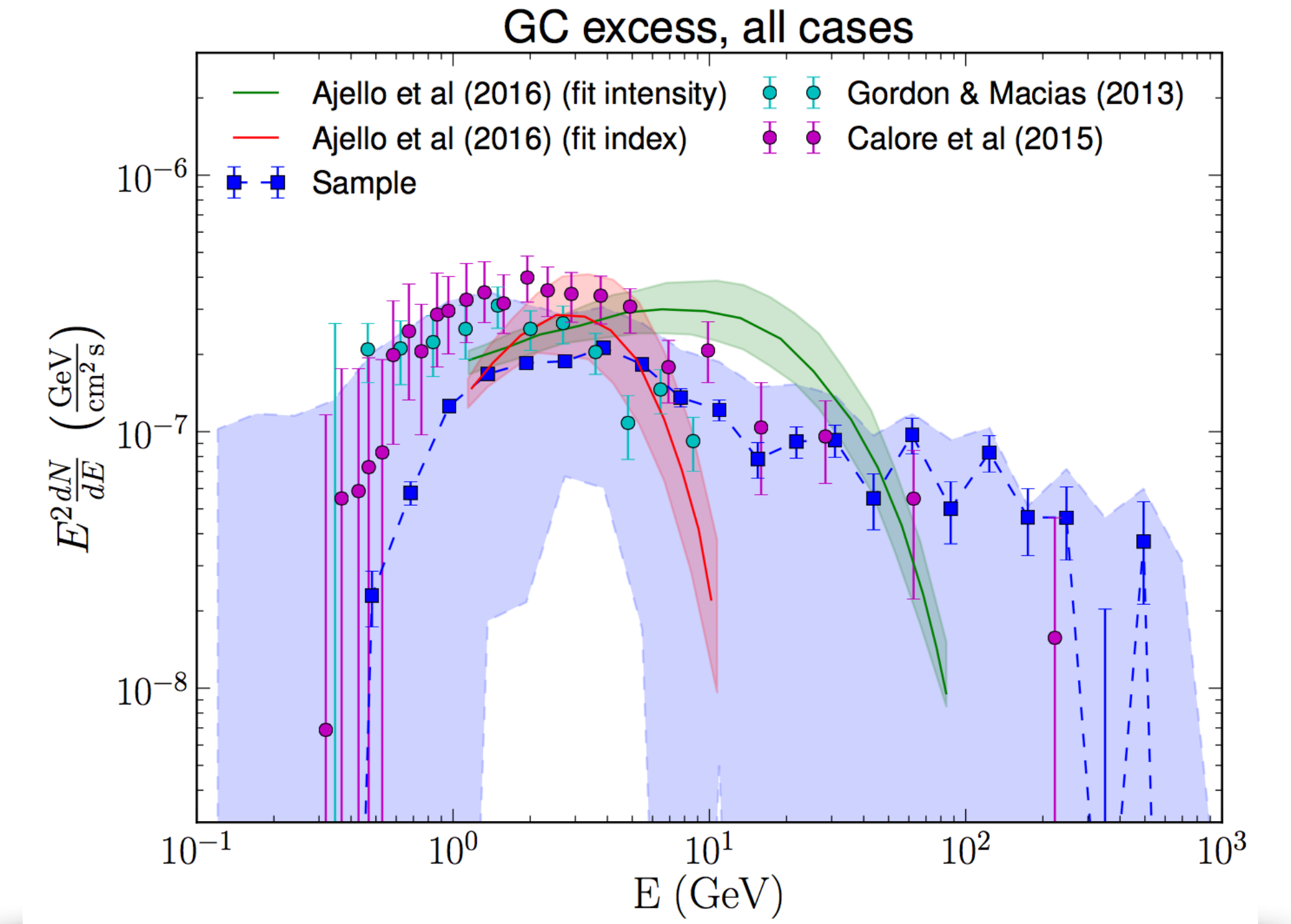
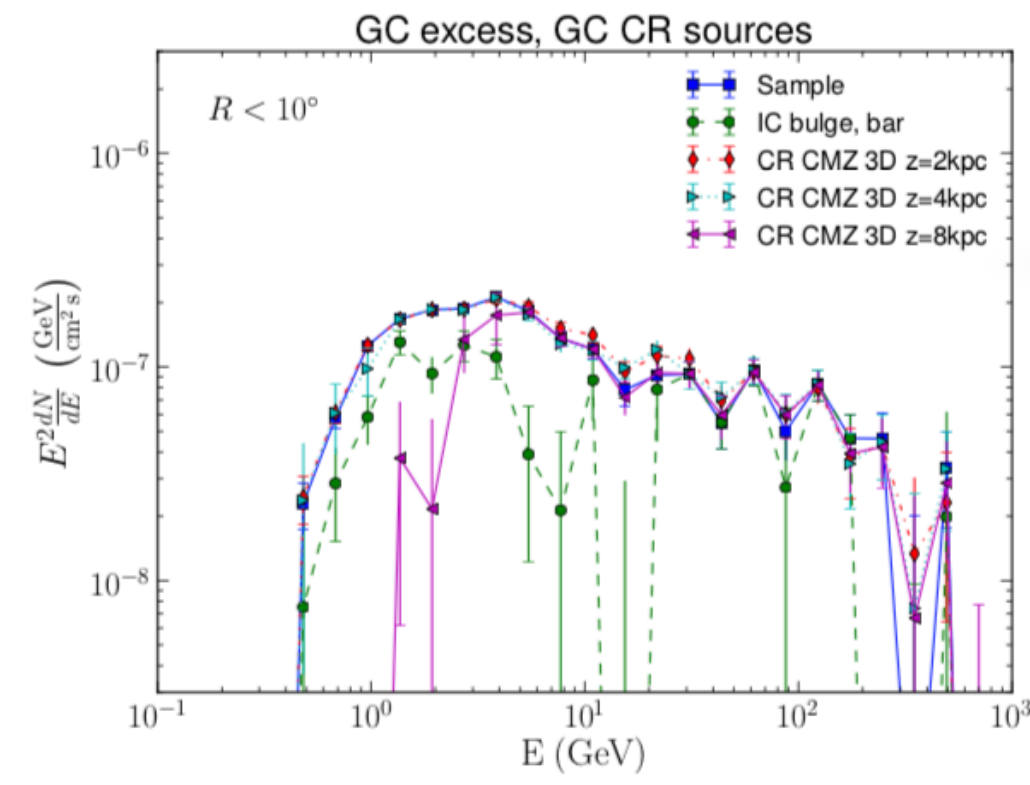
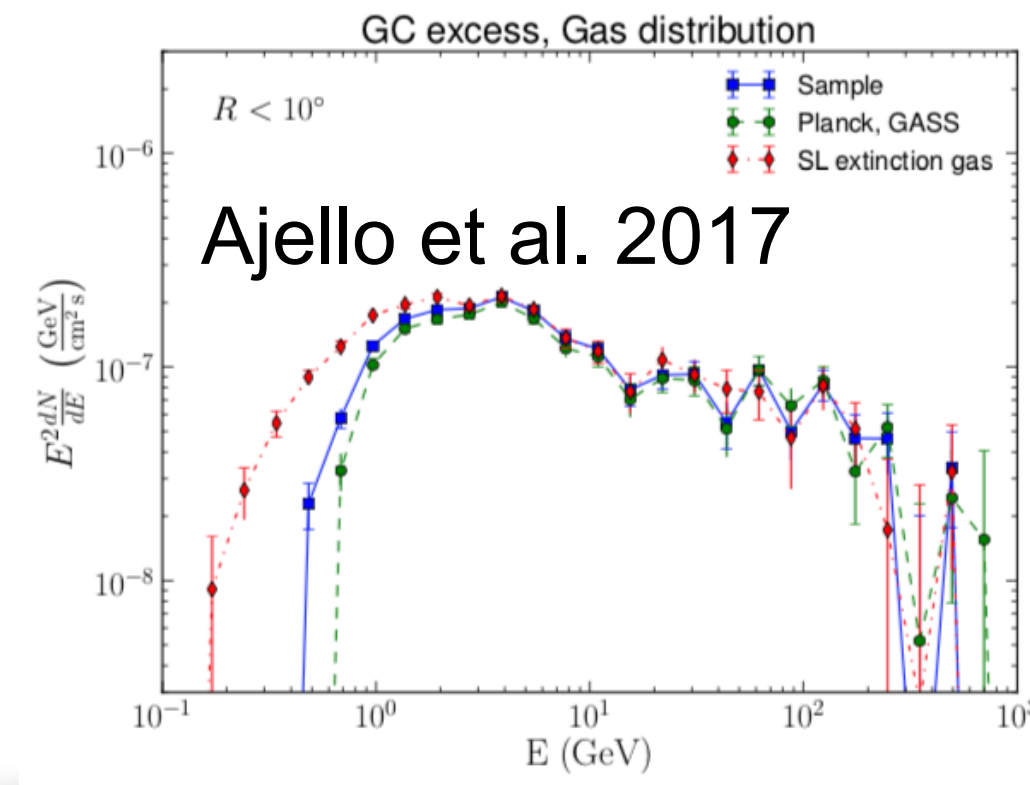
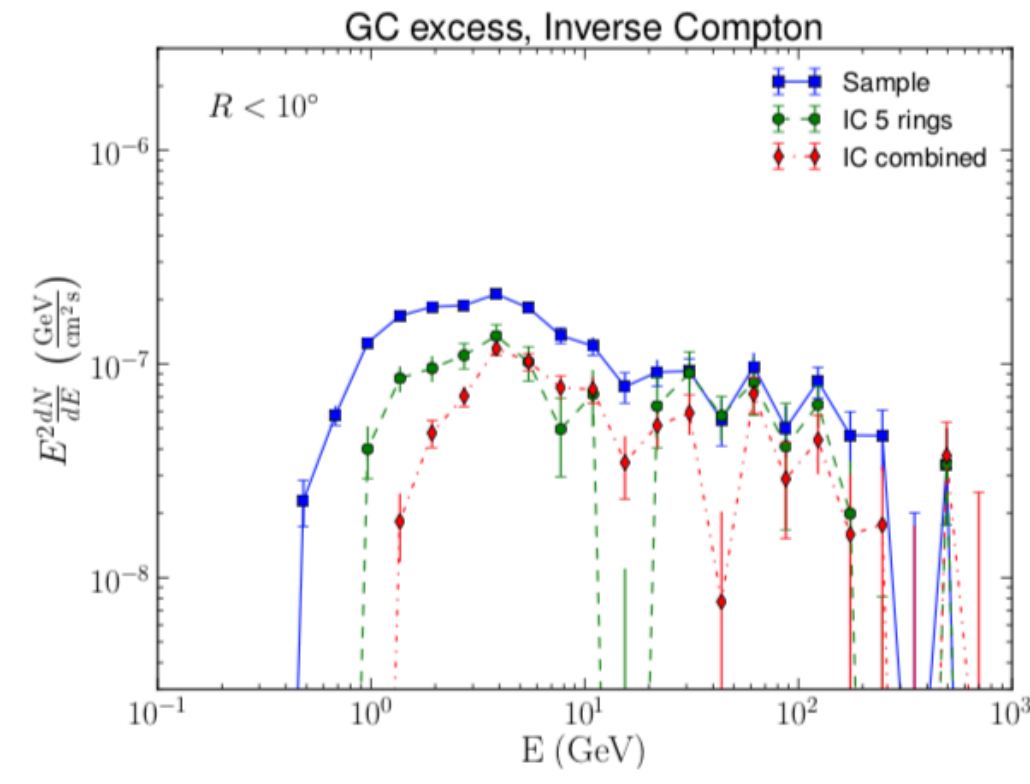
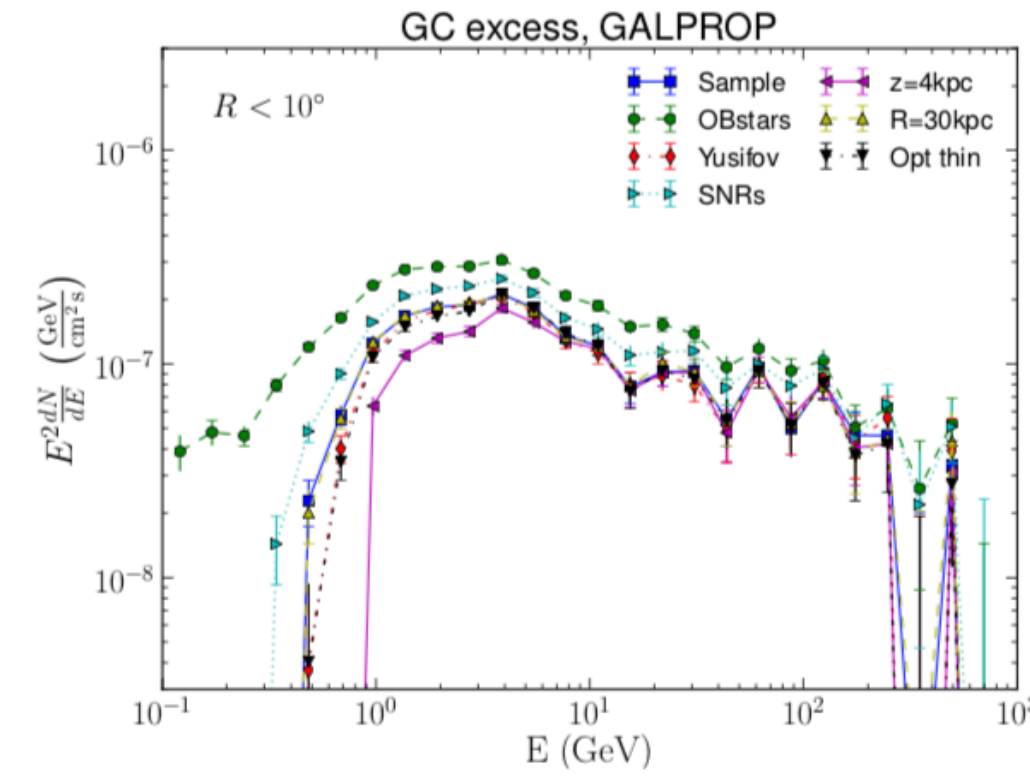
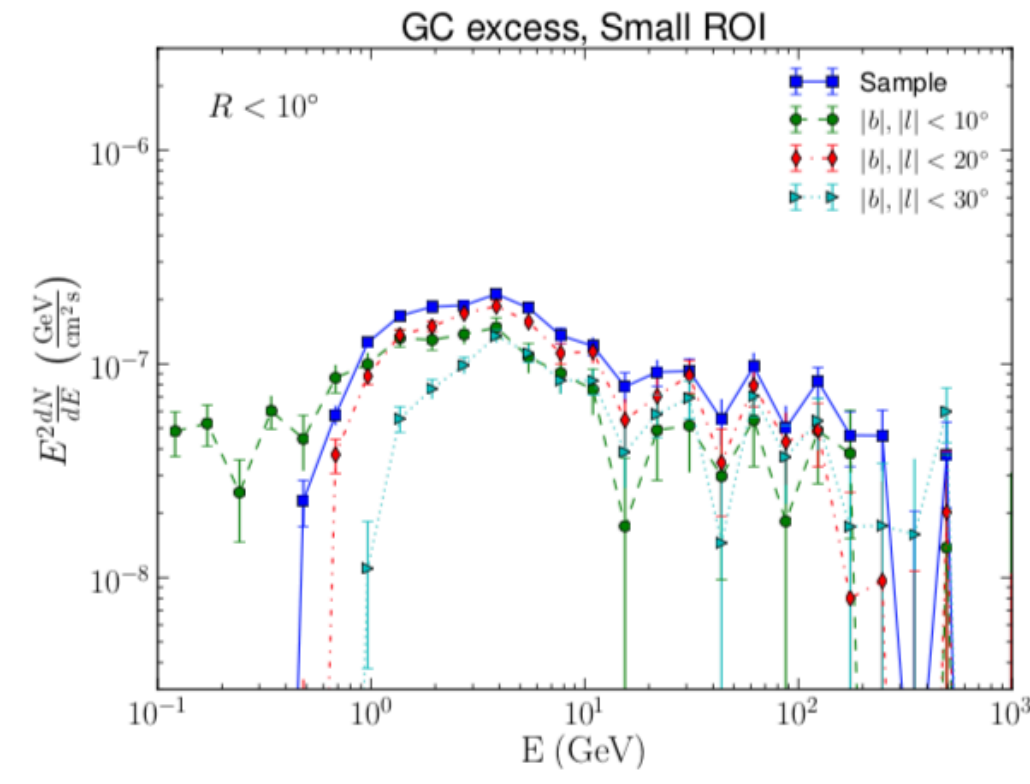
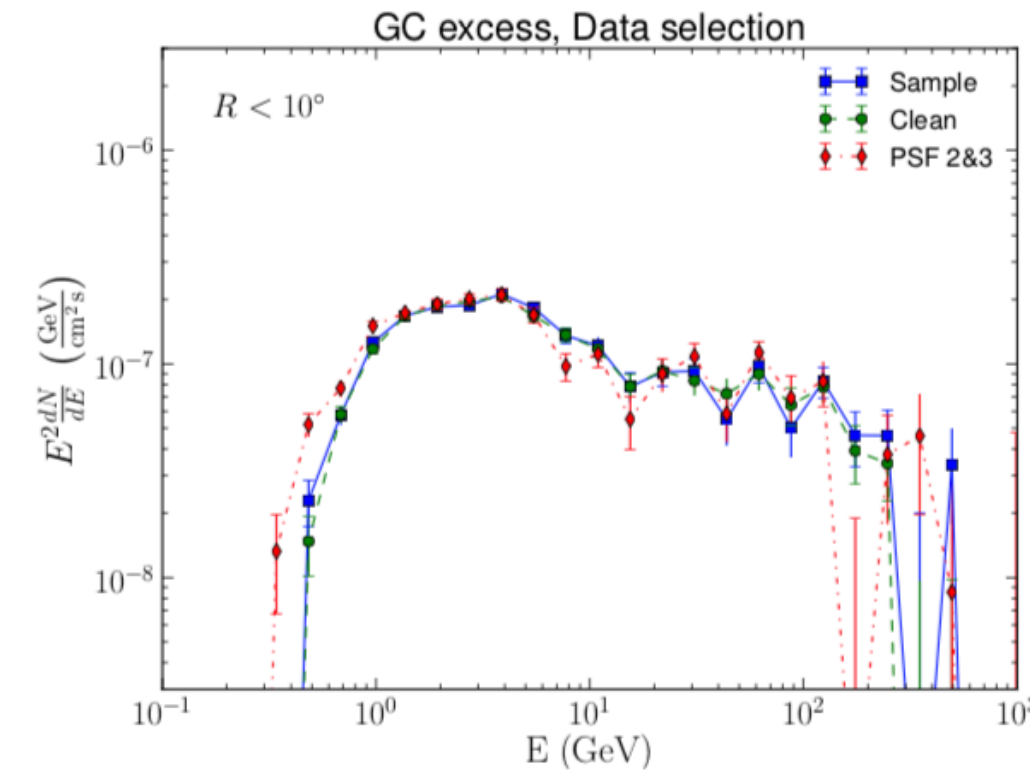


Cosmic-ray and radiation experiments

- Currently, there are precise experiments of cosmic ray and radiation.
- The future will be even more interesting!



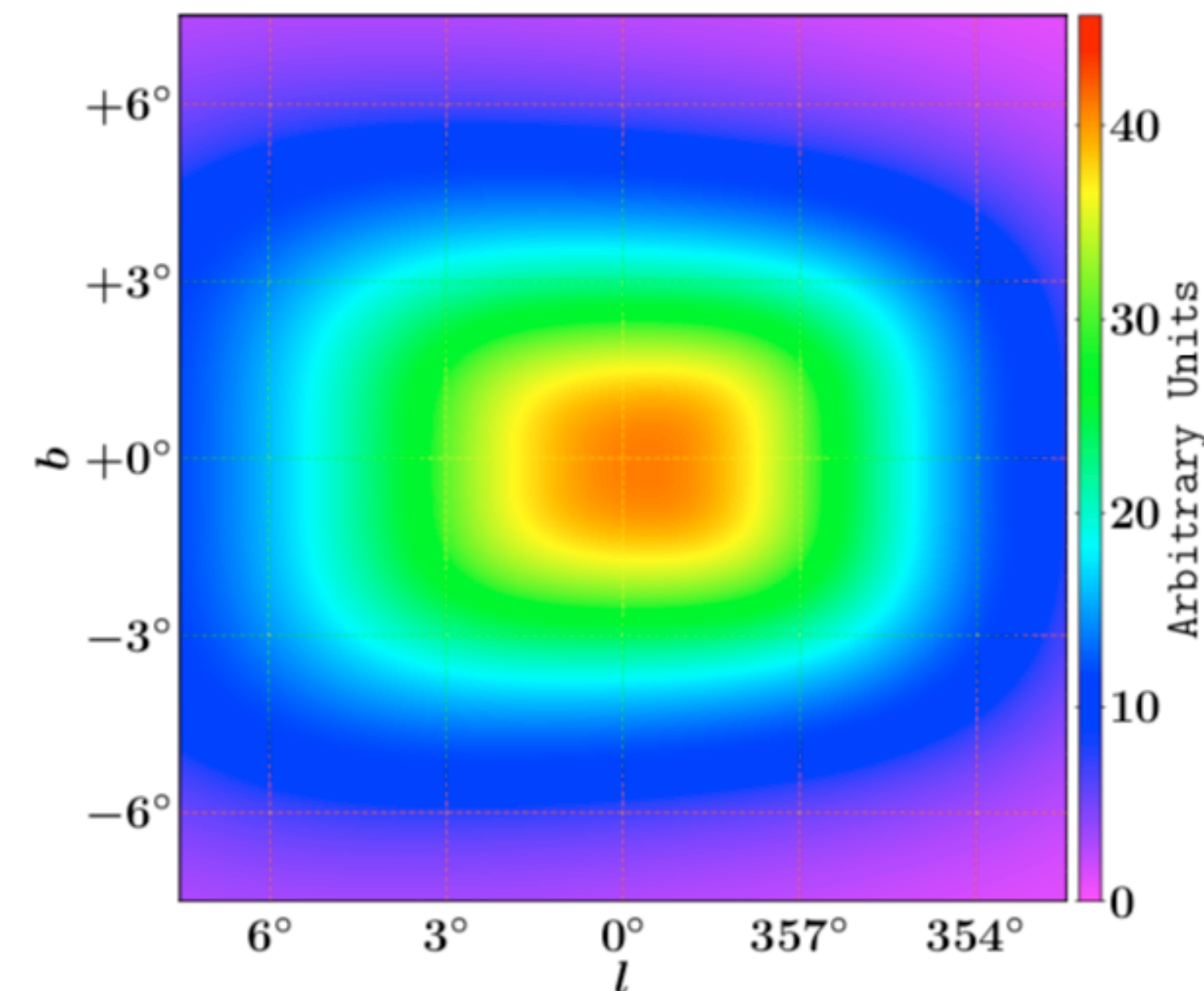
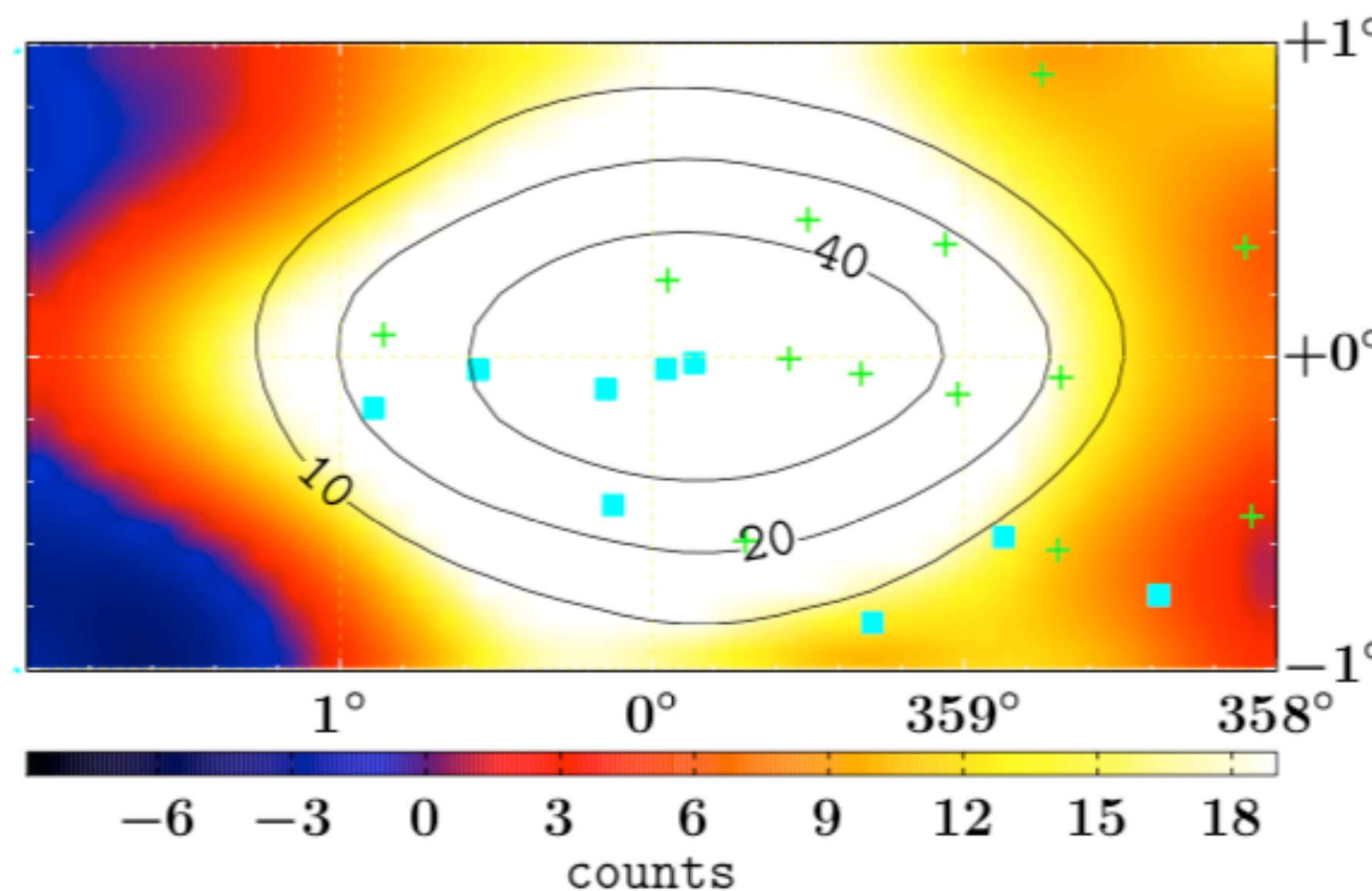
Uncertainties in the GCE flux



Galactic bulge

- **Macias et al. 2016-2020:**

- The GCE is better described by the stellar over-density in the Galactic bulge and the nuclear stellar bulge, rather than a spherical excess.
- Given its non-spherical nature, they argue that the GCE is not a dark matter phenomenon but rather associated with the stellar population of the Galactic bulge and nuclear bulge.



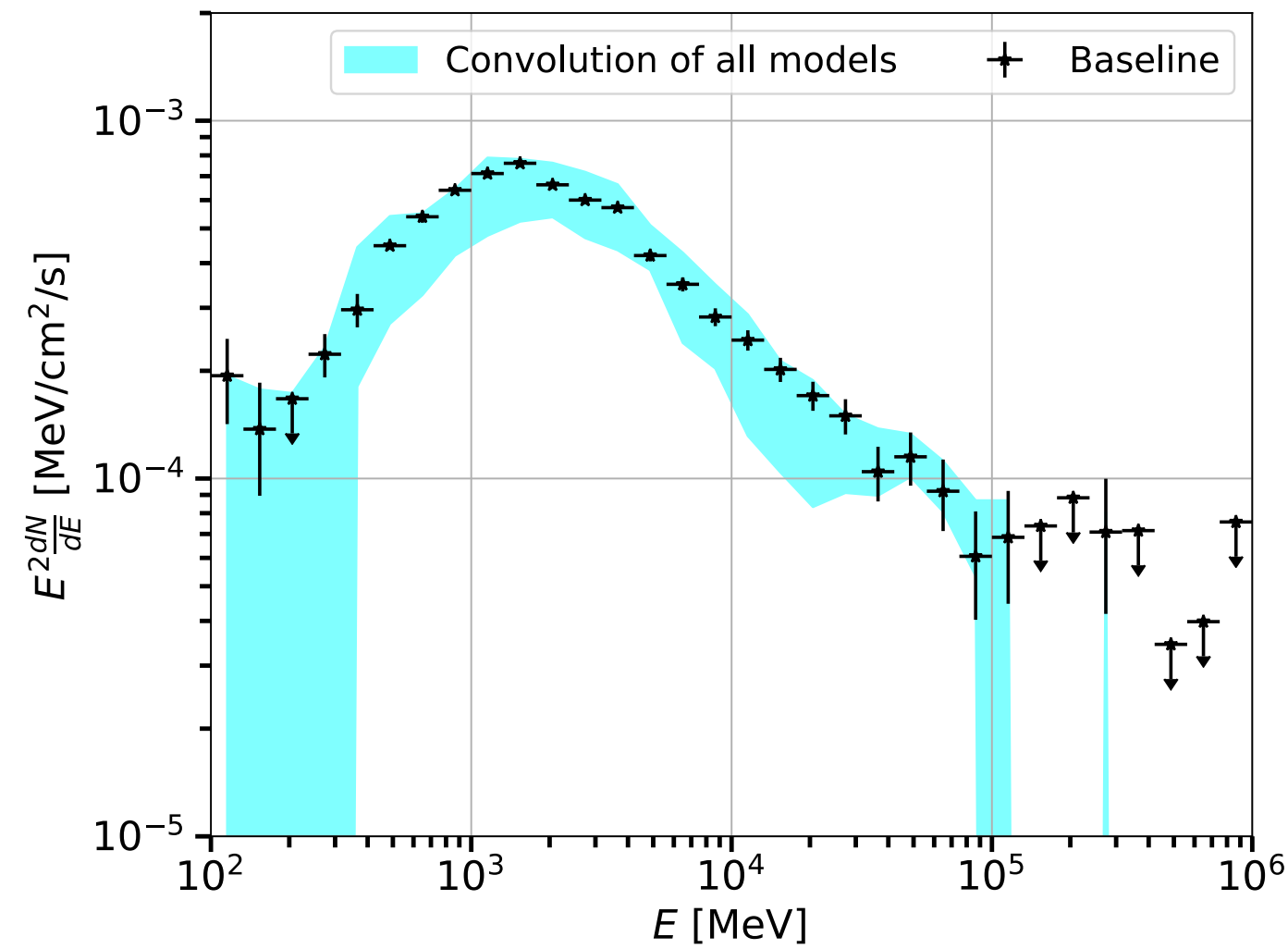
Most recent papers

- *Leane et al. 2019 and Chang et al. 2019*: the NPTF can misattribute to point sources or DM un-modeled point sources imperfection in the modeling of data.
- *Zhong et al. 2019* applied a wavelet method with 4FGL, and **do not find any evidence** of a faint population of un-modeled sources.
- *Buschmann et al. 2020*: They use a state-of-the-art model IEM find that the NPTF results continue to favor the interpretation that **the GCE excess is due, in part, to unresolved astrophysical point sources**.
- *List et al. 2019*: we find that the NN estimates for the flux fractions from the background templates are consistent with the NPTF; however, **the GCE is almost entirely attributed to smooth emission**.

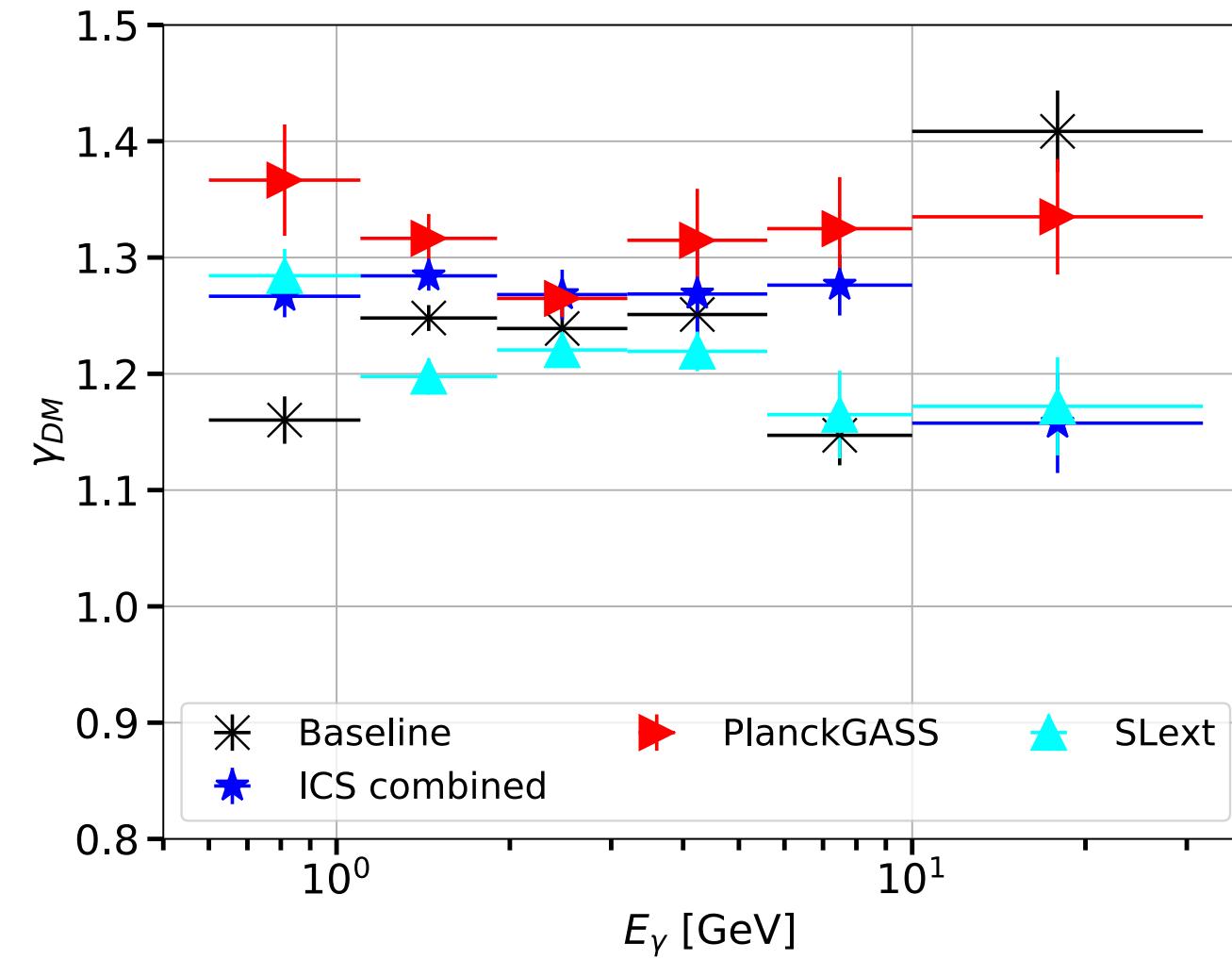
The situation is thus rather confusing and dark matter has recently gained interest.

Characteristics of the GCE: Summary

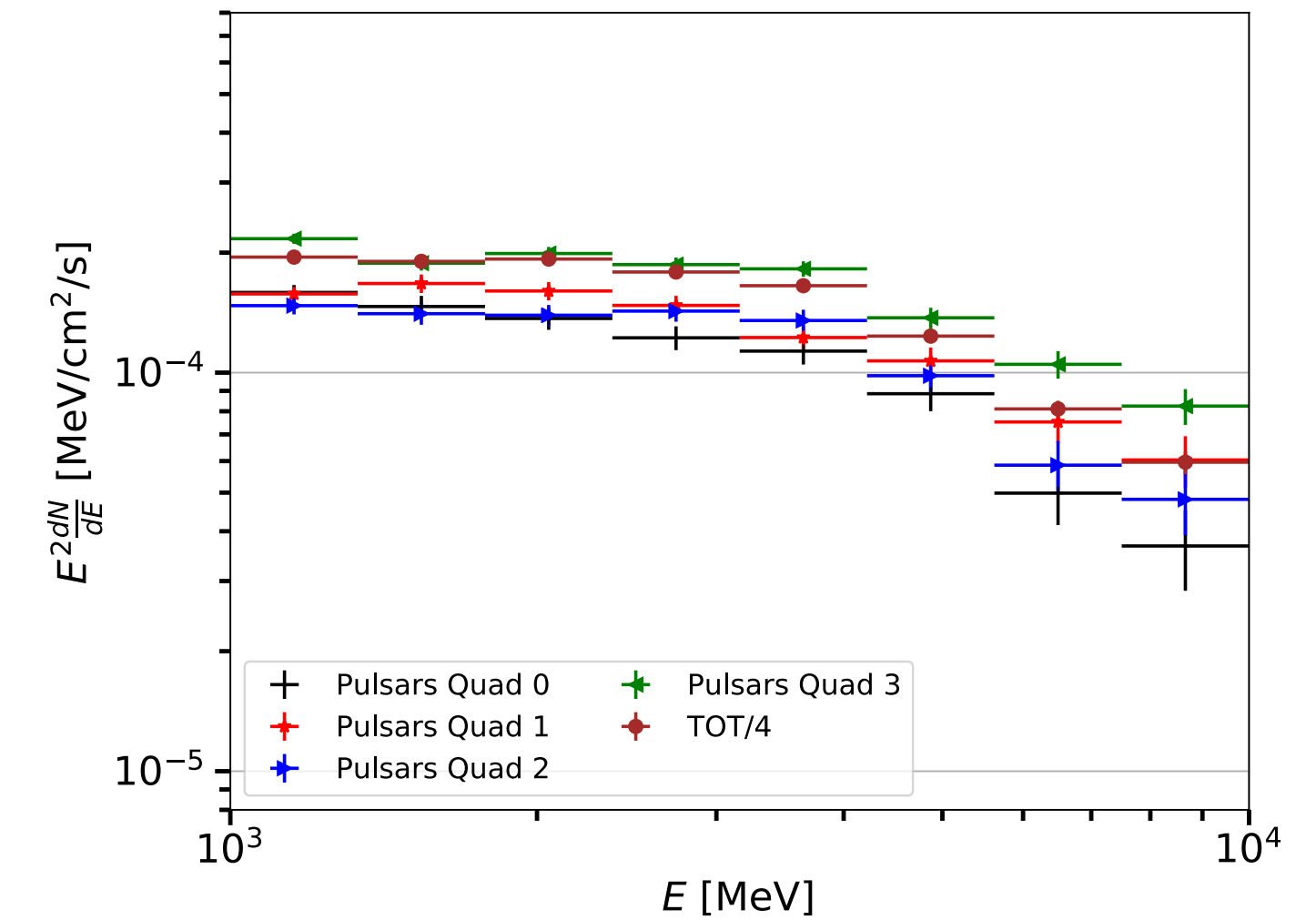
Spectrum peaked at a few GeV



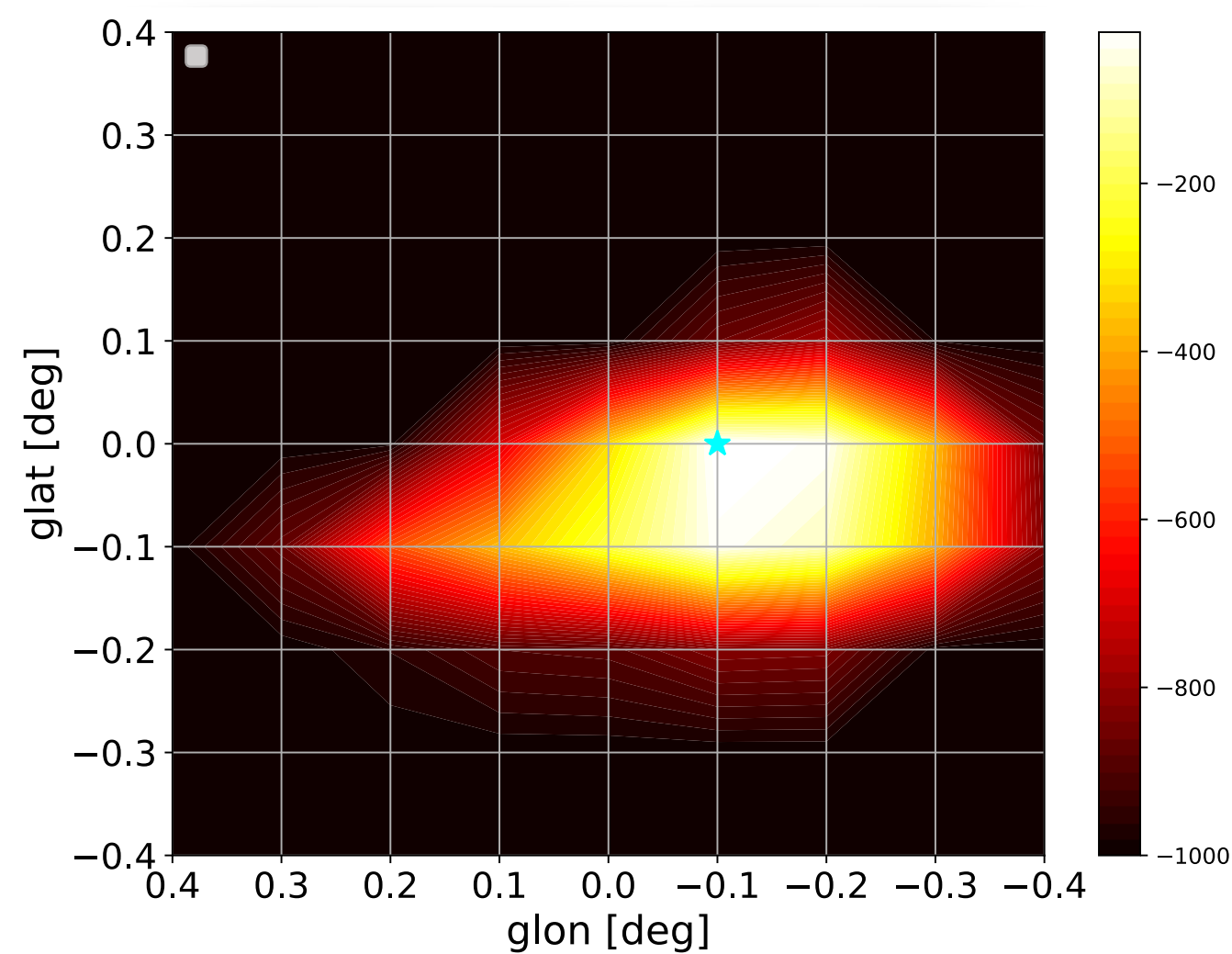
No energy dependence of spatial morphology.



The GCE is approximatively spherically symmetric.



Centered in the GC



gamma=1.25

